2008

Ceramide Kinase and Ceramide-1-Phosphate

Dayanjan Wijesinghe
Virginia Commonwealth University

CERAMIDE KINASE AND CERAMIDE 1 PHOSPHATE

A Dissertation submitted in partial fulfillment of the requirements for the degree of PhD at Virginia Commonwealth University.

by

DAYANJAN SHANAKA WIJESINGHE
BSc., University of Peradeniya, Sri Lanka, 2001
Grad. I. Chem. C., Institute of Chemistry, Sri Lanka, 1998

Director: CHARLES E. CHALFANT
ASSISTANT PROFFESSOR DEPARTMENT OF BIOCHEMISTRY AND MOLECULAR BIOLOGY

Virginia Commonwealth University
Richmond, Virginia
December 2008

DEDICATION

To my darling wife Piumini, my daughter Nisha, my Mother, Father and my Father and Mother-in-Law for their unconditional love and support.

Acknowledgement

I would like to express my heartfelt gratitude to my adviser, Dr. Charles E Chalfant for his guidance, counsel and advice without towards successful completion of this thesis. I am thankful to the members of my committee: Dr. Sarah Spiegel, Dr. Darrell L Peterson, Dr. Stephen T Sawyer and Dr. Lynne Elmore, for their valuable suggestions and time towards the successful completion of my degree.

I would like to thank Dr. William M Grogan for introducing me to all the great possibilities of mass spectrometry and for guiding me through the many trial and error days of learning. Many thanks Dr. Alfred Merrill Jr. and Dr. Cameron Sullards for the initial training they provided in lipid analysis by mass spectrometry. A huge thank you to Dr. Jeremy Allegood for filling in the gaps in my knowledge regarding mass spectrometry.

Thanks are also due to Dr. Darrell L Peterson, Mario A. Saavdera, Tom Sieger, and Dr. Bill Barton and Dr. Jessica Bell for all their insights and help in Ni-NTA purification of 6X his tagged proteins.

Many thanks to the members of the administration staff: Jodi, Carmelda, Gwen, Dan, Amy and Wilson for all the help and support given. You guys are the best!

Last but not least a huge thank you to all my friends Chaminda, Autumn, Kyle, Andreea, Preeti, Nadia, Luciana, Charu, Sanja and Alana for all their help and support. Also many thanks to other current members of the Chalfant Lab, Jackie and Rachel.

Table of Contents

Page

List of Tables

Page

List of Figures

Page

LIST OF ABBREVIATIONS

AA	arachidonic acid
C1P	ceramide-1-phosphate
Cer	ceramide
CERK	ceramide kinase
COX	Cyclooxygenase
$cPLA_2\alpha$	Group IVA cytosolic phospholipase A_2 alpha
DAG	di-acyl glycerol
DAGK	di-acyl glycerol kinase
ESI	electrospray ionization
FSK	foskolin
GFP	green fluorescence protein
HPLC	high pressure liquid chromatography
IL-1β	interleukin-1β
MRM	multiple reaction monitoring
PAPC	1-palmitoyl-2-arachidonyl-sn-phosphatidylcholine
PC	phosphatidyl choline
PGD_2	Prostaglandin D_2
PGE_2	Prostaglandin E_2
PGG_2	Prostaglandin G_2
PGHS	Prostaglandin H synthase
PKC	protein kinase C
PMA	phorbol 12-myristate 13-acetate
S1P	sphingosine-1-phosphate
SM	sphingomyelin
SMase	sphingomyelinase
SPHK1	sphingosine kinase 1
SPHK2	sphingosine kinase 2
PH	Pleckstrin homology
CerS	Ceramide synthase
CERT	Ceramide transport protein
LPA	lyso phosphatidic acid
PA	phosphatidic acid
GPCR	G-protein coupled receptor
PKA	protein kinase A
SPR	Surface Plasmon Resonance
TXA_2	Thromboxane A_2

Abstract

SUBSTRATE SPECIFICITY AND REGULATION OF ACTIVITY OF CERAMIDE KINASE

By Dayanjan Shanaka Wijesinghe, Ph.D.

A Dissertation submitted in partial fulfillment of the requirements for the degree of Ph.D. at Virginia Commonwealth University.

Virginia Commonwealth University, 2008

Major Director: Charles E. Chalfant, Ph.D.
Assistant Professor, Department of Biochemistry and Molecular Biology

Ceramide-1-phosphate (C1P) is a bioactive lipid that has been implicated in many biological processes. Our laboratory has conclusively demonstrated its role in inflammation via activation of $cPLA_2\alpha$. The only known enzyme to date responsible for direct synthesis of C1P is ceramide kinase. Very little was known about this enzyme in terms of its enzyme kinetics substrate specificity. As CERK is an enzyme that acts on membrane lipids, its kinetics cannot be studied using standard bulk dilutions methods. Thus we developed a surface dilution approach using Triton X 100 mixed micelles for studying the kinetics of CERK. We discovered that ceramide kinase has an affinity for naturally occurring long chain ceramides while ceramides containing shorter than 8 carbons are very poor substrates for the enzyme. Also of note is the discovery that there is

now discrimination between the naturally occurring long chain ceramides leading to the conclusion that the preponderance of D-e-C_{16} C1P in cells are due to an availability effect. We also investigated the chain length specificity of interaction between C1P and $cPLA_2\alpha$. Our data indicate that $cPLA_2\alpha$ is activated by C1P's containing acyl chains longer than two carbons. The study showed C_2 C1P as being unable to activate $cPLA_2\alpha$ thus establishing a tool for the investigation of $cPLA_2\alpha$ dependent and independent effects of C1P. In the course of the study we investigated the ethanol/dodecane delivery system as a means of safely delivering lipids to cells. Our data conclusively demonstrate that this delivery system successfully delivers lipids to the internal membranes where their biological action takes place and that at low lipid concentration (<1μM), is non toxic to cells. A significant technical hurdle in the study of C1P was the lack of accurate and reproducible method of quantitatively and qualitatively analyzing the lipid. Using a mass spectrometric approach we developed an accurate technique that now allows us to quantify the lipids in cells. Using this and radiolabeling studies we discovered evidence for production of C1P from S1P via an acyl transferase pathway. Further studies are currently being carried out to identify the enzyme/s responsible for this pathway.

INTRODUCTION

LIPIDS AND THEIR MANY FUNCTIONS

Of the major classes of biomolecules that make up a cell (nucleic acids, proteins, lipids and carbohydrates), lipids until recently, were not given the consideration deserved. While nucleic acids and proteins are necessary for cell survival, it is the lipids that are responsible for a cells existence. These are the molecules that through their special properties of self aggregation, walled off sections of the primordial soup giving rise to separate microenvironments that eventually became life. Thus if it is not for the lipids, life as we know would not exist.

Lipids are broadly defined in most textbooks as any lipophylic naturally occurring molecule. This broad category of compounds include fats, oils, waxes, cholesterols, sterols, fat soluble vitamins, mono and diglycerides etc. A much more refined definition of lipids would be that they are hydrophobic or amphiphilic small molecules that originate entirely or in part from either ketoacyl or isoprene groups. Using this definition, lipids can be categorized into eight different classes as fatty acyls, glycerolipids, glycerophospholipids, sphingolipids, saccharolipids, polyketides, sterol lipids and prenol lipids. Glycerophospholipids are the principal lipids found in membranes. Of the phospholipids, PE, PS and PI are found primarily in the inner leaflet of the membranes while PC is mainly found on the outer leaflet. While phospholipids do not flip between the membranes on their

own, the action of a group of enzymes called scramblases can catalyze this movement (1). In addition sphingomyelin, ceramides and sterols (mainly cholesterol) are also membrane constituents in animal cells. High caloric content of triglycerides have made them the ideal choice for energy storage by animals. In addition to these functions, certain lipids have other attributes specific to them. Vitamins A, D, K and E are essential isoprene based lipids and are stored in the liver and fatty tissues. Acyl carnitines are involved in the transport and metabolism of fatty acids in and out of mitochondria where they undergo beta oxidation. Polyprenols and their phosphorylated derivatives are important in transportation. Cardiolipins, a lipid that is found in the inner mitochondrial membranes are thought to be important in the activation of enzymes involved in oxidative phosphorylation.

SPHINGOLIPIDS

Sphingolipids are a major class of lipids that are conserved in all eukaryotic organisms. Sphingolipids are also found in some prokaryotic organisms, especially the genus *Sphingobacterium* (2). Loss of the ability to synthesize sphingolipids are lethal and has been shown to cause cell death in yeast (3) cell death in fly (4) and embryonic lethality in mouse (5).

The main classes of sphingolipids are the long chain bases, long chain base 1 phosphates, ceramides and their phosphates, sphingomyelins and glucosyl and galactosyl ceramides.

All sphingolipids are characterized by the presence of a sphingoid backbone containing a primary hydroxyl group at C1, an amino group on C2 and a secondary hydroxyl group on C3. This constitutes a hydrophilic head group and a hydrophobic tail group. All ceramide species contain an acyl chain attached to the sphingoid backbone via an amide bond through the amino group. The high stability of the amide bond renders ceramide species resistant to alkaline hydrolysis allowing for selective purification of sphingolipid species from glycerolipids in biological samples. The primary hydroxyl group allows for the attachment of various head groups via an ester or ether linkage. Specific examples include attachment of phosphocholine head group via a phosphodiester linkage giving rise to sphingomyelin, attachment of one or more glucose or galactose groups via an ether linkage, giving rise to multiple glucosyl or galactosyl ceramides.

A simple abbreviated nomenclature for sphingolipids is defined by the lipidmaps consortium (6). Accordingly the number of hydroxyl groups are defined by d (di), t (tri) followed by the number of carbons in the sphingoid backbone and then the number and position of the double bonds. For example, $d_{18:0}$ for sphinganine $d_{18:1}^{\Delta 4}$ for sphingosine, $d_{18:1}^{\Delta 4,8}$ for sphingadienine and $t_{18:0}$ for 4D-hydroxysphinganine. Sphingoid base 1-phosphates are denoted as $d_{18:1}$-P. When denoting sphingosine or any other species containing the sphingosine backbone, the position of the double bond is generally omitted. When denoting N-acylated sphingolipids, after the denotation for sphingoid backbone the number of carbons of the acyl chain is indicated followed by the number of double bonds

and their position. For example ceramide species with 18 carbon acyl chain with one double bond is denoted as $d_{18:1/18:1}$

Table 1: General structure of sphingolipids.

	R1	R2	R3
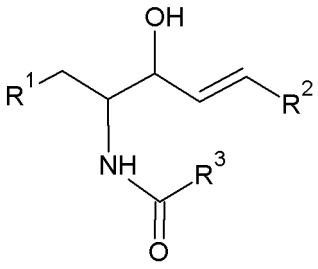	=OH Ceramide	Alkyl chain	Acyl chain length C2 to C26 Saturated or unsaturated
	= Glucose Glucosyl ceramide		
	= Galactose Galactosyl ceramide		
	= phosohatidyl choline Sphingomyelin		

The major form of the sphingoid backbone contains a trans double bond at the 4,5 position. The desaturation of the 4,5 bond occurs at a later stage of the denovo synthesis of sphingolipids. Thus significant quantities of 4,5 dihydro sphingosine and diydro ceramide species are also found in all of the eukaryotic cells. The major sphingoid base found in mammals are $d_{18:1}^{\Delta 4}$ while plant and fungi predominantly has phytosphingosine which carries an OH group at the C4 position ($t_{18:0}$). Mammals do have phytosphingosine; however they are limited mainly to the skin small intestines and the kidney. In addition mammalian skin has an unusual sphingoid base that contains an OH group at the 6 position (6-hydroxy-4-sphinganine) denoted $t_{18:1}^{\Delta 4}$ (7). Sphingoid base chain length can also vary between species. Among mammals it is predominantly 18. However 16, 18 and 20 carbons are found in yeast (8).

SYNTHESIS AND METABOLISM OF SPHINGOLIPIDS.

De novo synthesis of sphingolipids occur in the ER and start with the condensation of serine and palmitoyl Co-A by the action of serine palmitoyltransferase to produce 3-ketosphinganine. This is the rate limiting step in the synthesis of sphingolipids. 3-ketosphingainine is then reduced, N-acylated and desaturated to add a 4,5 double bond in a series of enzymaticaly catalyzed steps that include ceramide synthase (CerS) to give ceramide in the cytosolic leaflet of the ER (9). Ceramide thus synthesized is transported to the golgi where further modification produce complex sphingolipids like glucosylceramides and sphingomyelins. This transport of ceramide to the golgi is carried out either via a vesicular transport system involving COPII coated vesicles (10) or by non vesicular means via the ceramide transport protein (CERT) (9).

Mammals have six ceramide synthases currently identified with variable specificity for different acyl CoA groups. CerS1 for C_{18}, CerS5 and 6 for C_{16}, and CerS 2 and 4 for C_{22} and C_{24} (11-13). The attachment of the phosphocholine group to produce sphingomyelin is carried by sphingomyelin synthases of which two are present in mammalian cells SMS1 and SMS2 (14, 15). Glucosylation is carried out by the ceramide glucosyltransferase (16) and galactosylation is carried out by ceramide galactosyltransferase (17). Further glucosylation and galactosylation of glucosyl and galactosyl ceramide leads to hundreds of glycosphingolipids. Ceramide is phosphorylated in mammalian cells to produce ceramide-

1-phosphate via a kinase and a non kinase pathway (18). Ceramide kinase is the only known mammalian enzyme to date to produce ceramide 1 phosphate(19).

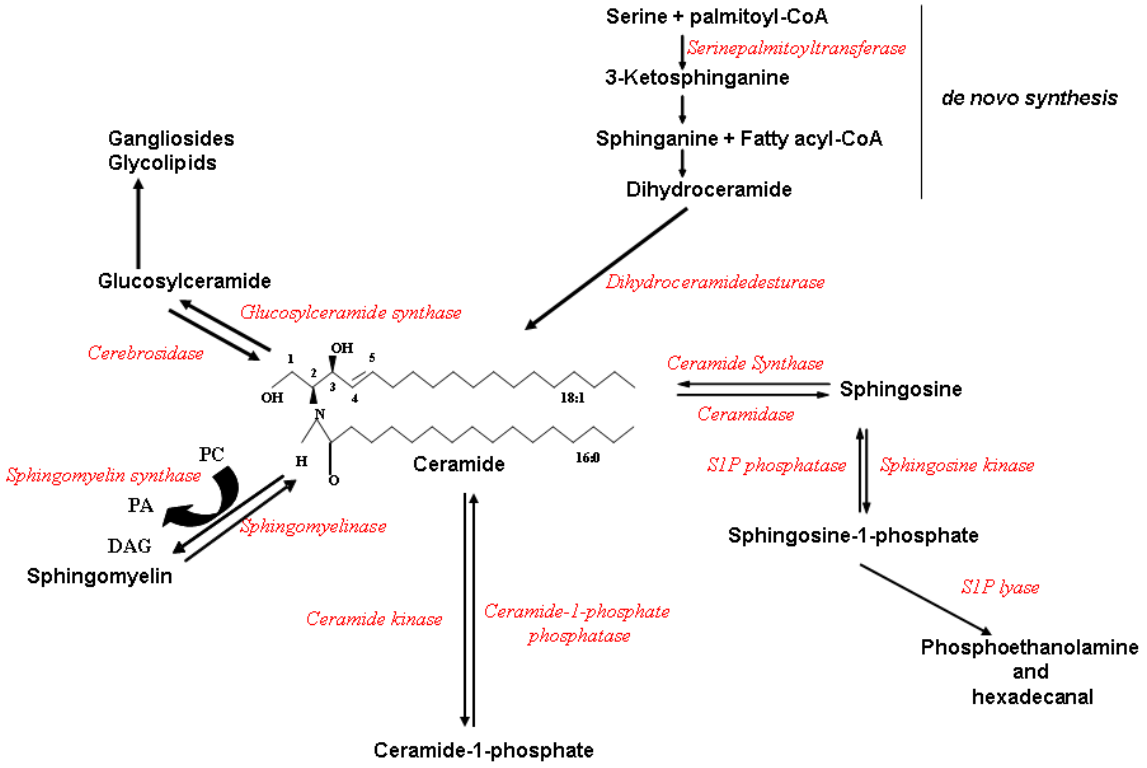

Figure 1. The synthesis and metabolism of sphingolipids. Ceramide is the central molecule in sphingolipid metabolism giving rise to all the major forms of sphingolipids in the cell.

Modified from: Pettus, et al. *Biochim, Biophys Acta* 2002, **1585**: 114-25.

LIPIDS AND CELL SIGNALLING

The ability of lipids to act as signaling molecules has been known for a long time. As early as 1930 cysteinyl leukotrienes have been known as slow reacting substances of anaphylaxis. Around the same time prostaglandins were found to cause vasodilation. It is now known that all these are metabolites of arachidonic acid. Thus a single lipid can have diverse downstream effects based on final products of its further metabolism.

Phosphatidylinositols are another well known group of lipid second messengers. Around 1980 it was discovered that phosphatidylinositol 4,5 bis phosphate could be hydrolyzed by phospholipase C (PLC) producing diaclyglycerol and inositol-1,4,5-tris phosphate. Both of these products are second messengers. DAG activates protein kinase C (PKC) while l Ins(1,4,5)P_3 causes Ca^{+2} release from internal stores. Other inositol polyphosphates are involved in different signaling events. For example PtdIns(3,4,5)P_3 is a signaling molecule that modulates cell growth, proliferation and motility. In addition to acting as direct signaling molecules, phosphoinositides act as localization agents for membrane signaling complexes. Another very potent signaling lipid is lysophosphatidic acid (LPA). These can act in an autocrine and paracrine manner through GPCR (20, 21).

The sphingolipids ceramides and sphingosines are lipids that have proapoptotic and antiproliferative actions. Their phosphorylated compounds ceramide 1 phosphates (C1P) and sphingosine 1 phosphate (S1P) are also potent signaling molecules. S1P is a well known potent cell proliferative agent while C1P among other things is a potent inducer of inflammation.

Disruptions and unusual changes in signaling lipids contribute to progression of diseases like chronic inflammation, autoimmunity, allergy, cancer atherosclerosis, hypertension, heart hypertrophy and metabolic and degenerative diseases etc.

LIPID SIGNALING AND INFLAMMATION.

Affecting lipid metabolisms to treat inflammation is not new to western medicine. Records as long ago as 400 BC from the Father of modern medicine, Hippocrates show the use of a brew from willow tree (*Salix alba*) to relieve fever and pain. Many centuries later the active ingredient was found to be salicilin, which in the body gets converted to salicylic acid that binds a pocket in cyclooxygenase leading to its irreversible inhibition and thereby shutting down prostaglandin synthesis. The identification of the binding site also led to the discovery of the highly effective COX-2 inhibitors.

Some of the major lipids involved in the inflammatory response are prostaglandins, leukotrienes and thromboxanes all of which are metabolites of arachidonic acid.

Arachidonic acid is produced by the hydrolysis of phosphatidylcholine containing arachidonic acid at the Sn2 position by the action of $cPLA_2$. Upon receipt of an inflammatory stimulus a whole cascade of signaling events ultimately lead to the increase in intracellular Ca^{+2} through the opening of store operated calcium channels. This leads to the activation of a whole host of lipid enzymes which include PKC, CERK, 5-lipoxygenase and prostaglandin H_2 synthase (PGH_2) thus priming the cell for the inflammatory cascade. $cPLA_2$ is activated by Ca^{+2} which neutralizes charges on the enzyme allowing it to bind PC rich membranes. This association is further enhanced by the action of ceramide kinase which produces C1P that increases the residence time of $cPLA_2$ once it binds membranes. In addition multiple protein kinases phosphorylates $cPLA_2$(22) which further supports its movement to the golgi peri nuclear region. Upon binding membranes, the activated $cPLA_2$ hydrolyses PC containing AA at the Sn2 position thus liberating AA. AA takes part in further metabolism to produce prostaglandins, thromboxanes and leukotrienes. These eicosanoids give rise to the classical features of inflammation and promote a wide range of disease states including chronic inflammation, allergy, cardiovascular diseases and cancer(23). Eicosanoids act extracellularly through GPCR. These inflammatory mediators promote bronchial constrictions, increased vascular permeability and diameter and the invasion of leukocytes which when in excess cause tissue destruction in late allergy and inflammation(24)

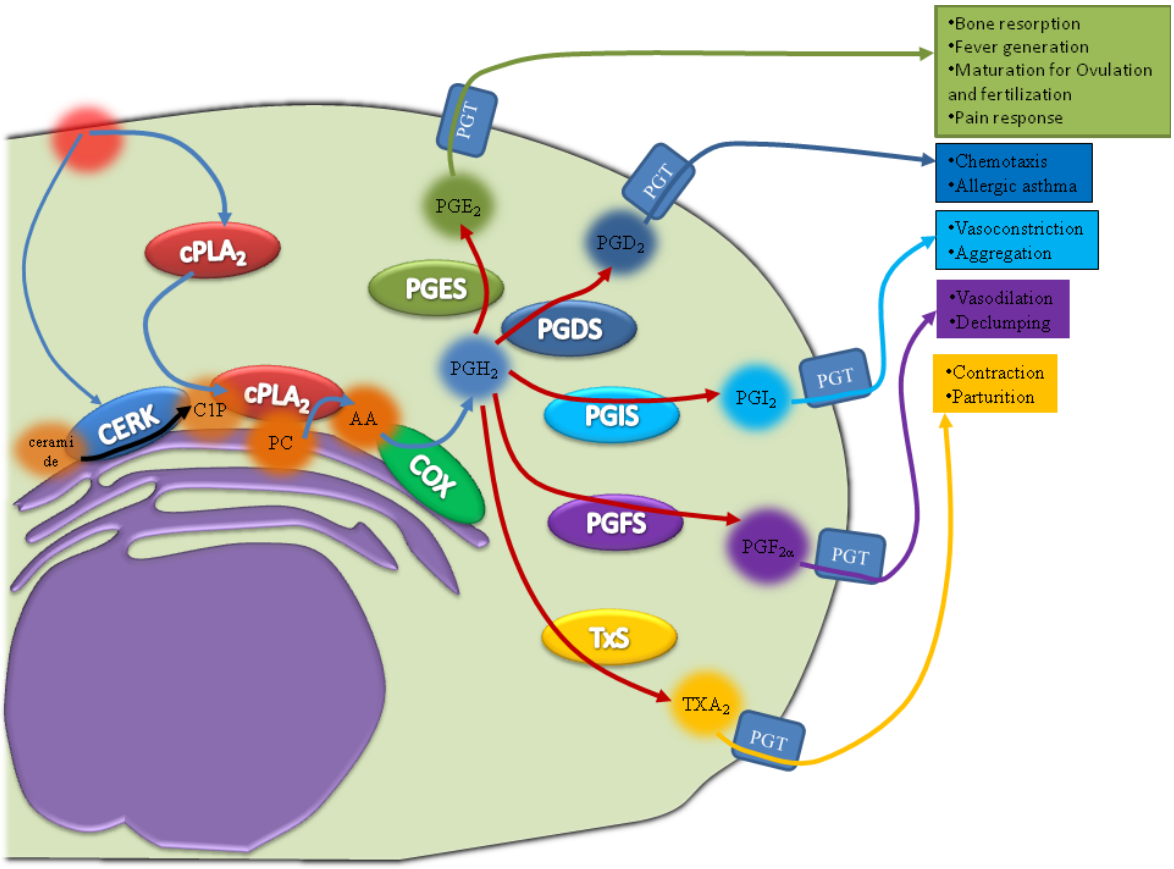

Figure 2. Biosynthesis and Biological effects of the various prostaglandins. Upon the receipt of a stimulus cPLA$_2$α is translocated from the cytoplasm to the golgi membrane where it liberates arachidonic acid from PC. This AA is then acted upon by the various prostaglandin and thromboxane synthases to produce the various prostaglandins and thromboxanes that in turn give rise to a multitude of biological responses.

CHAPTER 1: Ceramide Kinase and Ceramide-1-Phosphate

INTRODUCTION

The sphingolipid, C1P, is a direct metabolite of ceramide produced in the mammalian cells. The only known pathway for it's synthesis at present is via the phosphorylation of ceramide by ceramide kinase (CERK) (Figure 1). CERK was first described as a lipid kinase found in brain synaptic vesicles in 1989 by Bajjalieh and coworkers (25). This research group demonstrated that this activity was specific for the conversion of ceramide to C1P without effects on the closely related glycerol lipid, diacylglycerol (25). Just months after this initial finding, Kolesnick and coworkers reported the existence of C1P in human leukemia (HL-60) cells (26). They demonstrated that during stimulation, C1P was produced from ceramide derived from sphingomyelin, but not from glycosphingolipids. Later the same year, Kolesnick and coworkers also reported a CERK activity distinguishable from diacylglycerol kinase (DGK) activity in HL-60 cells verifying the findings of Bajjalieh and coworkers (27). To date, in mammalian cells, C1P has only been shown to be derived from the phosphorylation of ceramide by a specific CERK activity.

In 2002, the cDNA sequence for CERK was cloned by Sugiura and coworkers from Jurkat acute T-cell leukemic cells (19). The enzyme was found to be mainly expressed in heart, kidney, brain, and hematopoietic cells (19). Human CERK was also found to be a 537

amino acid protein closely related in structure and amino acid homology to sphingosine kinase 1 (SphK1) and 2 (SphK2). CERK was found to contain the five conserved domains (C1-C5) previously identified for SphK1 and 2. The first three of these domains, C1-C3, are found within a putative diacylglycerol kinase domain (DGK domain) (amino acids 126-342). The C4 region consists of a short 28 amino acid stretch designated the central homology region located just after the DGK catalytic domain, and the C5 region (amino acids 385-537) is located in the C-terminus of the enzyme (19) (Figure 1.1).

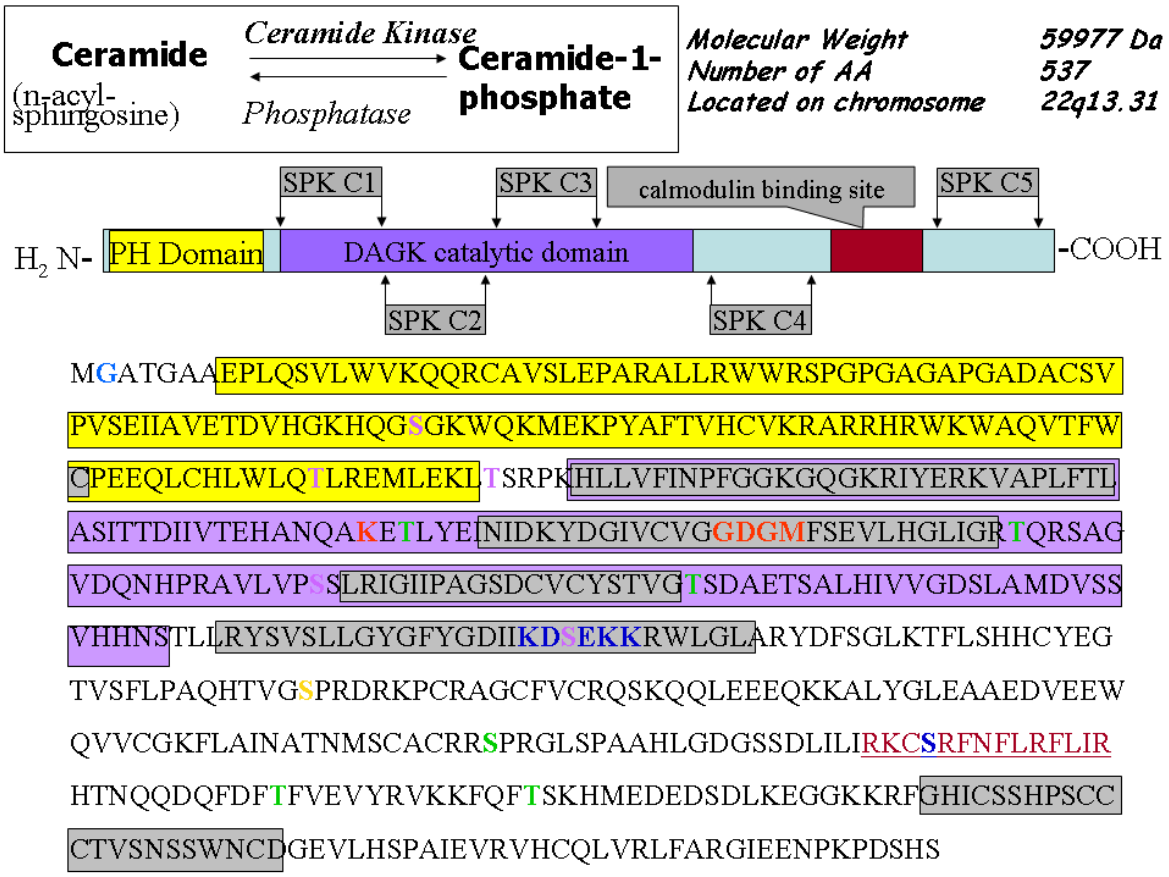

Figure 1.1: Important structural features of CERK: Schematic representation of the domain structure and conserved sequences of CERK with the corresponding primary structure. PH-Domain; Pleckstrin Homology domain (yellow), DAGK catalytic domain; diaclyglycerol kinase catalytic domain (purple), SphK C1 to C5 conserved regions within CERK (grey), calmodulin binding region (maroon).

REGULATION OF THE ACTIVITY OF CERAMIDE KINASE

CERK also contains additional conserved regions across several species (*M. musculus*, *D. melanogaster*, *C. elegans*, and *O. sativa*). These include a PH-domain in its N-terminus known to bind the β/γ subunit of heterotrimeric G-proteins, phosphoinositol-4,5-bisphosphate, and phosphorylated tyrosine residues (19). CERK is a calcium stimulated enzyme. However there are no binding sites for Ca^{+2} on CERK but contains a calcium/calmodulin binding motif of the 1-8-14 type B spanning residues 422-435 ((F/I/L/V/W) XXXXXX (F/A/I/L/V/W) XXXXX (F/I/L/V/W) with a net charge of $^{2+}$ to $^{4+}$) (19). These conserved domains have been shown to play a regulatory function for the enzyme. For example, Igarashi and coworkers and Bornancin and coworkers have both demonstrated that the PH-domain is required for the activity of CERK *in vitro* as well as proper localization of the enzyme in cells (28, 29). In regards to the calmodulin binding motif, Igarashi and coworkers recently demonstrated that calmodulin interacts with CERK and acts as a calcium "sensor" for the enzyme (30). Thus, these conserved domains play distinct roles in regulating CERK activity *in vitro* and in cells.

CERK has several putative phosphorylation sites of which some are highly conserved (Table 1). Treatment of A_{549} cells transfected with recombinant CERK has shown CERK to be phosphorylated in response to PKC and PKA agonists (Figure 1.1)

Table 1.1: Putative phosphorylation sites on CERK

Protein Kinase	Putative phosphorylation site
PKC	S^{72*}, T^{118*}, T^{127*}, S^{230*}, S^{300***}, S^{340*}
PKA	S^{424**}

* Conserved in mouse CERK
**Conserved in both mouse and drosophila CERK.
***Conserved in SPHK of all multicellular organisms

Another less understood mechanism of regulation of CERK is via lipid co-factors a. It has been known for quite some time that cardiolipin was able to activate CERK and in fact in its absence the *in vitro* activity of the enzyme is absent. A literature survey revealed that the motif KNKEKK is capable of binding cardiolipin (31). A similar motif (KDSEKK-Figure 1.1) is present on CERK that may have a role in binding to cardiolipin. The serine found on this (S^{300}) sequence is highly conserved in all eukaryotes and is a putative PKC phosphorylation site. CERK has been shown to be phosphorylated in response to the PKC agonist PMA and also in response to forskolin (Figure 1.2). Site directed mutagenesis of the S^{300} to E resulted in a complete loss of enzyme activity where as it's mutagenesis to A did not affect the enzyme activity by much (Figure 1.3).

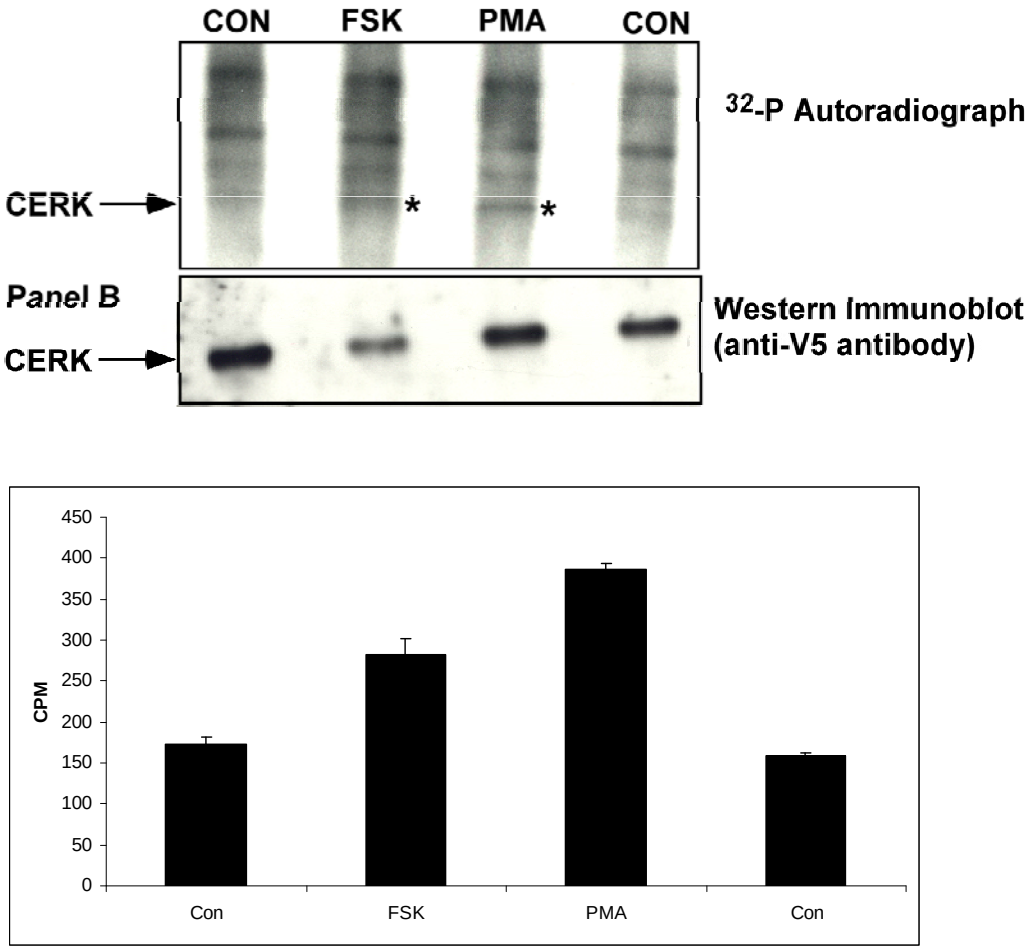

Figure 1.2: CERK is phosphorylated in response to PKA agonist forskolin and PKC agonist phorbol myristoyl acetate. A_{549} cells transfected with 6X His and V5 tagged CERK were treated with either the pan PKC agonist PMA or the PKA agonist forskolin. The cells were lysed and ceramide kinase was subjected Ni-NTA purification. The proteins were separated by SDS PAGE and subjected to autoradiography. In a parallel gel was subjected to western blotting to confirm the presence of CERK. Following autoradiography the P^{32} labeled CERK bands were excised and counted by scintillation.

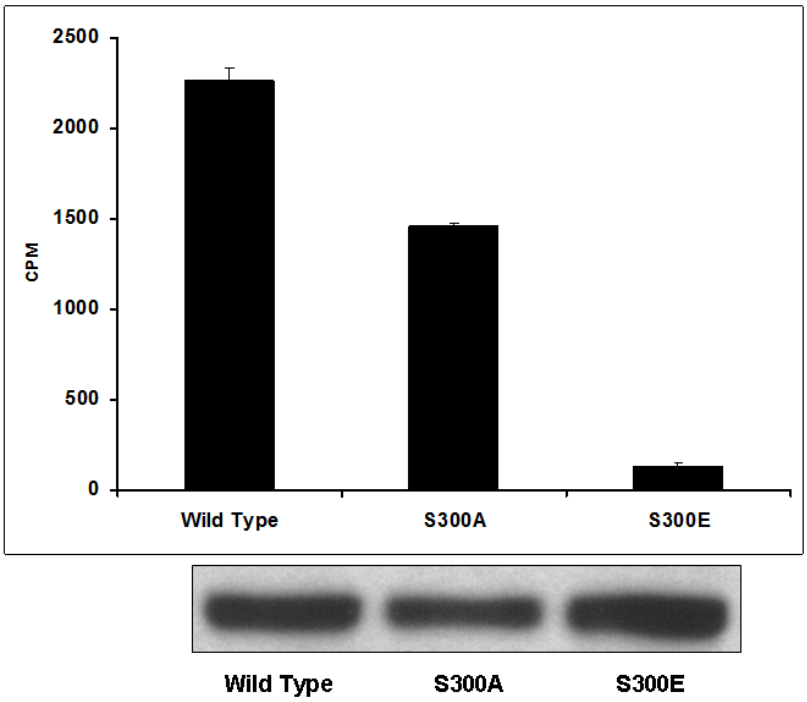

Figure 1.3: Serine 300 is a possible regulator of activity of CERK. A549 cell lysates were tested for ceramide kinase activity following transfection with wild type, S300A or S300E mutants of CERK. Western analysis revealed similar levels of recombinant CERK present in the lysates.

BIOLOGICAL ACTIVITIES ATTRIBUTED TO C1P

In the last few years, a large number of reports have demonstrated distinct biological mechanisms regulated by C1P. For example published findings from our laboratory demonstrated that C1P is a direct activator of $cPLA_2\alpha$ through interaction with the C2/CaLB domain (32). These results coupled with the previous findings that CERK/C1P pathway is required for PLA_2 activation in response to calcium ionophore and cytokines (33) demonstrated that C1P is a "missing link" in the eicosanoid synthetic pathway. Mechanistic studies demonstrated that the interaction of C1P and $cPLA_2\alpha$ was very specific as closely-related lipids and metabolites were unable to activate $cPLA_2\alpha$ *in vitro* and in cells (32, 34). Furthermore, these studies demonstrated that C1P interacted with $cPLA_2\alpha$ in the C2 domain via a novel and previously undescribed interaction site. Lastly, the studies also defined the mechanism of $cPLA_2\alpha$ activation: 1) decreasing the dissociation constant of $cPLA_2\alpha$ with membranes, and 2) acting in a manner similar to a positive allosteric activator (34). A role for CERK and its product, C1P, in a separate pathway of allergic/inflammatory signaling has also been recently reported in mast cells. Igarashi and coworkers demonstrated that treatment of RBL-2H3 cells or overexpression of CERK in these cells enhanced the degranulation induced by A23187 (35).

Another biological mechanism regulated by CERK and C1P was demonstrated by Shayman and coworkers. Specifically, they demonstrated that CERK was activated in the context of phagocytosis in neutrophils after challenging the cells with formyl peptide and

antibody-coated erythrocytes (FMLP/EIgG) (36). Thus, these data demonstrated that C1P may play a distinct role in membrane fusion possibly explaining the early finding that high levels of C1P are found in synaptic vesicles (25).

The first report of a biological effect for C1P was by Brindley, Gomez-Munoz, and coworkers. They demonstrated that short chain (not naturally found in cells) C1P induced DNA synthesis in Rat-1 fibroblasts (37). Later, Gomez-Munoz and coworkers also demonstrated that treatment of T17 fibroblasts with natural ceramide-1-phosphate induced a potent increase in DNA synthesis and the levels of proliferating nuclear antigen (38). The most recent report was from the Gomez-Munoz laboratory demonstrating that C1P prevented cell death in bone marrow-derived macrophages (BMDMs) after withdrawal of macrophage colony-stimulating factor (M-CSF)(39). Treatment of these cells with C1P effectively blocked the activation of caspases and prevented DNA fragmentation upon serum removal. In the same study, they also demonstrated that C1P treatment inhibited ceramide generation from acid sphingomyelinase (A-SMase). Lastly, A-SMase was shown to be a direct target of C1P inducing inhibition of this enzyme(39).

In conclusion, C1P and ceramide kinase have recently been shown to play significant biological roles in a variety of cell signaling cascades. In this chapter, we describe the methodologies for examining CERK function and C1P-specific effects *in vitro* and tissue culture systems.

RECOMBINANT EXPRESSION OF CERK

Principle

Production of CERK of sufficient quantity and purity is essential for producing consistent and reproducible results for *in vitro* kinetic analysis. Currently, there are several ways to purify endogenous CERK. The first method was described by Bajjalieh and coworkers using membrane synaptic vesicles from rat brains(25). A second method involves extracting the membrane fractions that are generally high in CERK activity. Neither method produces CERK of sufficient purity or quantity for detailed kinetic analysis. In addition, there is currently an absence of an antibody for efficient immunoprecipitation of the enzyme. Recently, our laboratory has demonstrated that the use of recombinant technology is an option available to obtain CERK of sufficient quantity and purity for *in vitro* kinase assays.

For large scale production of recombinant CERK, baculoviral-mediated expression in insect cells is recommended for several reasons. First, the post-translational modifications of insect cells are comparable to that of mammalian cells (Kost *et al*., 2005; Possee, 1997). This allows for CERK to be obtained in a form that resembles mammalian CERK. Second, insect cells can be cultured in large quantities allowing for large scale purification of CERK. Third, bacterially-expressed CERK may be contaminated by non-specific lipid

kinases due to aggregation unlike the use of baculovirus. Adenoviral-mediated expression of CERK is also the method of choice for the expression of CERK in human cell lines. However, adenoviral-mediated gene expression allows only for the transient expression of CERK as the adenoviral genome does not get incorporated into the genome. Furthermore, large quantities of recombinant CERK from human cells is costly in comparison to insect cells.

Reagents

Sf-9 cells and SF-900 media were obtained from Invitrogen Corporation. *Sf-9* cells are stored in liquid nitrogen and the media is stored at 4°C until use. pBlueBac4.5/V5-His-TOPO® vector, the pBlueBac4.5/V5-His-TOPO® TA kit, pcDNA™ 3.1D/V5-His-TOPO, pcDNA™3.1 Directional TOPO® Expression Kit and Back-n-Blue™ DNA were obtained from Invitrogen Corporation and are stored at -20°C. Cellfectin® was also obtained from Invitrogen Corporation and is stored at 4°C. The pTRE Shuttle vector and BD Adeno-X™ Tet-Off Expression system 1, were purchased from Clontech and is stored at -20°C until use. MOPS, KCl, glycerol, Triton X-100, Imidazole, and PMSF are obtained from Sigma-Aldrich and is stored at room temperature. Aprotinin, Leupeptin, and Pepstatin were also obtained from Sigma-Aldrich. These are stored at -80°C. DTT was also obtained from Sigma-Aldrich and upon receipt a 500 mM solution is made, aliquoted and stored at -80°C. Ni-NTA resin was obtained from Qiagen Corporation. XK columns are purchased from

Amersham Biosciences. Anti-6XHis and Anti-V5 antibodies were obtained from Santa Cruz Biotechnology and are stored at 4°C.

Buffers

Cell Lysis buffer:

10 mM MOPS, pH 7.2, 150 mM KCl, 10% Glycerol, 0.5% Triton X-100, 0.001 mg/ml Leupeptin, 0.01 mg/ml Aprotinin, 0.005 mg/ml Pepstatin, 1 mM PMSF

Buffer A for Ni-NTA His purification (Ni-NTA wash buffer):

10 mM MOPS pH 7.2, 150 mM KCl, 10% Glycerol

Buffer B for Ni-NTA His purification:

10 mM MOPS pH 7.2, 150 mM KCl, 10% Glycerol, 250 mM Imidazole

Dialysis buffer:

10 mM MOPS pH 7.2, 150 mM NaCl, 2 mM EGTA, 50% glycerol, 1 mM DTT

RECOMBINANT EXPRESSION OF CERK IN INSECT CELLS.

Ceramide kinase was PCR amplified (high fidelity) from an A549 cDNA library and then cloned into pBlueBac4.5/V5-His-TOPO® vector using the pBlueBac4.5/V5-His-TOPO® TA expression kit. The cDNA was verified by sequence analysis. To produce CERK baculovirus, this CERK plasmid is transfected into *sf9* insect cells simultaneously with Back-n-Blue^{TM} DNA using Cellfectin® transfection reagent in serum free medium following the manufacturers recommended protocol. Recombinant viral genome is produced through homologus recombination leading to the production of infective baculoviral particles. The recombinant virus is identified by the presence of blue plaques in the presence of X-gal. The viral particles from the individual blue plaques are used to infect new *sf9* cells growing in separate wells of 12 well plates. DNA is extracted from a portion of the resultant P0 viral stock and PCR amplified for 15 cycles (94°C, 30s; 58°C, 30 s; 72°C, 1 min) using the primer pair 5'-TCGTCTGTGTCGGCGGAGAT-3' and 5'-CTTTGCCACCAACCCAGAACG -3' to verify the presence of the sequence of interest. The primers cross one exon/intron boundary eliminating the possibility of amplifying contaminating genomic DNA from *Sf-9* cells. Presence of a 355 bp band upon gel electrophoresis of the PCR product verifies the presence of CERK in the viral genome. The remaining P0 viral stock from PCR verified viral particles are then amplified twice to produce 1 L of P2 viral stock. This viral stock is titered by endpoint dilution and is used to infect *sf9* cells at a density of 1.2-1.5x10^6 cells/ml in a 50 ml culture. Optimal transfection/expression is determined at 1 MOI of baculovirus for 72 hours post infection. The cells are harvested by centrifugation at 400xg.

RECOMBINANT EXPRESSION OF CERK ADENOVIRUS IN MAMMALIAN CELLS.

Ceramide kinase cDNA library was obtained from an A549 cDNA library using high fidelity PCR and cloned into pcDNA™3.1D/V5-His-TOPO® vector using the pcDNA™3.1 Directional TOPO® expression kit. CERK expression in the adenoviral genome was carried out using BD Adeno-X™ Tet-Off Expression system. CERK with V5 and 6XHis tags (on C-terminus) was excised from the pcDNA vector using BamHI and PmeI and inserted into the pTRE Shuttle vector. Recombinant CERK containing the adenoviral expression cassette was excised from pTRE shuttle and ligated to Adeno-X™ viral DNA according to manufacturer's protocol and amplified in *E. coli*. After amplification in *E. coli*, the recombinant CERK adenovirus is obtained by transfection of the linearized adenoviral genome containing the recombinant CERK expression cassette into HEK 293 cells, and the recombinant adenoviral particles produced are harvested according to manufacturer's protocol. Cotransfection of mammalian cells with these adenoviral particles along with the Adeno Tet-Off® regulatory virus allows for the transient overexpression of CERK in mammalian cells. Optimal transfection/expression is determined at 150 MOI each of Adeno-CERK and Adeno Tet-Off® virus infecting 2 x 10^6 A549 cells growing in 15 cm plastic culture dishes in normal A549 media (DMEM/RPMI containing 10% serum and 2% Penicillin/Streptomysin). The cells are exposed to the virus for 48 hrs and then harvested for CERK purification.

PURIFICATION OF RECOMBINANT CERK.

Recombinant CERK expressed in either of above methods can be purified using Ni-NTA affinity column chromatography. Large scale purification of baculoviral-mediated CERK expression in *Sf-9* cells is recommended. The following protocol was used for large scale purification of CERK from infected *Sf*-9 cells. The cell paste is suspended in ten volumes of lysis buffer, and cells lysed by douncing 10 times per sample using a dounce homogenizer with a type B pestle. 100 ml sample is used at a time and kept chilled on ice. The lysates are then centrifuged at 16,000xg for 45 minutes at 4 °C. Simultaneously, 100 ml of Ni-NTA superflow resin is equilibrated in 5 column volumes of Ni-NTA wash buffer. The supernatant is then batch bound with the equilibrated Ni-NTA for 1.5 hours at 4 °C with nutation. The resin is then transferred to a 5 cm XK column, and the column is washed until baseline absorbance at 280 nm with Ni-NTA wash buffer at 4 ml/min flow rate using fast protein liquid chromatography (FPLC). Thereafter, the column is washed with a 19.5 mM imidazole wash buffer at 4 ml/min until baseline absorbance at 280 nm. CERK is eluted from the column using 250 mM imidazole in Ni-NTA wash buffer at 5 ml/min flow rate collecting the elutions in fractions. The eluted fractions are analyzed by SDS PAGE to assess the purification and by western blotting to identify the presence of recombinant CERK using Anti-His and Anti-V5 antibodies. All fractions containing CERK are pooled, and DTT is added to a final concentration of 1 mM. The pooled samples are dialyzed against the dialysis buffer overnight at 4 °C with stirring using dialysis tubing

with a 12-14,000 molecular weight exclusion. The dialyzed sample is centrifuged at 31,000xg to remove any precipitant, and the total protein is quantified by Bradford assay. The protocol yields recombinant CERK that is 60-70% (Figure 2) pure with a specific activity of approximately 0.19 (µmol C1P produced/min/mg protein) towards D-*erythro*-$C_{16:0}$ ceramide (Figure 3). Glycerol is added to the pooled samples to 50%. The samples are then aliquoted and stored at -80 °C. Under these conditions CERK is stable for approximately 1 year. Note: For mammalian cells the same protocol can be utilized, but a type A pestle or sonication is recommended for cell lysis. Furthermore, this is a one day procedure. The enzyme needs to be purified and stored at -80°C as soon as possible for stability purposes.

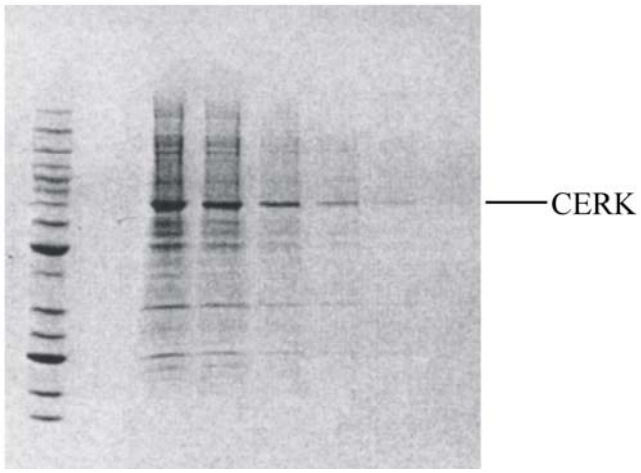

Figure 1.4: SDS PAGE analysis of Ni-NTA purified CERK from *Sf-9* cells: Cell lysates were subjected to purification by 6XHis Ni-NTA purification. The pooled fractions with the highest levels of CERK were dialyzed overnight against the storage buffer. An aliquot of purified CERK was separated on a 10% SDS-PAGE gel followed by coomassie staining to visualize the purity of the protein. Lane 1: BenchMark Protein ladder, lane 2: 15 µg protein, lane 3: 10 µg protein, lane 4: 5 µg protein, lane 5: 2.5 µg protein.

IN VITRO KINETIC ANALYSIS OF CERK ACTIVITY USING MIXED MICELLAR ASSAYS

Principle

For the following assays D-*erythro*-$C_{16:0}$ ceramide and adenosine triphosphate (ATP) are routinely utilized for kinetic analysis. However, in terms of solubility, D-*erythro*-$C_{18:1}$ ceramide is more soluble and better suited for measuring endogenous CERK activity *in vitro*. In the methods described here, the activity of CERK was assayed by measuring the levels of ceramide-1-phosphate formed using a detergent micelle system for substrate presentation. Since endogenous CERK acts on membrane lipids, the presentation of its substrate in this form compatible to a biological membrane is appropriate. When studying the activity of CERK, one has to take into account the enzymes diffusion in a 3D cellular matrix (locating the membranes) and the diffusion in 2D (locating and utilizing its substrate in the membrane) bound to the membrane. Thus, the true kinetic behavior of the enzyme is best studied using a model that takes into account both bulk and surface diffusion. Surface dilution kinetics, first introduced in 1973 by Dennis, is an excellent means of studying this type of enzyme behavior *in vitro*. This technique can be coupled to both detergent micelles and lipid vesicles, but the use of vesicles as a mean of delivering the substrate is not suitable for the study of kinetics of CERK for several reasons. First, the number of substrate molecules per vesicle is not constant. Second, substrate molecules in

the inner membrane are not accessible to the enzyme. Lastly, mixed vesicles lack uniformity in size. Mixed micellar assays are better suited for the study of kinetics in being uniform in size with the same number of substrate molecules being present in each micelle. Thus, mixed micellar assays are the method of choice for *in vitro* assays when studying the kinetics of CERK.

β-octylglucoside and Triton X-100 are the two published methods for the presentation of substrate to CERK as mixed micelles (40, 41) β-octylglucoside based method is the traditional method used in the assay of CERK (40). This system would be ideal for investigating substrates of ceramide. However, molecular modeling studies have shown micelles of β-octylglucoside to have an irregular surface (42), thereby preventing equal presentation of all substrate molecules to the enzyme. This tends to be a drawback when studying the kinetics of a lipid kinase. Also compared to Triton X-100, β-octylglucoside has a very high CMC, thus the amount of detergent required to achieve CMC is about 100 times greater.

Compared to β-octylglucoside method, Triton X-100 micelles provide several advantages. First, they provide an inert surface for CERK. Second, the size of the micelles is relatively independent of ionic strength and temperature within the physiological range (43-45). Third, mixed micelles up to 20 mol% phospholipids are similar in structure to pure Triton X-100 micelles, but proportionally larger (43-45). Lastly, pure Triton X-100 micelles do not coexist with mixed micelles. Thus, Triton X-100 is an excellent method of choice in

the assaying of CERK activity. Both the β-octylglucoside and Triton X-100 assays are detailed below.

Reagents

CERK was prepared as mentioned above using baculoviral-mediated expression followed by Ni-NTA 6XHis purication. Triton X-100 was obtained from Pierce Biotechnology as a 10% solution (~155 mM). D-*erythro*-$C_{16:0}$ ceramide was from Avanti Polar Lipids. Upon receipt a 0.82mM solution is prepared by dissolving in $CHCl_3$ and is stored at -20 °C until use. Cardiolipin also was obtained as a 6.67 mM solution in $CHCl_3$ from Avanti Polar Lipids and is stored at -20°C upon receipt. MOPS, NaCl, DETAPAC, and glycerol were obtained from Sigma-Aldrich and are stored at room temperature. DTT was also from Sigma-Aldrich and upon receipt a 500 mM solution is made and stored at -80°C. TLC plates were purchased from VWR and are stored desiccated at RT. 13x100 mm borosilicate glass tubes were obtained from Fisher Scientific.

Buffers

Reaction buffer for β-octylglucoside assay:

20 mM MOPS, pH 7.2, 50 mM NaCl, 1 mM DTT, 3 mM $CaCl_2$, 51.24 mM β-octylglucoside, 1 mM cardiolipin, and 0.2 mM diethylenetriaminepentaacetic acid

Reaction buffer for Triton X-100 assay:

20 mM MOPS, pH 7.2, 50 mM NaCl, 1 mM DTT, 3 mM $CaCl_2$, 1 mM cardiolipin, and 0.2 mM diethylenetriaminepentaacetic acid

Experimental Procedures

1. Solubilization of ceramides.

a. β-octylglucoside methods

First described by Bajjalieh and coworkers, this method utilizes the β-octylglucoside as the micelle detergent (25). octlyglucoside is nonionic detergent that forms micelles of 27 molecules each at a critical micellar concentration of 23-25 mM. Micelle solubilization of ceramide in this method is carried by sonicating ceramide in reaction buffer. The preparation of β-octylglucoside micelles for CERK assay is described below.

25 mg of cardiolipin is dried under a stream of dry nitrogen gas followed by dissolving in 3.333 ml water containing 256 mM β-octylglucoside and 1 mM DETAPAC to obtain a 5 mM cardiolipin solution. To prepare the reaction buffer, 160 µl of this solution was mixed with MOPS, NaCl, $CaCl_2$ and DTT such that the final concentrations are 20 mM MOPS (pH 7.2), 50 mM NaCL, 1 mM DTT, 3 mM $CaCl_2$, 51.24 mM β-Octylglucoside, 1 mM Cardiolipin and 0.2 mM DETAPAC. 640 nmol ceramide is dried down under a stream of

dry nitrogen gas followed by micellar solubilization in 720 µl of the above reaction buffer. A Misonix 3000 probe sonicator with a microtip probe (tip diameter of 3mm) is used in the sonication (using three pulses of 1 minute duration with 10 second intervals in between, on ice). 180 µl of this mixture is used per reaction as explained below.

b. Triton X-100 method.

First described for CERK by Wijesinghe *et al.*, this method uses the nonionic detergent Triton X-100 for the preparation of mixed micelles (Wijesinghe *et al.*, 2005). Triton X-100 differs from β-octylglucoside in having 140 molecules per micelle and a CMC of 0.24 mM. The preparation of Triton X-100 mixed micelles containing D-*erythro*-$C_{16:0}$ ceramide at its K_m^b (0.36 mol%) and cardiolipin is described below.

43.35 nmol ceramide is dried down with 250 nmol cardiolipin under a stream of dry Nitrogen gas. 5.75 µmol Triton X-100 in water is then added to the dried lipids such that the final volume is 500 µl and the final concentrations are 8.67 µM ceramide, 0.5 mM cardiolipin and 11.5 mM Triton. A Misonix 3000 probe sonicator with a microtip probe (tip diameter of 3 mm) is used to sonicate this mixture. Sonication is carried out on ice using three pulses of 1 minute duration with a 10 second resting interval (on ice) in between each pulse. 40 µl of this mixture containing the mixed micelles is added to 140 µl of reaction buffer (20 mM MOPS, pH 7.2, 50 mM NaCl, 1 mM DTT, 3 mM $CaCl_2$, and 0.2 mM diethlenetriaminepentaacetic acid) for a total volume of 180 µl.

In both methods, care must be taken to prevent the ceramide solution from heating. This is achieved by carrying out the sonication on ice. Also “frothing” of the mixture must be avoided at all costs. The mixed micelles, thus prepared, can be kept on ice up to a day. It is recommended that they not be stored for longer.

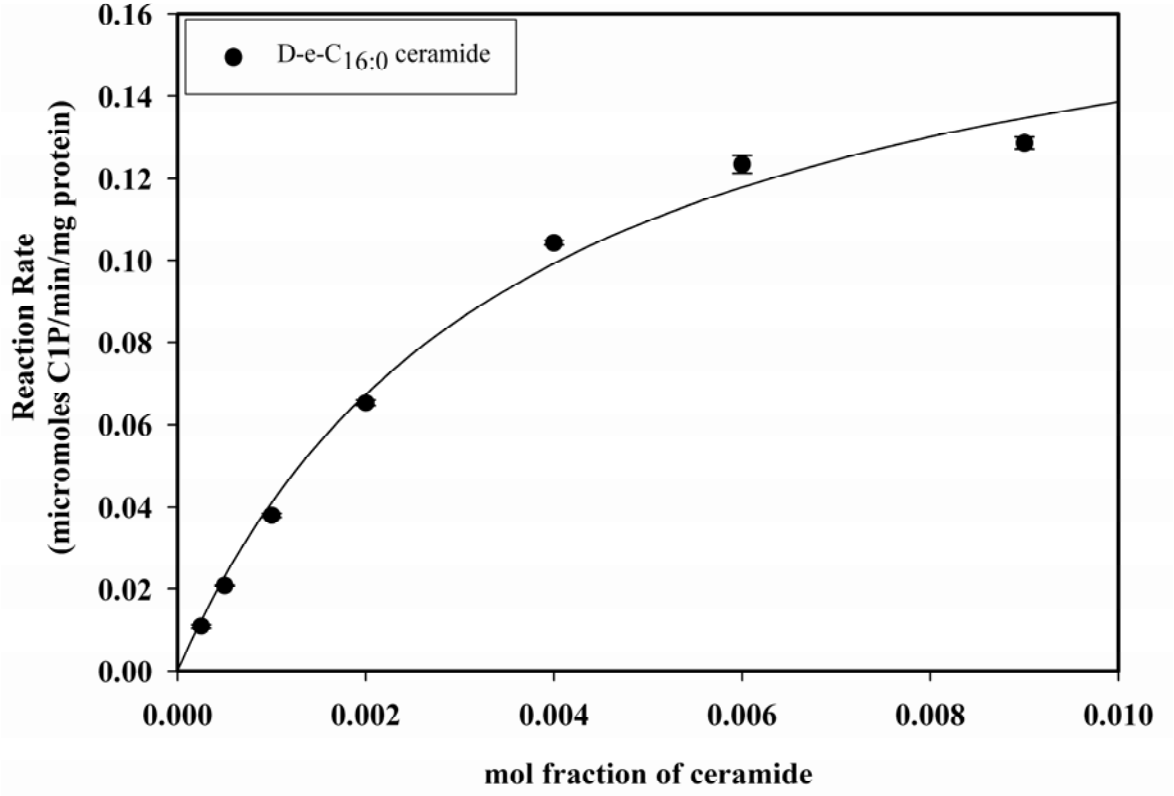

Figure 1.5. Surface dilution kinetics for CERK using Triton X-100 mixed micellar assay: Michaelis-Menten curve for D-*erythro*-$C_{16:0}$ ceramide assayed at 0.025, 0.05, 0.1, 0.2, 0.4, 0.6, 0.9, and 1.4 mol%. The graph depicts micromoles of C1P produced per minute per milligram of CERK (baculovirus-expressed) versus the mole fraction of ceramide to obtain V_{max} and K_m [b]. Data are presented as means SEM and are representative of three separate determinations.

2. Ceramide Kinase Assay.

Reactions are carried out in 13x100 mm borosilicate glass tubes. 180 µl of micellar solubilized ceramide in reaction buffer from either the a or b sections above is used in the reaction. Recombinant/purified ceramide kinase is diluted to 0.1 µg/µl in lysis buffer (if using unpurified cell lysates from CERK overexpressed cells, the crude lysate is diluted 1 µg/µl in lysis buffer). 10 µl of the diluted CERK is added to each reaction, mixed by gently pipetting up and down and incubated at 37 °C for 10 minutes. The reaction is then started by the addition of 10 µl of ATP from a stock solution of 20 mM such that the final concentration is 1 mM (the total reaction volume is 200 µl). The mixture is incubated at 37°C for 15 minutes and the reaction is stopped by the addition of 1.2 ml 1:1 v/v $CHCl_3$:MeOH. Thereafter, 500 µl of 1 M KCl in 20 mM MOPS (pH 7.2) is added followed by vigorous vortexing and separation of phases by centrifugation at 250xg.

3. Quantification of the C1P produced:

There are three different methods used in the quantification of C1P produced *in vitro* in the above reaction. They are quantification using TLC (Bielawska *et al*., 2001), quantification by direct scintillation counting (Bectas *et al*., 2003) and quantification using mass spectrometry (ESI-LC/MS/MS) (Merrill *et al*., 2005). The first two methods involve labeling a portion of C1P produced using [γ-^{32}P] ATP, and the reaction is started by adding

a mixture of labeled and unlabelled ATP such that final concentration in the reaction is 0.05 μCi and 1 mM ATP. The TLC method, while being time consuming and cumbersome, allows for the elimination of any other contaminating lipid species (radiolabeled) from contributing to the total radioactivity assayed producing for more accurate results. This technique is best suited for instances where tissues levels of active ceramide kinase are to be investigated. The direct scintillation counting method is a faster method of analyzing CERK activity. However, any other lipid radiolabelled by contaminating lipid kinases will also be present. Thus, this method is best suited for instances where the enzyme is highly expressed such that contribution from other lipid kinases are negligible, or when using purified CERK.

Another method of quantifying CERK activity is ESI LC/MS/MS. The main advantage of ESI LC/MS/MS method is the ability to assay C1P levels without using hazardous radioactive material. This allows for the reactions to be carried out on any laboratory bench without shielding. The high selectivity of the method allows for separation of C1P from other lipid phosphates, from the activity of other lipid kinases and lipid substrates. Thus, the technique is good for measuring CERK activity in tissues as well. However, in terms of sensitivity, the radiolabeled assays are currently superior to mass spectrometric assays.

a) Quantification by thin layer chromatography

An aliquot of the organic phase is spotted on a TLC plate, and lipids are separated in chloroform/acetone/methanol/acetic acid/water (10:4:3:2:1, v/v). Radioactive bands are visualized with a phosphoimager (Bio-Rad), and [^{32}P]-ceramide-1- phosphate is quantitated by densitometry or scintillation counting. (See Table 1 for R_f values of various C1P species)

Table 1.2: *R*f Values for Lipid Standards Resolved in Solvent System: Chloroform–Acetone–Methanol–Acetic Acid–Water (10:4:3:2:1; v/v) (*Bielawska et al.*, *2001)*

Standards	*R*F value
D-e-C2:0 ceramide phosphate	0.36
D-e-C6:0 ceramide phosphate	0.49
D-e-C12:0 ceramide phosphate	0.58
D-e-C14:0 ceramide phosphate	0.61
D-e-C16:0/D-e-C18:0 ceramide phosphate	0.63
D-e-C24:0/D-e-C24:1 ceramide phosphate	0.68
D-e-C2:0 dihydroceramide phosphate	0.37
D-e-C6:0 dihydroceramide phosphate	0.53
D-e-C16:0/D-e-C18:0 dihydroceramide phosphate	0.68
a-OH-D-e-C6:0 ceramide phosphate	0.40
C26:0 phytoceramide phosphate	0.63
a-OH-C24:0 phytoceramide phosphate	0.51

b) Quantification by direct scintillation counting.

After the reaction is stopped the organic layer is washed 4 times using 500 µl of 1M KCl in 20 mM MOPS (600 µl). The amount of C1P produced is quantified by counting 100 µl organic phase using a Beckman-Coulter LS 6500 scintillation counter. The presence of C1P can be confirmed by TLC as detailed above in section A.

c) Quantification using electron spray ionization liquid chromatography tandem mass spectrometry (ESI LC/MS/MS)

To the organic phase obtained from above, a known quantity of internal standard, ideally an unnatural C1P (e.g. C_{12} C1P or C_{17} C1P) is added. The organic phase is then dried, and the residue is brought up in sample buffer (Merrill, *et al.*, 2005). The C1P produced can be identified and quantified by MRM using either $[M+H]^+$ (molecular ion) , and 264.4 (ceramide) ion pair in the positive ion mode, or $[M-H]^-$ (molecular ion) and 78.9 (phosphite) ion pair, in the negative mode. More information on mass spectrometric analysis of CERK can be found in Chapter 4.

CHAPTER 2: SUBSTRATE SPECIFICITY AND KINETIC ANALYSIS OF HUMAN CERAMIDE KINASE

INTRODUCTION

Understanding of the important role played by sphingolipids in the regulation of intracellular processes began with the discovery by Hannun *et al* (46) of the inhibition of protein kinase C (PKC) by sphingosine. Since then ceramides and a number of its metabolites have been identified to regulate important cellular processes by regulating the activity of key regulatory enzymes (47-54). These include specific serine threonine kinases (27, 52), protein phosphatases (55), PKCξ (56), Jun nuclear kinases (JNK) (57, 58), mitogen-activated protein kinases (MAPK) (39, 40), phospholipase A_2 (PLA_2) (59), phospholipase D (PLD) (42, 43) and protein kinase B (PKB) (60, 61).

The interconvertable ceramide-derived metabolite, ceramide-1-phosphate (C1P) is emerging as an important biological mediator. In mammalian cells, C1P is produced by the phosphorylation of ceramides. To date, CERK is the only enzyme known to catalyze this reaction in mammals, and CERK was first described as a lipid kinase found in brain synaptic vesicles by Bajalieh and coworkers (62). CERK is a calcium-dependent lipid kinase specific for phosphorylation of ceramides, but not the structurally related diacylglycerol (19, 25, 27). Dressler and Kolesnick also reported the existence of C1P

derived from sphingomyelin in human leukemia (HL-60) cells (63). Later, Kolesnick and Hemer verified the findings of Bajalieh *et al* by reporting CERK activity distinguishable from diacylglycerol kinase activity in HL-60 cells (27). More recently, Hinkowska-Galcheva *et al* and also Rile *et al* reported the CERK activity in human neutrophils (36, 64). CERK activity has also been shown in cerebellar granule cells (65) and also in epithelial-derived A549 lung carcinoma cells (33).

Increasingly, ceramide-1-phosphate (C1P) is reported in the scientific literature as a regulator of intracellular processes. Gomez-Munez *et al* showed that C1P was a potent stimulator of DNA synthesis as well as promoting cell division in rat fibroblasts (37) and blocking apoptosis in bone marrow derived macrophages (39). Carpio *et al* has also shown C1P to cause Erk-2 phosphorylation in osteoblastic cells (66). CERK was also implicated in the process of phagolyzosome formation during phagocytosis (36). Finally, published findings from our laboratory demonstrated for the first time, a role for C1P in signal transduction in the inflammatory response (32, 67). Incubation of A549 lung carcinoma cells, with Il-1β and A23187 (a Ca^{+2} ionophore) caused an induction of C1P levels that coincided with activation of CERK within the time frame of AA release (67). Down-regulation of CERK by RNA interference technology caused a concomitant down-regulation of AA release in response to IL-1β, ATP and A23187. In the presence of excogenous C1P however, CERK down-regulation had no effect upon the agonist-induced AA release. Further studies also disclosed that C1P interacts with the CaLB/C2 domain of $cPLA_2$, acting as a positive allosteric activator of $cPLA_2$ and enhancing the interaction of

the enzyme with phosphatidylcholine (34). These findings established a role for CERK and C1P in the inflammatory pathway. Therefore, with the loss of Vioxx and Bextra as therapeutics for inflammation, the characterization of other mediators of inflammation such as CERK is warranted.

In this study, we examined the structural requirements within the ceramide molecule necessary for recognition and substrate utilization by human CERK. The results disclose that even slight modifications to the sphingoid backbone greatly decrease the ability of the lipid to identify its substrate and to catalyze the reaction. Thus, the presented study shows a high degree of specificity for ceramide by CERK, and identifies key features for the development of sphingoid-based inhibitors of the enzyme.

EXPERIMENTAL PROCEDURES

Materials: Serinol and all general chemicals were purchased from Aldrich. Phytosphingosine (2S, 3S, 4R), D-*erythro*-$C_{24:0}$, $C_{24:1}$ were purchased from Avanti. D-*erythro*-C_{16} ceramide and various structural analogs were obtained from the Lipidomics Core at the Medical University of South Carolina synthesized as previously described (68-72). All lipids were quality controlled by ^{1}H-NMR spectra, recorded using a Bruker AVANCE 500 MHz spectrometer equipped with Oxford Narrow Bore Magnet. Chemical shifts are given in parts per million (ppm) downfield from tetramethylsilane as internal

standard and the listed J values are in Hz. Mass spectral data were obtained in positive ion electrospray ionization (ESI) mode on a Finnigan LCQ ion trap mass spectrometer. Samples were infused in methanol solution with an ESI voltage of 4.5 kV and capillary temperature of 200 ^{o}C. The purity of all synthesized lipids was >95% as estimated by TLC and ^{1}H-NMR analysis.

Recombinant expression of CERK using baculovirus: Recombinant human CERK (hCERK) was expressed in Sf9 cells with a 6XHis-tag using a baculovirus expression system and purified using a modified protocol as previously described (73, 74). Briefly, Sf9 cells were grown in suspension culture and infected with high titer recombinant baculovirus at a multiplicity of infection of 1.0 and 72 hours post-infection. The cells were then harvested and the cell paste was re-suspended in a 10 x cell paste volume lysis buffer (10mM MOPS pH 7.2, 150 mM KCl, 10%glycerol, 0.5% Triton, 0.01 mg/ml leupeptin, 0.01 mg/ml aprotinin, 0.005 mg/ml pepstatin, 1mM PMSF). The cells were broken by 10 strokes with a dounce homogenizer. The cell lysate was clarified by centrifugation at 16000xg for 45 mins at 4^{0}C. The soluble supernatant was batch bound to 100ml Ni-NTA superflow resin for 1.5 hours at 4^{0}C with nutation. The column was washed first, with Ni-NTA wash buffer (10mM MOPS pH 7.2, 150 mM KCl, 10%glycerol) and then with 19.5mM imidazole at a rate of 4ml/min until A280 baseline absorbance. The column was eluted with a step elution to 250 mM imidazole in NI-NTA wash buffer (10mM MOPS pH 7.2, 150 mM KCl, 10%glycerol, 250mM imidazole) at 5ml/min. The fractions were analyzed by SDS-PAGE and fractions containing significant amounts of cPLA2α were

pooled and dialyzed against storage buffer (10 mM Tris pH 7.2, 0.1 M NaCl, 2mM EGTA, 50% glycerol, 1mM DTT). The dialyzed material was then centrifuged at 39,000xg for 30 mins to remove precipitation and aliquoted into 10 ml fractions. Recombinant CERK was assayed at 70% purity by coomassie stain, and retained all of the characteristics (eg. Ca^{+2} sensitivity, pH optimum, etc.) as hCERK overexpressed in mammalian cells (19).

Recombinant expression of CERK in mammalian cells: Recombinant CERK was expressed in HeLa cells by transfecting the plasmid construct (hCERK in pcDNA3.1 His TOPO®) using Effectene reagent (Qiagen Corp.) following the standard procedure. Briefly, HeLa cells are plated at 40 to 50% confluency in 150 x 15 mm tissue culture dishes 24 hours prior to transfection. Cells are transfected with 6 µg of plasmid under conditions specified by the manufacture. After 24 hours, the cells were harvested and the crude HeLa extracts were obtained by sonicating in lysis buffer (20mM MOPS, 2mM EGTA,0.5 mM DTT with added Sigma® P-8340 protease inhibitor cocktail at 1/250 dilution). 10 µg protein of the crude extract was used per assay.

***Cell Culture*:** HeLa cells are cultured in DMEM with L-glutamine supplemented with 10% fetal bovine serum and 2% penicillin/streptomycin. Incubation conditions are 5%CO_2, 37^0C, and 95% humidity.

Ceramide Kinase Assays

a)β-Octylglucoside mixed micellar assay: 160 nmol ceramide were micellar solubilized by sonication in 180 ul of reaction buffer (20 mM MOPS (pH 7.2), 50 mM NaCL, 1 mM DTT, 3 mM $CaCl_2$, 51.24 mM β-Octylglucoside, 1 mM Cardiolipin , 0.2 mM DETAPAC). 10µg of crude human CERK (crude lysate of hCERK overexpressed in HeLa cells) or 0.9µg of baculovirus expressed CERK was added per reaction and incubated at 37^0C for 5 minutes. The reaction was started by adding 11µl of ATP (1µl □^{32}P ATP (10µCi/µl) + 10 µl 20 mM ATP in 100 mM $MgCl_2$). All reactions were carried out in triplicates and with D-e-C_{16} ceramide as a positive control. The reaction was allowed to continue at 37^0C for 40 minutes, and stopped by the addition of 1.2 ml 1:1$CHCl_3$:MeOH followed by 500 µl of 1M KCl in 20 mM MOPS. The mixture was then vortexed and phases separated by centrifugation at 650xg for 5 mins. As previously described (75), the organic phase was washed thrice with 500 µl aliquots of 1M KCL and 100 µl of the organic phase was counted directly. All results (as to substrate utilization) obtained with the Triton X-100 based assay (see below) were verified with this previously described CERK assay (43).

b) Surface dilution assay with Triton X-100 mixed micelles: Briefly, 0.003, 0.006, 0.012, 0.024, 0.048, 0.072, 0.109, 0.170 mM ceramide solutions were sonicated with 11.5 mM Triton X-100® and 0.5 mM cardiolipin to obtain 0.025, 0.05, 0.1, 0.2, 0.4, 0.6, 0.9, and 1.4 mol% ceramide solutions. 40µl each of these solutions were used per 200 µl reaction containing 20 mM MOPS (pH 7.2), 50 mM NaCL, 1mM DTT, 3 mM $CaCl_2$, and 0.2 mM DETAPAC. 0.9µg of baculovirus expressed or 10µg of crude hCERK (crude lysate of hCERK overexpressed in HeLa cells) was used per reaction. The reaction was started by

adding 11µl of ATP (1µl λ^{32}P ATP (10µCi/µl) + 10 µl 20 mM ATP in 100 mM $MgCl_2$). All reactions were carried out in triplicates. The reaction was incubated at 37^0C for 15 minutes and stopped by the addition of 1.2 ml 1:1$CHCl_3$:MeOH. The organic phase was washed four times with 500 µl of 1M KCl in 20 mM MOPS. The mixture was then vortexed and phases separated by centrifugation at 650xg for 5 mins. as previously described (75), The amount of ^{32}P-C1P produced was quantified as previously described (75) and confirmed by TLC as previously described (76).

Data analysis: Data analysis was done using Enzyme Kinetics Module™ 1.1 together with SigmaPlot version 8.02A. Mole fraction of ceramide was plotted against reaction velocity (µmol of C1P produced/min/mg protein) to obtain $K_m{}^b$ and V_{max}. The data obtained is the mean of triplicate data sets +/-standard error. Two way ANOVA was performed using Microsoft Excel.

RESULTS

Previously, CERK was shown only to phosphorylate ceramides and not the closely related lipids, diacylglycerol and sphingosine (27). To determine the molecular basis of the interaction between CERK and its substrate, ceramide, our laboratory focused on key features in the ceramide molecule required for substrate recognition and specificity. These include the stereochemistry at the C2, C3, C4, and C5-positions, the requirement of the acyl chain length, the effect of the functional groups in the sphingoid-backbone, the

requirement of the secondary amide bond, and the requirement of the primary and secondary hydroxyl-groups (Figure 2.1). Additionally, the saturation, desaturation, configuraion, and hydroxylation of the natural *trans* C4-C5 double bond and the role of the alkyl chain of the sphingoid-backbone were also investigated (Figure 2.1). The data presented in this manuscript is from the CERK assay utilizing mixed micelles of Triton X-100. The previously described assay for CERK was used to verify these results (data not shown) (43).

Also of note, V_{max}/K_m is used in these studies as a measure of the relative rates of enzymatic reactions for different substrates under identical conditions. Therefore, V_{max}/K_m is a measure of the specificity of an enzyme to different substrates. A statistically significant difference in V_{max}/K_m is generally considered to denote an actual difference in substrate specificity. In this study, we utilized this parameter to investigate the differences in substrate specificities of CERK, and all differences in substrate specificity mentioned hereafter are statistically relevant.

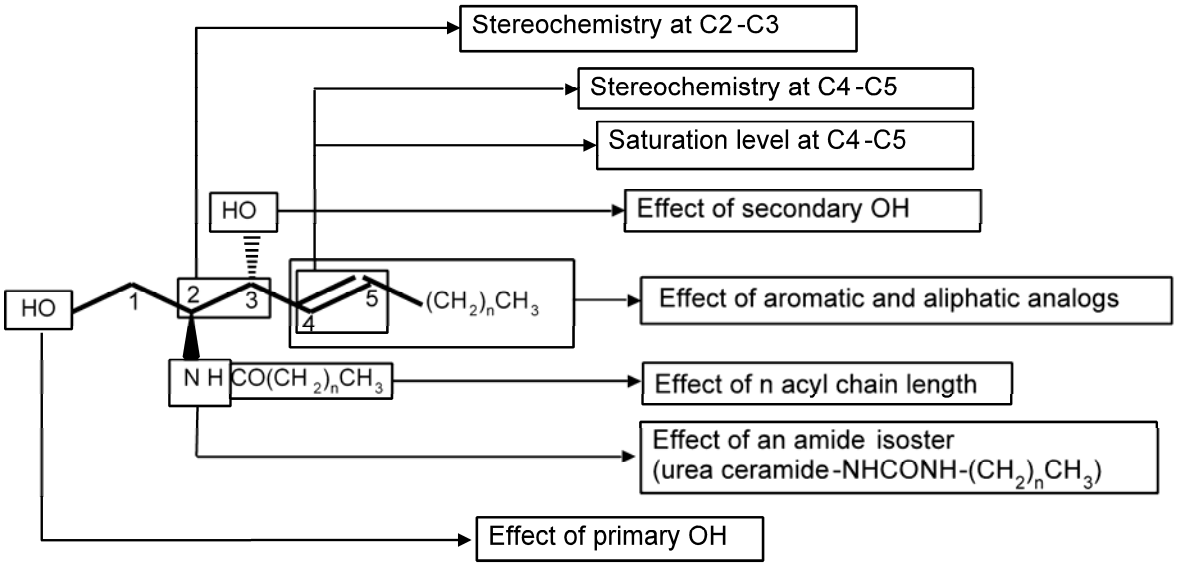

Figure 2.1. The investigated structural features of ceramide.

Stereochemistry.

There are two asymmetrical carbon atoms within the ceramide molecule, and thus, four stereoisomers are possible. D-*erythro*-C_{16} ceramide (2S, 3R) is the naturally occurring configuration, with L-*erythro*-C_{16} ceramide (2R, 3S) being its enantiomer. Additionally, enantiomeric pairs of the *threo*-diastereoisomers can be formed, L-*threo* (2S, 3S) and D-*threo* (2R, 3R). In this study only the D-*erythro* configuration of ceramide was converted to ceramide-1-phosphate. CERK demonstrated no activity towards the other stereoisomers of ceramide. Thus, CERK only phosphorylates the naturally occurring D-*erythro* ceramides (Table 1).

Table 2.1

K_m and V_{max} of all the ceramides and ceramide analogs examined for CERK (baculovirus expressed).
Values represent the mean from three separate determinations

Ceramide tested	K_m[b] *mol fraction (μM)*	V_{max} *μmolC1P/min/mg protein*	V_{max}/K_m
D-e-$C_{2:0}$-Cer	NS	NS	NS
D-e-$C_{4:0}$-Cer	NS	NS	NS
D-e-$C_{6:0}$-Cer	0.1109 (299.36)	0.4456	4.0180
D-e-$C_{8:0}$-Cer	0.0657 (168.77)	0.6843	10.42
D-e-$C_{10:0}$-Cer	0.0186 (45.49)	0.4408	23.75
D-e-$C_{12:0}$-Cer	0.0086 (20.82)	0.3357	39.11
D-e-$C_{14:0}$-Cer	0.0026 (6.26)	0.1590	60.46
D-e-$C_{16:0}$-Cer	0.0036 (8.67)	0.1882	52.53
D-e-$C_{16:0}$ dehydro-Cer	0.0018 (4.33)	0.0338	18.70
D-e-$C_{16:0}$ dihydro-Cer	0.0034 (8.19)	0.0723	21.33
D-e-$C_{16:0}$ -*cis*-Cer	0.0506 (127.91)	0.5485	10.85
D-e-$C_{16:0}$ (R)-α-hydroxy Cer	0.0026 (6.26)	0.0294	11.14
D-e-$C_{16:0}$ (S)-α-hydroxy Cer	0.0030 (7.22)	0.0070	2.34
D-e-$C_{18:0}$-Cer	0.0028 (6.74)	0.1557	56.56
D-e-$C_{18:0}$ phytoceramide	0.0023 (5.53)	0.0451	19.82
D-e-$C_{24:0}$-Cer	0.0033 (7.95)	0.1626	49.29
D-e-$C_{24:1}$-Cer	0.0068 (16.43)	0.3059	44.93
1-0-methyl $C_{16:0}$ -Cer	NS	NS	NS
3-0-methyl $C_{16:0}$ -Cer	0.0049 (11.82)	0.0247	5.04
D-e-C_{16} Urea Cer	0.0008 (1.92)	0.0097	11.54
L-e-C_{16} Urea Cer	NS	NS	NS
N-methyl $C_{16:0}$ -Cer	NS	NS	NS
D-t- $C_{16:0}$-Cer	NS	NS	NS
L-e- $C_{16:0}$-Cer	NS	NS	NS
L-t- $C_{16:0}$-Cer	NS	NS	NS
D-t-$C_{6:0}$-Cer	NS	NS	NS
L-e-$C_{6:0}$-Cer	NS	NS	NS
L-t-$C_{6:0}$-Cer	NS	NS	NS
(R)α-hydroxy-C16-1,3-Acetoinide of Ceramide	NS	NS	NS

(1S, 2S) B13	NS	NS	NS
(1R, 2R) B13	NS	NS	NS
N-palmitoyl-serinol (C16 Serinol)	NS	NS	NS

The effect of the chain length of the acyl chain.

Since sphingosine has been shown not to be a substrate for CERK, we examined various acyl chain lengths of ceramide to determine the minimum size for substrate recognition. We found no statistically significant effects on substrate specificity for chain lengths $\geq C_{12:0}$ (Figure 2.2A, 2.21B, and Table 2.1). With decreasing acyl chain lengths, however ($<C_{12:0}$), CERK showed a proportionate, statistically significant, decrease in enzymatic activity indicated by increasing $K_m{}^b$ and decreasing specificity ($V_{max}/K_m{}^b$). Both C_2- and C_4-ceramide were found not to be substrates for CERK. Thus, a minimum of 14 carbons are required for full recognition of ceramide as a substrate by CERK, and ceramides with an acyl chain <6 carbons are not recognized as substrates. These data indicate that ceramides with chain lengths observed to occur in cells are preferred substrates of CERK (45-47).

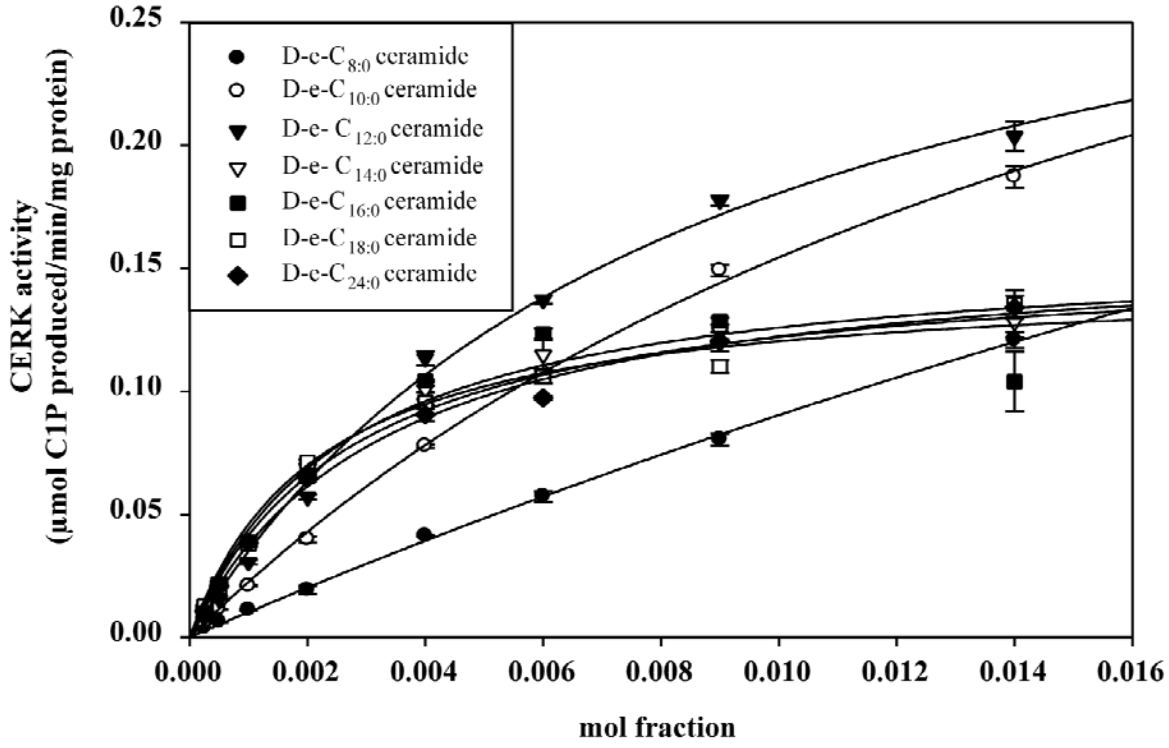

Figure 2.2 Panel A: Michaelis-Menton curves for ceramides of different acyl chain lengths. Specificity of ceramides of different acyl chain lengths were assayed at 0.025, 0.05, 0.1, 0.2, 0.4, 0.6, 0.9, and 1.4 mol% as described in materials and methods. The graph depicts the µmoles of C1P produced per minute per mg of CERK (baculovirus expressed) versus mol fraction of ceramide to obtain V_{max} and the intrafacial Michaelis-Menton constant (K_m^b). Data are presented as mean ± standard error and are representative of three separate determinations. D-e-$C_{8:0}$ ceramide (●), D-e-$C_{10:0}$ ceramide (○), D-e-$C_{12:0}$ ceramide(▼), D-e-$C_{14:0}$ ceramide( ), D-e-$C_{16:0}$ ceramide (■), D-e-$C_{18:0}$ ceramide (□), D-e-$C_{24:0}$ ceramide (♦). Note: for both $C_{6:0}$ (not depicted) and $C_{8:0}$, a higher range (concentration of ceramide) was utilized to establish K_m^b and V_{max} due to their poor substrate specificity constant (higher range concentrations not depicted).

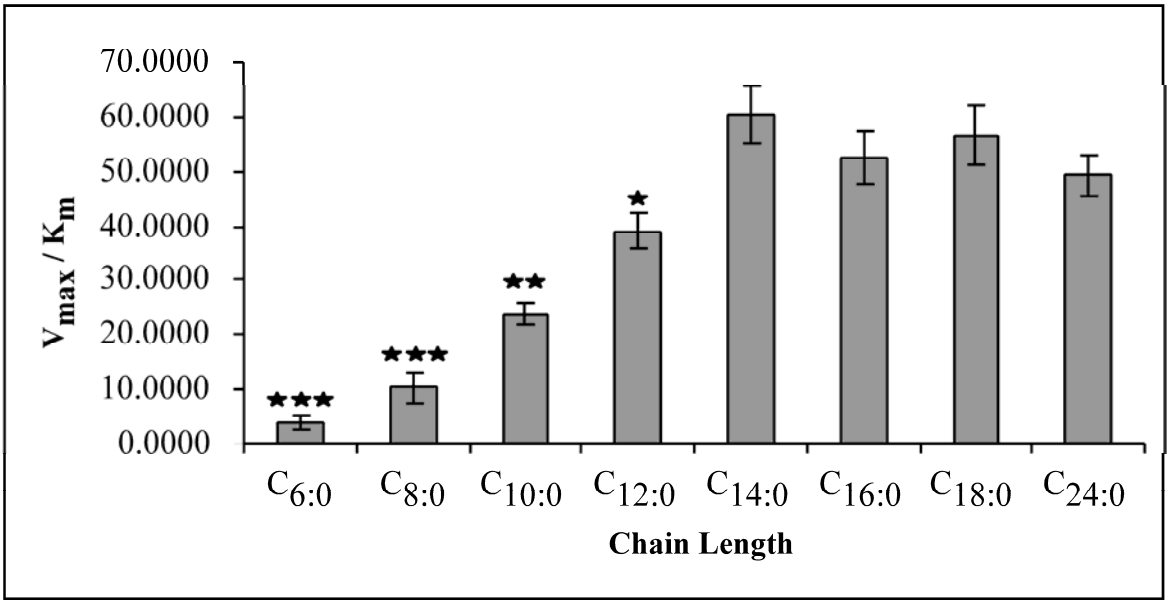

Figure 2.2 Panel B: Specificity constants for the different acyl chain lengths of ceramide. Data presented are the specificity constants (V_{max}/K_m^b) for D-e-$C_{8:0}$, $C_{10:0}$, $C_{12:0}$, $C_{14:0}$, $C_{16:0}$, $C_{18:0}$ and D-e-$C_{24:0}$ ceramide ± standard error. Data are representative of three separate determinations. Significance of the differences in specificity constants when compared to D-e-$C_{16:0}$ ceramide was examined by two way ANOVA, $p < 0.1$(★), $p < 0.01$ (★★), $p < 0.005$ (★★★).

Saturation state of the acyl chain.

The main forms of ceramide found in mammalian cells are D-e-$C_{16:0}$ ceramide and D-e-$C_{24:1}$ ceramide (77-79). In this study, we examined whether CERK possessed any selective characteristics for saturated or unsaturated acyl chains of ceramide, using D-e-$C_{24:0}$ ceramide and D-e-$C_{24:1}$ ceramide (Figure 2.3 and Table 2.1). Although the saturated ceramide showed a lower K_m compared to the unsaturated ceramide, this was accompanied by a proportionate change in the V_{max}. As a result, no statistically significant difference was observed in the specificity constant (V_{max}/K_m^b). Thus, differences in the K_m and V_{max} may be attributed to the higher solubility of the monounsaturated form. A similar pattern was observed between D-e-$C_{18:0}$ ceramide D-e-$C_{18:1}$ ceramide (data not shown). Thus CERK seem to equally recognize ceramides containing both saturated and unsaturated fatty acyl chains.

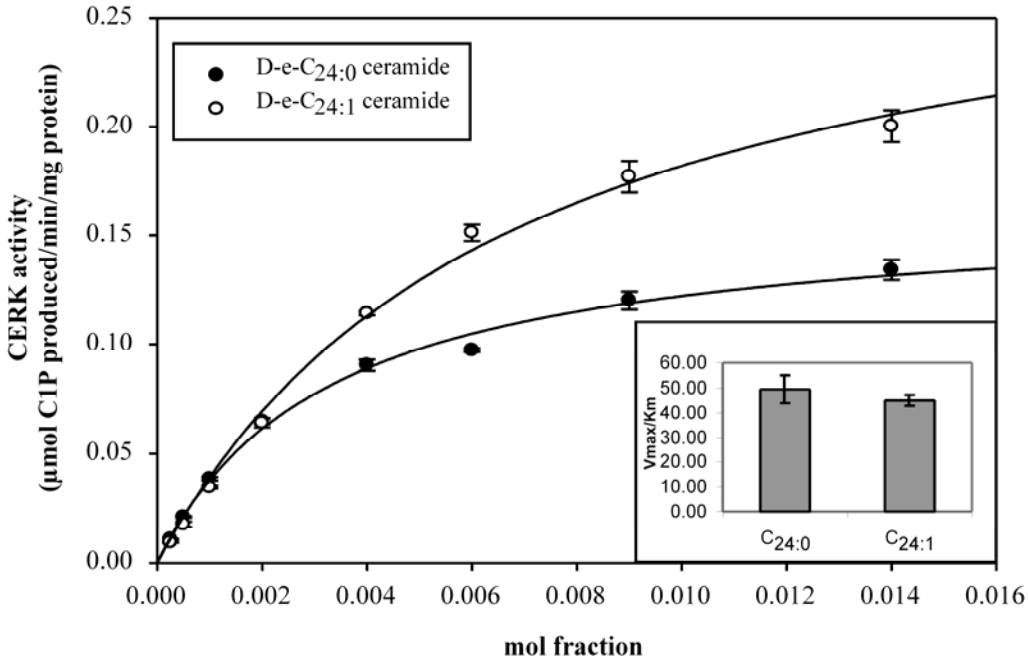

Figure 2.3: The saturation state of the acyl chain does not affect the substrate specificity of CERK. Ceramides with saturated ($C_{24:0}$) and unsaturated ($C_{24:1}$) acyl chains were assayed at 0.025, 0.05, 0.1, 0.2, 0.4, 0.6, 0.9, and 1.4 mol% as described in materials and methods. The graph depicts µmoles of C1P produced per minute per mg of CERK (baculovirus expressed) versus mol fraction of ceramide to obtain V_{max} and the intrafacial Michaelis-Menton constant (K_m^b). Data are presented as mean ± standard error and are representative of three separate determinations. D-e-$C_{24:0}$ ceramide (●), D-e-$C_{24:1}$ ceramide (○). **Inset: Specificity constants for D-e-$C_{24:0}$, and D-e-$C_{24:1}$ ceramide**. Data presented are the specificity constants (V_{max}/K_m^b) for D-e-$C_{24:0}$ and D-e-$C_{24:1}$ ceramide ± standard error. Data are representative of three separate determinations.

Effect of α hydroxylated fatty acids.

Ceramidase, another ceramide utilizing enzyme, is capable of utilizing ceramides with α hydroxy fatty acids as a substrate (80). Therefore, the ability of CERK to utilize α hydroxylated ceramides was also investigated (Table 2.1). CERK was able to phosphorylate both R and S, D-e-$C_{16:0}$- α hydroxyl ceramides, but demonstrated a lower specificity constant compared to the naturally occurring long chain ceramides (Table 2.1). Thus, CERK possesses the ability to phosphorylate α hydroxylated ceramides, and an α hydroxylated C1P may exist in cells.

Sphingoid Moiety

The sphingoid-backbone modifications shown in figure 2.1 were introduced into the ceramide molecule. First, the requirement for the 4-5 double bond within the sphingoid moiety was examined. Saturation of the 4-5 double bond produces D-*erythro*-dihydroceramide, an anabolic precursor of ceramide, which has been shown to be biologically inactive in cells (70). CERK showed significantly reduced specificity ($p<0.005$) towards the dihydroceramides as compared to ceramide (Figure 2.4A and Table 2.1).

To further examine the necessity of the 4-5 double bond of ceramide for use as a substrate for CERK, this moiety was further unsaturated to D-*erythro*-dehydro-C_{16} ceramide producing a triple bond between the 4 and 5 carbons of the sphingoid backbone. This compound also showed a decreased specificity ($p<0.005$) compared to the natural ceramides (Figure 2.4A and Table 2.1). Since natural ceramide has the 4-5 double bond in the *trans*-configuration, the nature of the 4-5 double bond was further examined by modifying the configuration from *trans* to *cis*. CERK also showed a significant decrease ($p<0.005$) in specificity for this substrate as well (Figure 2.4A and Table 2.1).

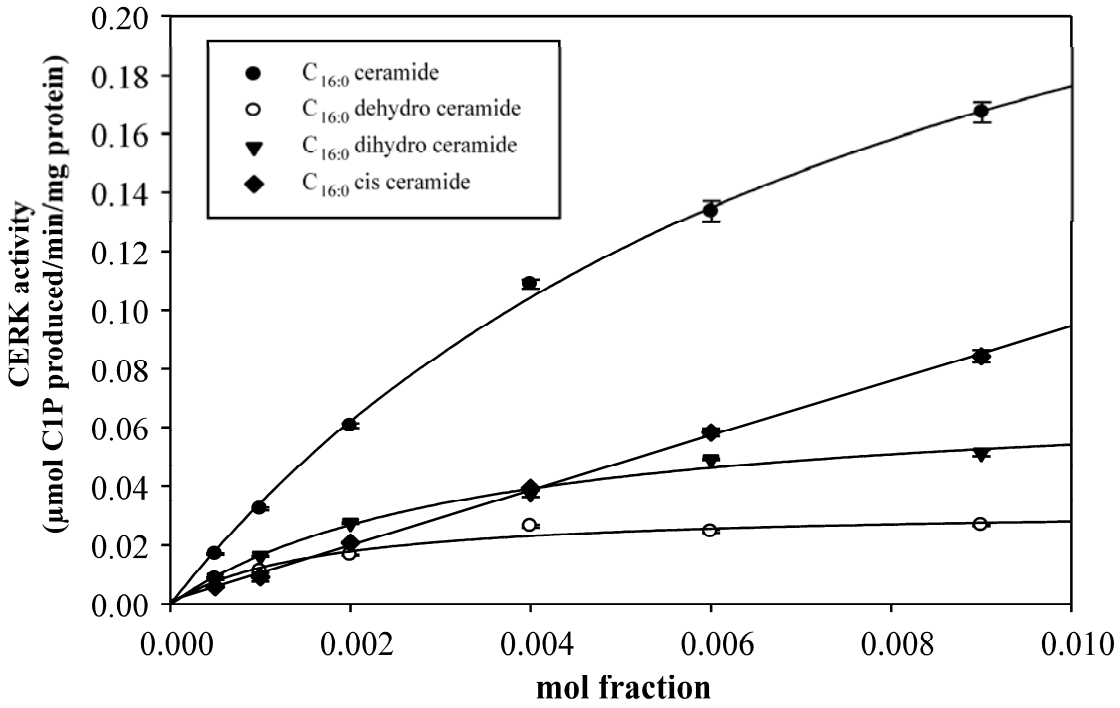

Figure 2.4: Alteration of the 4,5 double bond of ceramide significantly affects the recognition of ceramide by CERK. Panel A. Michaelis-Menton curves for C_{16} ceramides with different 4,5 bonds. D-e-$C_{16:0}$ *trans*, $C_{16:0}$ *cis*, $C_{16:0}$ dehydro, $C_{16:0}$ dihydro ceramides were assayed at 0.025, 0.05, 0.1, 0.2, 0.4, 0.6, 0.9, and 1.4 mol% as described in materials and methods. The graph depicts the µmoles of C1P produced per minute per mg of CERK (baculovirus expressed) versus mol fraction of ceramide to obtain V_{max} and the intrafacial Michaelis-Menton constant (K_m^b). Data are presented as mean ± standard error and are representative of three separate determinations. D-e-$C_{16:0}$ ceramide (●), D-e-$C_{16:0}$ dehydro ceramide (○), D-e-$C_{16:0}$ dihydro ceramide (▼), D-e-$C_{16:0}$ *cis* ceramide (♦).

Recently, phytoceramides were described in mammalian cells, (81-83) thus, the use of phytoceramides (4-hydroxy-dihydroceramides) as substrates for CERK were also investigated. $C_{18:0}$-phytoceramide showed a decreased specificity constant ($p<0.005$) when compared against $C_{18:0}$ ceramide (Figure 2.4B and Table 2.1). Thus, these data demonstrate that CERK has a marked preference for the saturation level and the *trans*-orientation of double bond at the 4-5 position.

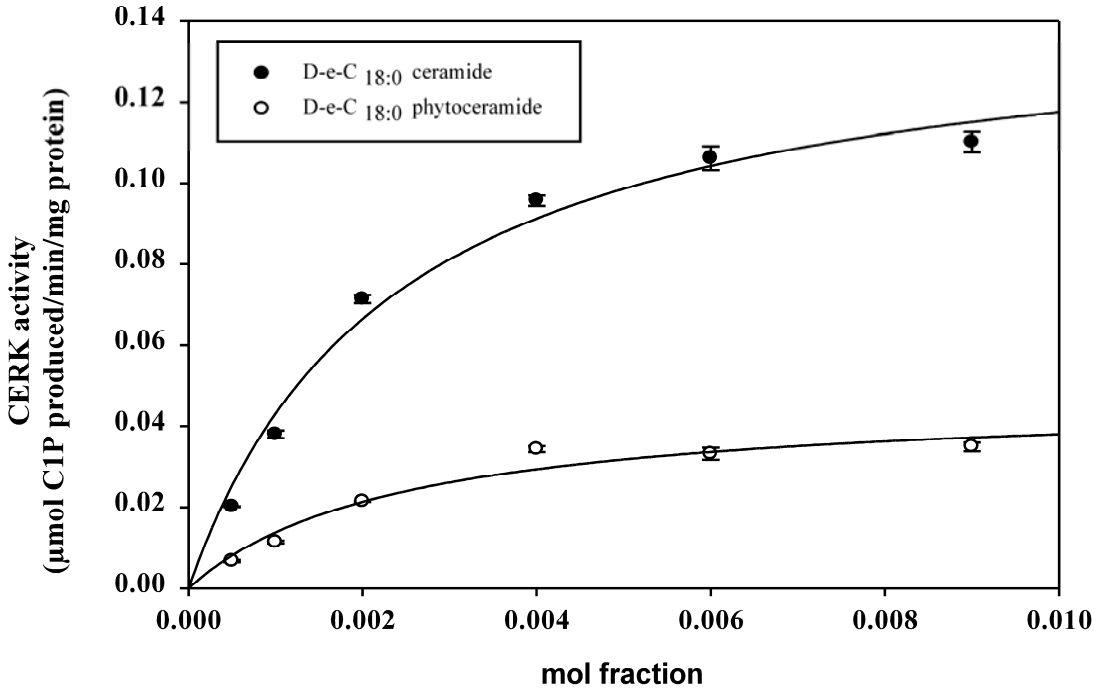

Figure 2.4 Panel B: Michaelis-Menton curves for $C_{18:0}$ ceramide and $C_{18:0}$ phytoceramide. D-e-$_{18:0}$ ceramide and D-e-$C_{18:0}$ phytoceramide were assayed at 0.025, 0.05, 0.1, 0.2, 0.4, 0.6, 0.9, and 1.4 mol% as described in materials and methods. The graph depicts the µmoles of C1P produced per minute per mg of CERK (baculovirus expressed) versus mol fraction of ceramide to obtain V_{max} and the intrafacial Michaelis-Menton constant (K_m^b). Data are presented as mean ± standard error and are representative of three separate determinations. D-e-$C_{18:0}$ ceramide (●), D-e-$C_{18:0}$ phytoceramide (○).

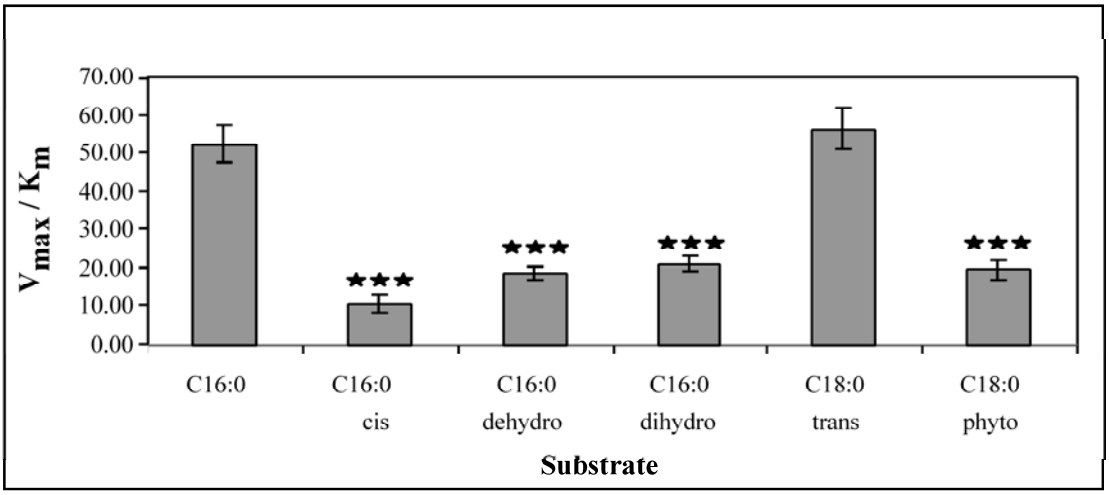

Figure 2.4 Panel C. Specificity constants for the ceramides with different 4,5 bonds. Data presented are the specificity constants (V_{max}/K_m^b) for D-e-$C_{16:0}$ *trans*, $C_{16:0}$ *cis*, $C_{16:0}$ dehydro, $C_{16:0}$ dihydro, $C_{18:0}$ *trans* ceramides and $C_{18:0}$ phytoceramides ± standard error. Data are representative of three separate determinations. Significance of the differences in specificity constants when compared to D-e-$C_{16:0}$ ceramide (for D-e-$C_{16:0}$ dehydro, dihydro and *cis* ceramide) and D-e-$C_{18:0}$ (for D-e-$C_{18:0}$ phytoceramide) were examined by two way ANOVA, $p < 0.005$ (★★★).

The necessity of other sphingoid structural features were also examined. Clearly, from other published findings, the free sphingoid bases, sphingosine and dihydrosphingosine, are not substrates of CERK (19). The question remains, however, if the sphingoid-base chain is necessary for the recognition of ceramide as a substrate for CERK. To this end, serinol ceramide (a ceramide analog with a truncated sphingosine-backbone containing only the C1-C3 part from serine) was synthesized and tested *in vitro* (69). The results show that N-hexadecanoyl-serinol (serinol ceramide) was not a substrate (Table 1). The structural features of the sphingoid moiety were further investigated by replacing the sphingoid alkenyl chain with an aromatic phenyl group producing two enantiomers, (1R,2R)-2-(N-Myristoylamino)-1-(4'-nitrophenyl)-1,3-propandiol (1R,2R-B13) and (1S,2S)-2-(N-Myristoylamino)-1-(4'-nitrophenyl)-1,3-propandiol (1S,2S-B13). Neither of these compounds were substrates for CERK (Table 1). Therefore, the sphingosine chain is necessary for CERK to recognize ceramide as a substrate.

Amide group

To determine the importance of the secondary amide group –NHCO- in the ceramide structure, we synthesized urea-isosters of ceramide bearing –NHCONH- instead of the -NHCO- group, producing two enantiomers, 2S,3R (*i.e.* D-*erythro*) and 2R,3S (*i.e.* L-*erythro*)-urea-C_{16} ceramide. D-*erythro*-urea-C_{16} ceramide was a substrate for CERK, but demonstrated significantly lower specificity ($p<0.005$) compared to the naturally occurring ceramides (Figure 2.5 and Table 2.1). Also, similar to L-*erythro*-C_{16} ceramide, L-*erythro*-

urea-C_{16} ceramide was not a substrate (Table 2.1). These results indicate that the N-acyl-amide bond is required for the complete recognition of the substrate by CERK. Next, the role of the hydrogen atom from the amide bond –NHCO- was examined using N-methyl-C_{16} ceramide as a model. This compound was also not a substrate of CERK (Table 1), demonstrating the necessity of the free hydrogen in the secondary amide group for recognition by CERK.

Primary and Secondary Hydroxyl-groups

The necessity of the free primary and secondary hydroxyl groups of the ceramide molecule was examined by using 1-O-methyl-C_{16} ceramide and 3-O-methyl-C_{16} ceramide (Figure 2.1). Methylation of the primary hydroxyl group completely eradicated the ability of CERK to phosphorylate ceramide. Methylation of the secondary hydroxyl group showed dramatically decreased specificity ($p<0.005$) for the substrate by CERK (Figure 2.5 and Table 2.1). To further investigate the importance of the primary and the secondary hydroxyl groups, the ability of CERK to phosphorylate $C_{16:0}$-1,3-acetoinide was tested. This compound was also not a substrate of CERK (Table 2.1). These data confirm that primary hydroxyl group is the site of phosphorylation by CERK and that the secondary hydroxyl group although not involved in direct phosphorylation, is still important for substrate recognition.

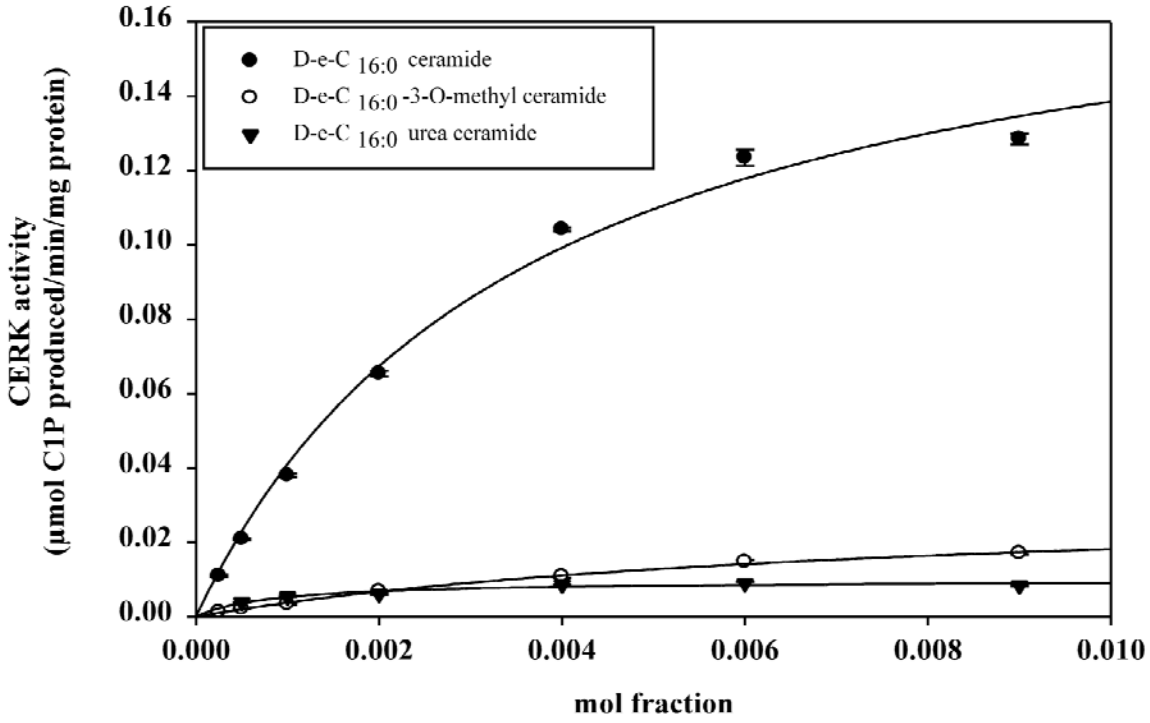

Figure 2.5. The secondary amide and the secondary hydroxyl groups of ceramide are important for substrate recognition by CERK. Panel A. Michaelis-Menton curves for $C_{16:0}$, $C_{16:0}$ -3-O-methyl, and $C_{16:0}$ urea ceramide. D-e-$C_{16:0}$, $C_{16:0}$-3-O- methyl, and $C_{16:0}$ urea ceramides were assayed at 0.025, 0.05, 0.1, 0.2, 0.4, 0.6, 0.9, and 1.4 mol% as described in materials and methods. The graph depicts the µmoles of C1P produced per minute per mg of CERK (baculovirus expressed) versus mol fraction of ceramide to obtain V_{max} and the intrafacial Michaelis-Menton constant (K_m^b). Data are presented as mean ± standard error and are representative of three separate determinations. D-e-$C_{16:0}$ ceramide(●), D-e-$C_{16:0}$-3-O- methyl ceramide (○), and D-e-$C_{16:0}$ urea ceramide (▼).

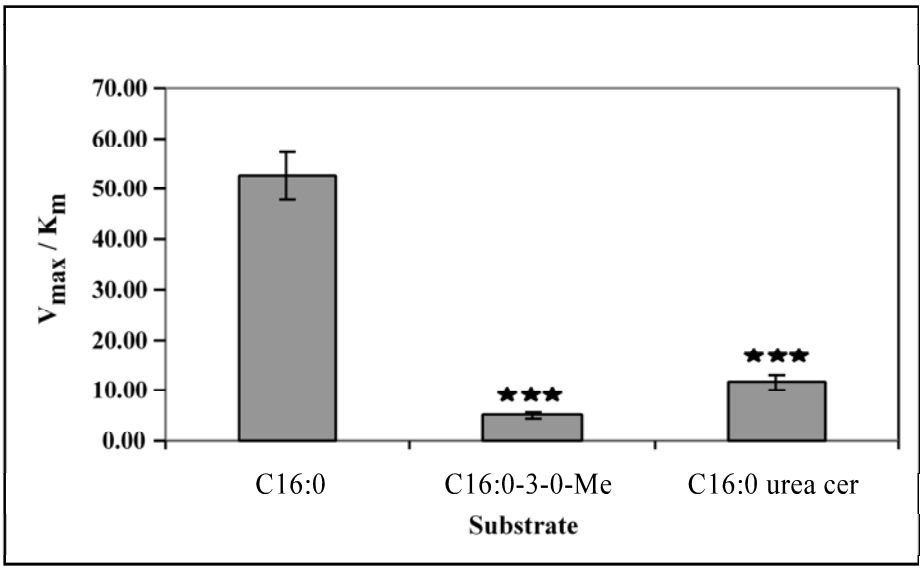

Figure 2.5. Panel B. Comparative specificities of CERK towards modifications to the secondary amide and hydroxyl group. Data presented are the specificity constants (V_{max}/K_m^b) for $C_{16:0}$, $C_{16:0}$-3-O- methyl, and $C_{16:0}$ urea ceramides ± standard error. Data are representative of three separate determinations. Significance of the differences in specificity constants when compared to D-e-$C_{16:0}$ ceramide was examined by two way ANOVA, $p < 0.005$ (★★★).

DISCUSSION

In this study, we demonstrate the strict structural requirements of ceramide for recognition as a substrate by CERK. The understanding of this action of recognition is important for several reasons. First, these studies begin to identify features for ceramide-based inhibitors of CERK, allowing for the possible designing of new anti inflammatory compounds. Second, these studies add to our knowledge of the biochemical mechanisms of CERK and sphingolipid enzymes in general. Lastly, these studies further disclose that this interaction between ceramide and CERK has implications for the physiological regulation of the enzyme.

Previously published kinetic studies on CERK were accomplished using a bulk dilution technique and mixed micelles of β-OG (40). In this regard, molecular modeling studies show β-OG to have an irregular surface (42), thus, all the substrate in the micelle is not presented equally to the enzyme. Furthermore, as ceramides are found in membranes, the true kinetic behavior of the enzyme can only be studied using a model that takes into account both bulk and surface diffusion of the enzyme. Therefore, in this study, surface dilution kinetics (34, 84) utilizing Triton X-100 mixed micelles were used to characterize the substrate specificity of CERK. Triton X-100 micelles provide several advantages. First, they provide an inert surface for CERK containing an average of 140 molecules/micelle.

Second, the size of the micelles are relatively independent of ionic strength and temperature within the physiological range (43-45, 85). Lastly, mixed micelles up to 20 mol % phospholipids are similar in structure to pure Triton X-100 micelles, but proportionally larger (43, 45, 85), and pure Triton X-100 micelles do not co-exist with mixed micelles. Therefore, the new Triton X-100 based assay presented in these studies provided an excellent means of studying the kinetics of CERK.

Using this assay, the presented study corroborates the findings of Sugiura *et al* (86) in that, C_2 ceramide is not a substrate of CERK. In addition C_4 ceramide was also found not to be phosphorylated by CERK, thus greater than a C_4 acyl chain is required for recognition by CERK. These previous studies by Sugiura and co-workers also showed C_8 and C_6 ceramides to be good substrates of CERK based on activity at fixed concentrations, which would be a reflection of the differences in their V_{max} (19). In contrast, the Michaelis-Menton constant, K_m^b, was taken into account in this study as well as V_{max} to study the substrate specificity (V_{max}/K_m^b), since this is a more accurate indication in comparing the affinity of an enzyme to different substrates. Therefore, although the V_{max} of C_6 and C_8 ceramides are in general greater than long chain ceramides, the ratio V_{max} : K_m is dramatically lower by comparison. Sugiura *et al* (86) also reported that C_8 dihydroceramide was a good substrate for CERK with a comparable V_{max} to long chain ceramides. Our study using naturally occurring D-e-C_{16} ceramides show saturation of the 4,5 double bond induces a significant decrease in substrate preference by CERK.

Therefore, these studies demonstrate the importance of examining the K_m and specificity constant for determining substrate preference for lipid kinases.

The presented study also examined the substrate preference of CERK in depth. As alluded to above, the presence of the 4,5 double bond of the sphingoid moiety is an important feature for recognition by CERK as dehydro, dihydro, and phytoceramide all showed decreased substrate specificity. In addition, the natural *trans* configuration of the double bond is also important as the *cis* configuration showed greatly reduced specificity. Thus, the 4,5 double bond of the sphingoid moiety is likely an important contact point for the substrate with CERK. Furthermore, results disclosed the importance of the sphingoid alkyl chain as replacement of the alkyl chain with an aromatic phenyl group caused a dramatic loss in phosphorylation. Thus, the sphingoid moieties of ceramide are essential for substrate recognition and phosphorylation by CERK explaining why CERK phosphorylates ceramide and not the closely related glycerol lipids like DAG. For the purpose of designing pharmacologic inhibitors of CERK based on sphingoid moieties, these required features of ceramide that affect the substrate specificities of CERK should be taken into account. For example, at least a six carbon acyl chain should be utilized as a shorter acyl chain length is not recognized by CERK. To this end, unpublished findings from our laboratory demonstrate that C_2 ceramide is not an inhibitor of CERK.

The structural requirements for substrate recognition by CERK also appear different from other ceramide-utilizing enzymes. CERK showed very high stereospecificity using only

the D-*erythro* ceramides as substrates. In contrast, glucosylceramide synthase (GCS) can use both D-*erythro* and L-*erythro* isoforms (87), while Stoffel *et al.* (88) reported that sphingomyelin synthase (SMS) prefers L-*threo* isoform over the D-*erythro*. In terms of chain length, neutral ceramidase (80) shows a marked preference for long chain and unsaturated ceramides. In contrast, CERK does not discriminate between a saturated and unsaturated ceramide. In addition, the phytoceramides, 4,5-*cis*-ceramide, and 3-O-methyl ceramides were not substrates for ceramidase (80). However, these are substrates for CERK although the substrate specificity is greatly reduced. CERK does show some similarities to neutral ceramidase in utilizing only the D-*erythro* isoform as a substrate and demonstrating decreased specificity for dihydro ceramides. Furthermore, as in the case of neutral ceramidase, CERK does not recognize N-methyl ceramides as substrates. Thus, the recognition of ceramide as a substrate by CERK is more similar to the substrate preferences of ceramidase than to other ceramide metabolizing enzymes like GCS and SMS. However there are still clear differences between the substrate preferences of CERK and ceramidase making CERK unique within the ceramide metabolizing enzymes.

These studies also suggest a mechanism for the intracellular utilization of ceramide by CERK. Unpublished findings from our lab demonstrate that the major form of C1P found in A549, HeLa, and J774.1 macrophage cells is D-e-$C_{16:0}$ ceramide. As CERK does not discriminate among the long chain ceramides, the prevalence of particular forms of C1P is likely due to substrate availability. Furthermore, a recent report by Baumruker (89) and coworkers localizes CERK to the Golgi apparatus, and ceramide transport protein (CERT),

the enzyme responsible for actively transporting ceramide to the Golgi apparatus demonstrates a preference for the D-e-C_{16} ceramide (90). These suggest that CERK produces predominantly D-e-$C_{16:0}$ C1P due to substrate availability regulated by the transport of ceramides to the Golgi apparatus by CERT.

In conclusion, CERK shows very high specificity towards the naturally occurring ceramides. This high specificity allows the enzyme to distinguish between ceramides and other structurally related compounds like sphingosine and diacylglycerol. Furthermore, substrate preference cannot explain the predominance of D-e-$C_{16:0}$ C1P in cells, and CERK demonstrates different requirements for sphingoid moieties than other sphingolipid enzymes. These structural features identified as essential for substrate recognition can now be used as a basis for the rational designing of inhibitors to CERK. Since CERK has an established role in the inflammatory pathway as an upstream activator of $cPLA_2\alpha$, inhibitors of CERK may become a new generation of anti-inflammatory drugs. With the COX-2 inhibitors, Vioxx (4-(4-methylsulfonylphenyl)-3-phenyl-5H-furan-2-one) and Bextra (4-(5-methyl-3-phenyl-isoxazol-4-yl)benzenesulfonamide), now withdrawn from the pharmaceutical market, the designing of novel anti-inflammatory compounds are a high priority as therapeutics for disorders like arthritis, asthma, multiple sclerosis and Alzheimer's disease.

CHAPTER 3: THE CHAIN LENGTH SPECIFICITY FOR THE ACTIVATION OF GROUP IV CYTOSOLIC PHOSPHOLIPASE A_2 BY CERAMIDE-1-PHOSPHATE.

INTRODUCTION

The first report of a biological effect for C1P was by Brindley and coworkers (37), which demonstrated that short chain (not naturally found in cells) C1P induced DNA synthesis in Rat-1 fibroblasts (37). Later, treatment of T17 fibroblasts with long chain, natural ceramide-1-phosphate was also demonstrated to induce a potent increase in DNA synthesis (38) and the levels of proliferating nuclear antigen. Following this line of research, a recent report demonstrated that C1P prevented programmed cell death in bone marrow-derived macrophages (BMDMs) after withdrawal of macrophage colony-stimulating factor (M-CSF) (91). Treatment of these cells with C1P effectively blocked the activation of caspases and prevented DNA fragmentation upon serum removal. In the same study, they also demonstrated that C1P treatment inhibited ceramide generation from acid sphingomyelinase (A-SMase). Lastly, A-SMase was shown to be a direct target of C1P inducing inhibition of this enzyme (39).

In the last few years, a number of reports have continued to demonstrate distinct biological mechanisms regulated by the sphingolipid, C1P, and the enzyme responsible for its

synthesis, ceramide kinase (CERK). For example, Shayman and coworkers demonstrated that CERK was activated in the context of phagocytosis in neutrophils after challenging the cells with formyl peptide and antibody-coated erythrocytes (FMLP/EIgG) (36). Thus, these data demonstrated that C1P may play a distinct role in membrane fusion possibly explaining the early finding that high levels of C1P are found in synaptic vesicles (25). Our laboratory has also demonstrated a biological function for C1P as a direct activator of $cPLA_2\alpha$ through interaction with the C2/CaLB domain (32). These results coupled with the previous findings that CERK/C1P pathway is required for $cPLA_2\alpha$ activation in response to calcium ionophore and cytokines (67) demonstrated that C1P was a "missing link" in the eicosanoid synthetic pathway. A role for CERK and its product, C1P, in a separate pathway of allergic/inflammatory signaling has also been reported in mast cells. Igarashi and coworkers demonstrated that treatment of RBL-2H3 cells or overexpression of CERK in these cells enhanced the degranulation induced by A23187 (35).

While there is a growing list of biological functions attributed to C1P, it is unclear whether an effect observed for different chain lengths of C1P can be extrapolated to all biological observations. In this regard, many chain lengths of C1P have been utilized exogenously to examine biological effects. For example, short chain C1Ps are ideal candidates for studying the biology of C1P as their higher solubility allows for relatively easy delivery to target cells. In this regard, Högback *et al* (2003) and Tornquist *et al* (2004) showed that C_2-C1P induced an increase in the intracellular Ca^{+2} levels in $FRTL_5$ cells and GH_4C_1 rat pituitary cells. Using the same lipid, Graf *et al* (2006) showed a correlation between

apoptosis and enhanced C_2-C1P formation upon C_2-ceramide treatment of CERK overexpressing COS cells. C_2, C_8 and long chain C1P have also been demonstrated to cause ^{3}H thymidine incorporation into DNA (37, 38). Our laboratory using the naturally occurring $C_{16:0}$ and $C_{18:1}$ C1P showed the lipid is a co-factor in the activation of cPLA$_2\alpha$ and synthesis of eicosanoids (32, 67). Since eicosanoids pathways have roles in calcium homeostasis (92, 93), cell survival (94), apoptosis (95), and cell growth (95), the question remains whether these biologies reported for C1P can be attributed to simply cPLA$_2\alpha$ activation. In addition, a recent paper by Bornancin and co-workers demonstrated that using dodecane to deliver phospholipids induced eicosanoid synthesis and loss of cell viability in a non-specific manner (96) casting doubts on the validity of this well-established method of lipid delivery.

In this paper, we show that while the ethanol/dodecane system successfully delivers all chain lengths of C1P to cells, not all chain lengths activate cPLA$_2\alpha$ *in vitro* and in cells. Thus, certain biologies attributed to C_2-C1P are not via activation of cPLA$_2\alpha$. In addition, we also demonstrate that at low concentrations, C1P exerts biological effects that are specific, non-toxic, and distinct from other structurally similar lipid molecules as well as the delivery medium. Therefore, this study shows that the alcohol/dodecane delivery system can be utilized to study lipid-specific effects if proper controls and appropriate lipid concentrations are utilized. Furthermore, the study demonstrates that certain reported biologies (e.g. calcium release) for C1P are not via activation of eicosanoid biosynthesis.

Materials and Methods

Materials: All cultured cells were obtained from American Type Culture Collection (ATCC). [γ-^{32}P]ATP (3000 Ci/mmol) was purchased from Amersham Pharmacia Biotech (Piscataway, NJ). D-e-$C_{18:1}$ ceramide-1-phosphate, D-e-$C_{16:0}$ ceramide-1-phosphate, D-e-$C_{6:0}$ ceramide-1-phosphate and D-e-$C_{2:0}$ ceramide-1-phosphate for the treatment of A549 were purchased from Avanti or produced via large scale phosphorylation of ceramide. C1P used in the treatment of NR8383 cells, Methanol, Ethanol and dodecane are from Sigma-Aldrich. Ceramide and PA were purchased from Avanti Polar Lipids. Dulbecco's modified Eagle's medium (DMEM), RPMI, fetal bovine serum (FBS) and Penicillin/Streptomycin (100 units/ml penicillin G sodium, and 100 µg/ml streptomycin sulfate) were obtained from Invitrogen Life Technologies, Carlsbad, CA.

Cell culture: A549 lung adenocarcinoma cells were grown in 50% RPMI 1640 and 50% Dulbecco's modified Eagle's medium-DMEM supplemented with L-glutamine, 10% (v/v) FBS, 2% (v/v) Penicillin/Streptomycin. Cells were maintained at less than 80% confluency under standard incubator conditions (humidified atmosphere, 95% air, 5% CO_2, 37 °C). RAW macrophages were grown in DMEM supplemented with L-glutamine, 10% (v/v) FBS, 2% (v/v) Penicillin/Streptomycin. For treatments, the medium was replaced 2 hours prior to the addition of the agonist by DMEM containing 2 % FBS and 2 % Penicillin/Streptomycin. Alveolar macrophage cells (NR8383) were cultured in Ham's F12 medium supplemented with 15% FBS, 2.74 mg/ml of glucose, 2% (v/v)

Penicillin/Streptomycin. Floating and adherent cells were collected after centrifugation, resuspended in fresh medium, and seeded in new culture dishes. They were then cultured in a humidified atmosphere containing 5%CO_2 at 37°C.

Dispersion of C1P in aqueous solution: C1P is dissolved in ethanol to make a 10 mM solution. The required amount of C1P from this stock solution is dried down under N_2 gas. Water is added to the dried ceramide to the desired concentration. The solution is then sonicated on ice until a clear solution is obtained and used soon thereafter.

Dispersion C1P in ethanol/dodecane: *E*thanol and dodecane is mixed at a ratio of 98:2, followed by vortexing and pre-warmed at 37 °C. Meanwhile, C1P is dissolved in chloroform:methanol 1:1. The required volume is then dried down under N_2 gas. The pre-warmed alcohol:dodecane mixture is added to the dried C1P such that the final concentration is 2.5 mM (a stock solution up to 10 mM can be made). This mixture is thoroughly vortexed and incubated at 37°C for a further 20 minutes followed by further vortexing. The stock solution, thus prepared, is diluted to the required concentration using ethanol/dodecane and used to treat the cells.

Treatment of cells with phospholipids: The stock solution of C1P in delivery medium is incubated at 37 °C followed by vortexing. C1P is diluted to the appropriate concentration in ethanol/dodecane solution, and added to cells at a dilution of 1:1000. This concentration is recommended to prevent adverse effects on cells by the delivery medium itself. 1-

palmitoyl-2-oleoyl-*sn*-glycero-3-phosphate (PA) and ceramide similarly prepared in ethanol/dodecane was included as a sham control at the same concentration as the treatment.

Mixed micelle assay for cPLA$_2$α: cPLA$_2$α activity was measured in a PC-mixed micelle assay in a standard buffer composed of 80 mM HEPES, pH 7.5, 150 mM NaCl, 10 µM free Ca^{2+}, and 1 mM dithiothreitol. The assay also contained 0.3 mM 1-palmitoyl-2-arachidonoylphosphotidylcholine (PAPC) with 250,000 dpm of [^{14}C]PAPC, 2 mM Triton X-100, 26% glycerol, and 500 ng of purified cPLA$_2$α protein in a total volume of 200 µl. To prepare the substrate, an appropriate volume of cold PAPC in chloroform, indicated phospholipids, and [^{14}C]PAPC in toluene/ethanol 1:1 solution were evaporated under nitrogen. Triton X-100 was added to the dried lipid to give a 4-fold concentrated substrate solution (1.2 mM PAPC). The solution was probe sonicated on ice (1min on, 1 min off for 3 min). The reaction was initiated by adding 500 ng of the enzyme and was stopped by the addition of 2.5 ml of Dole reagent (2-propanol, heptane, 0.5 M H_2SO_4; 400:100:20, v/v/v). The amount of [^{14}C]AA produced was determined using the Dole procedure as previously described (97). All of the assays were conducted for 45 min at 37 °C. Statistical and kinetic analysis was performed using Sigma-Plot Enzyme Kinetics software, version 1.1, from SYSSTAT software, Inc.

Quantification of arachidonic acid release: A549 cells (5 x 10^4) were labeled overnight with 5 μCi/ml [^{3}H]arachidonic acid (5 nM). Cells were washed and placed in Dulbecco's modified Eagle's medium supplemented with 2% fetal bovine serum for 2 h. Following treatment, medium was transferred to 1.5-ml polypropylene tubes, centrifuged at 10,000 x *g*, and [^{3}H]AA (and metabolites) cpm were determined by scintillation counting. Results were controlled for equivalent number of cells quantified by 3-(4,5-dimethylthiazol-2-yl)-2,5-diphenyltetrazolium bromide assay as described (32) and by verification of total AA labeling by scintillation counting. In arachidonic acid release experiments of NR 8383 cells, both adherent and floating cells were collected and seeded in 35 mm plates at a density of 1 x10^6 cells/ml. [3H]-Arachidonic acid (0.20 μCi/ml) was added and cells incubated overnight. The cells were then washed twice with Ham's F12 medium supplemented with 0.2% BSA, and experiments were performed in Ham's F12 medium supplemented with 0.1% BSA. Six hours after addition of appropriate agonist, the medium was collected and centrifuged at 10000 x g for 5 min. The radioactivity in the supernatants was measured using a liquid scintillation counter Packard Tri-Carb2700TR (Meriden, CT). An aliquot of the supernatant was used in some experiments for analysis of radiolabeled compounds confirming that most of the radioactivity was in arachidonate.

PGE_2 assay: The ELISA plate (Cayman Chemical), coated with goat anti-mouse IgG was loaded at 50 μL per well of standard/sample, where the sample was diluted at 1 in 40 in 1X EIA buffer, 50 μL of PGE_2 EIA AChE tracer (Cayman Chemical), and 50 μL of PGE_2 monoclonal antibody (Cayman Chemical). The control wells received 50 μL of 1X EIA

buffer along with 50 µL of PGE_2 EIA AChE tracer and 50 µL of PGE_2 monoclonal antibody. The plate was covered and kept at 4 ^{o}C for 16 hours. The plate was then washed and 200 µL of Ellman's reagent (Cayman Chemical) was added to each well and was allowed to develop in the dark with low shaking at room temperature for 90 minutes. Following the developing step, absorbance in each well at 405 nM was read using a microplate spectrophotometer (BMG Labtech FLUOStar Optima). This assay was normalized by WST-1 assay (Roche Diagnostics) following the manufacturer's instructions. WST-1 reagent (10 % of the total volume) was added to the cells and the plate was incubated at 37 °C for 30 minutes. The optical density was then measured (at 450 nM vs. a reference of 630 nM) using microplate spectrophotometer (BIO-TEK KC Junior).

Confocal microscopy: A549 cells were seeded onto 22×22 mm coverslips (Fisher) in 35 mm diameter plates in their appropriate media and incubated at 37 ˚C under 5 % CO_2 overnight. The following day, cells were transfected with adenovirus containing GFP-$cPLA_2$ at 10 MOI. After 48 hours incubation, the cells were treated with C1P or PA (1µM) solubilized in ethanol dodecane (98:2). Cells were washed twice with PBS to remove the excess of protein and then fixed on the coverslips with 100 % cold methanol for 10 min at -20 °C. Coverslips were mounted in 10 mM n-propagalate in gycerol, and were viewed using Olympus BX50WI confocal microscope at 488 nM (Fluoview detector) using a 40x liquid immersable lens with a 1.5x-enhanced magnification. microscopy.

Lipid uptake analysis by radiolabeled C1P: D-e-$C_{18:1}$ ceramide was subjected to enzymatic conversion to C1P in the presence of λ^{32}P labeled ATP as previously described (41, 75) and purified as previously described (41, 75). A549 cells were seeded onto 10 cm dishes at a density of 5 x 10^4 and incubated overnight under standard incubation conditions. On the day of treatment the cells were washed in PBS and transferred to media containing 2% serum and incubated under standard incubation conditions for two hours. Lipids were prepared by mixing radiolabeled and unlabeled C1P such that the final lipid concentration was 1mM. These lipids were solubilized either in EtOH/dodecane as described elsewhere, or by sonicating in water for five minutes. The resulting 1mM lipid solutions were added to the cells at a dilution of 1:1000 and incubated for two hours. At the end of the incubation period the cells were washed three times in ice cold PBS prior to fractionation.

Subcellular fractionation of plasma membrane versus internal membranes: The plasma membranes of the harvested cells were disrupted by four consecutive freeze thaw cycles. The internal membranes were separated from the plasma membrane by centrifugation at 10,000 g for 5 minutes. The two fractions were counted separately using a Beckman LS 6500 scintillation counter.

Subcellular fractionation of different organelle membrane fractions: A549 cells in 10 cm plates treated for lipid uptake, were suspended in buffer containing 20 mM HEPES (pH 7.4), 10 mM KCl, 2 mM $MgCl_2$, 1 mM EDTA, 0.25 M sucrose, and protease inhibitor

cocktail (Sigma). The plasma membranes of the harvested cells were disrupted by four consecutive freeze thaw cycles followed by homogenization by passing through a 23G needle 10 times. Subcellular fractionation was performed by differential centrifugation using a modification of the technique described by Maceyka *et al* (98). The postnuclear supernatants were centrifuged at 5,000 *g* for 10 min to generate the heavy membrane (mitochondria- and *trans*-Golgi-enriched fraction). The supernatants were then centrifuged at 17,000 *g* for 15 min to obtain the light membrane fraction (endoplasmic reticulum- and *cis*-Golgi-enriched fraction). The remaining supernatants were centrifuged at 100,000 *g* for 1 h to obtain the plasma membrane and the cytosol. 100 µl of each fraction was counted using a Beckman LS 6500 scintillation counter.

Mass spectrometric analysis: **(**1 x 10^6) A549 cells were seeded onto 10 cm dishes and incubated overnight under standard incubator conditions. The following day cells were washed with PBS and treated with 1µM solution of D-erythro-$C_{18:1}$ C1P or ceramide for 2 hours in 2% medium. Thereafter, the cells were washed and harvested in cold PBS as described (99). The cell pellets were stored at -80°C until extraction and analyzed by mass spectrometry. An aliquot of cells was taken for standardization (Total DNA). The lipids were extracted as described by Merrill *et al* (99) and quantified using liquid chromatography electrospray ionization tandem mass spectrometry using a Shimadzu HPLC system coupled to a 4000 QTRAP mass spectrometer (Applied Biosystems) as described (99).

Statistical analysis: Statistical differences between treatment groups were determined by a 2-tailed, unpaired Student t test when appropriate. P values less than or equal to 0.05 were considered significant.

Results

C1P activates cPLA$_2$α in a chain length-specific manner.

C1Ps ranging from acyl chain lengths of 14 to 26 carbons are present in mammalian cells with $C_{16:0}$, $C_{18:0}$ and $C_{24:1}$ generally being the more abundant. However, there are reports as to the existence of chain lengths as short as 2 carbons (100) and many studies have utilized C_2-C1P as an exogenous agonist (37, 101, 102). In this study the ability of various chain lengths of C1P to activate cPLA$_2$α was examined. To this end, we utilized C_2, C_6, C_{16} and $C_{18:1}$ C1P and an established *in vitro* assay for cPLA$_2$α. All chain lengths of C1P except C_2-C1P substantially activated cPLA$_2$α (Figure 3.1). C_2-C1P induced an insignificant increase in cPLA$_2$α activity similar to that of our previous reports of S1P, LPA and PA (Figure 3.1). C_4-C1P was also able to activate the enzyme to the same extent as $C_{18:1}$-C1P (data not shown). Thus, C1P requires an acyl chain length of ≥ 4 to 6 carbons for significant activation of cPLA$_2$α.

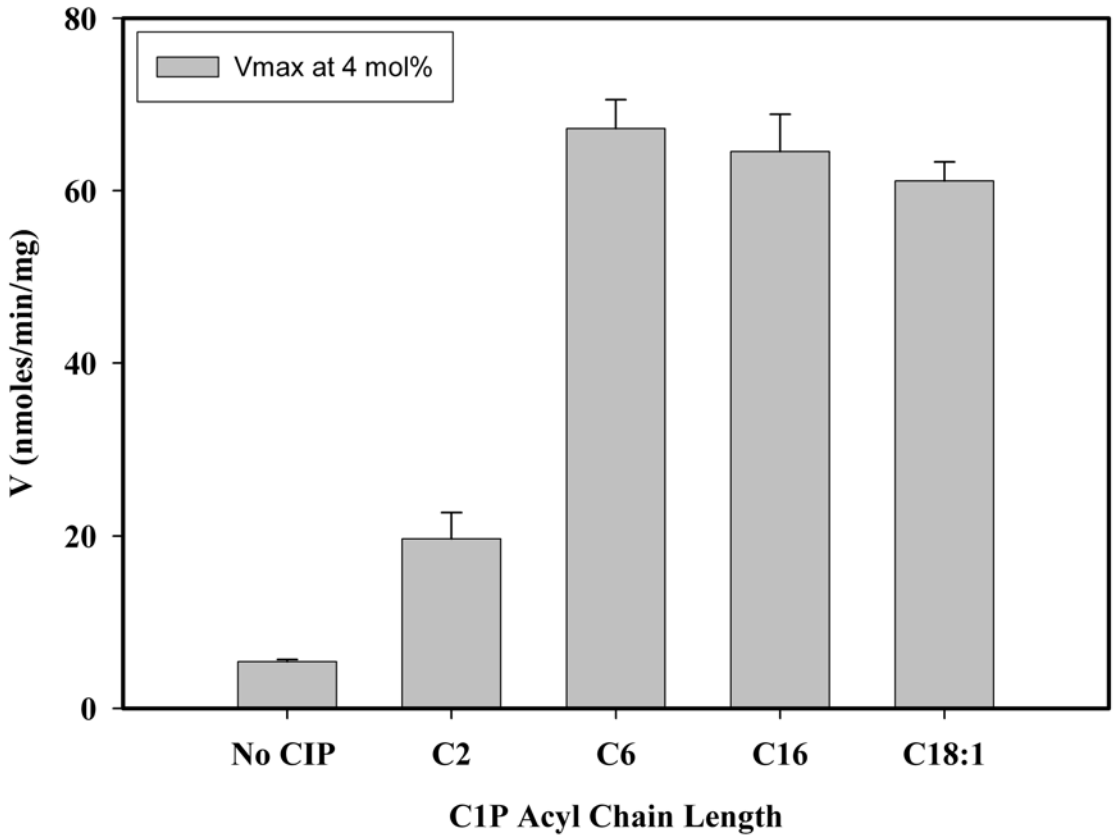

Figure 3.1. Activation of cPLA$_2$α by C1P is dependent on the acyl chain length. cPLA$_2$α activity was measured as a function of PC molar concentration in the absence and presence of 4 mol % D-*erythro* C_2, C_6, C_{16}, and $C_{18:1}$ C1P for 45 min at 37 °C as described under "Experimental Procedures". The PC mole fraction was held constant at 0.137. Data are presented as cPLA$_2$α activity measured as nanomoles of arachidonic acid produced/minute/milligram of recombinant cPLA$_2$α± S.E.

Natural ceramide-1-phosphate is a lipid-specific inducer of AA release, cPLA$_2$α activation and eicosanoid synthesis.

The recent report by Bornancin and coworkers (96) elegantly and comprehensively demonstrated that the biological effects on cells, in particular PGE_2 synthesis and cell death, were not lipid specific when: 1) high doses of lipids were used (10 μM), and 2) the lipids were delivered using ethanol/dodecane. In 2003, our laboratory demonstrated that a lipid-specific effect on the activation of cPLA$_2$α, induction of AA release, and eicosanoid synthesis was observed for C1P when low doses of lipids (≤ 1 μM) were utilized using the ethanol/dodecane delivery system (32, 67). Furthermore, a collaboratory study with Spiegel and co-workers demonstrated no loss of cell viability when < 5μM of C1P was delivered to cells via ethanol/dodecane. Therefore, we hypothesized that the dose of lipids utilized when delivered via ethanol/dodecane was the reason for these contrasting observations, and chose to validate this lipid delivery system before proceeding to examine the chain length specificity of C1P activation of cPLA$_2$α in cells. Therefore, we first examined the effects of related/similar lipids delivered via EtOH/dodecane (98:2 v/v) on cPLA$_2$α translocation, AA release, and eicosanoid synthesis. Treatment of A549 cells with D-erythro-$C_{18:1}$ ceramide-1-phosphate, a naturally occurring sphingolipid, rapidly induced an increase in AA release (Figure 3.2, Panel A) with concomitant increase in PGE_2 synthesis (Figure 3.2, Panel B). This effect was dose-dependent with an EC_{50} of 400 nM C1P at 2 hours with 200 nM C1P inducing a significant increase in AA release and PGE_2

synthesis. Therefore, treatment of cells with C1P induces activation of a PLA_2 species and induces a dose-dependent increase in AA release, which subsequently leads to eicosanoid production. As previously reported by our laboratory, C1P at ≤1μM had no effect on cell viability (Pettus el al *2003*, Mitra *et al* 2007, data not shown)

To demonstrate that the effect of C1P on AA and PGE_2 release was lipid-specific, A549 cells were also treated in the same experiments with various doses of the closely related lipid, di-oleolyl phosphatidic acid (PA), and a direct metabolite of C1P, and D-erythro $C_{18:1}$ ceramide (Cer) (Figure 3.2A). Both ceramide and PA had only marginal effects on AA release (approximately 2-fold) in the sub-micromolar range as compared to treatment of A549 cells with the vehicle control requiring at least 750 nM for the effect. PGE_2 synthesis followed a similar patter of induction (Figure 3.2B). Higher doses of PA (≥1μM) did induce dramatic AA release (62% as effective as C1P on AA release) in accord with the findings of Bornancin and co-workers (96) (data not shown). Thus, C1P is a potent and specific effector of AA and PGE_2 release in cells when sub-micromolar doses of lipids were added exogenously in ethanol/dodecane.

We then examined the lipid specificity of $cPLA_2\alpha$ activation. Upon activation, $cPLA_2\alpha$ is translocated from the cytosol to associate with the Golgi and perinuclear membranes in cells (32). Therefore, to determine the lipid specificity of $cPLA_2\alpha$ activation/translocation in cells, we examined whether C1P versus PA affects the association of $cPLA_2\alpha$ with cellular membranes using $cPLA_2\alpha$ fused to green fluorescent protein (GFP). Treatment of

A549 cells with 500 nM C1P for 2 hours induced a significant increase of cPLA$_2$α in the Golgi and perinuclear membranes (Figure 3.2C). The same doses of PA or the delivery medium alone had no effect on the translocation of cPLA$_2$α (Figure 3.2C).

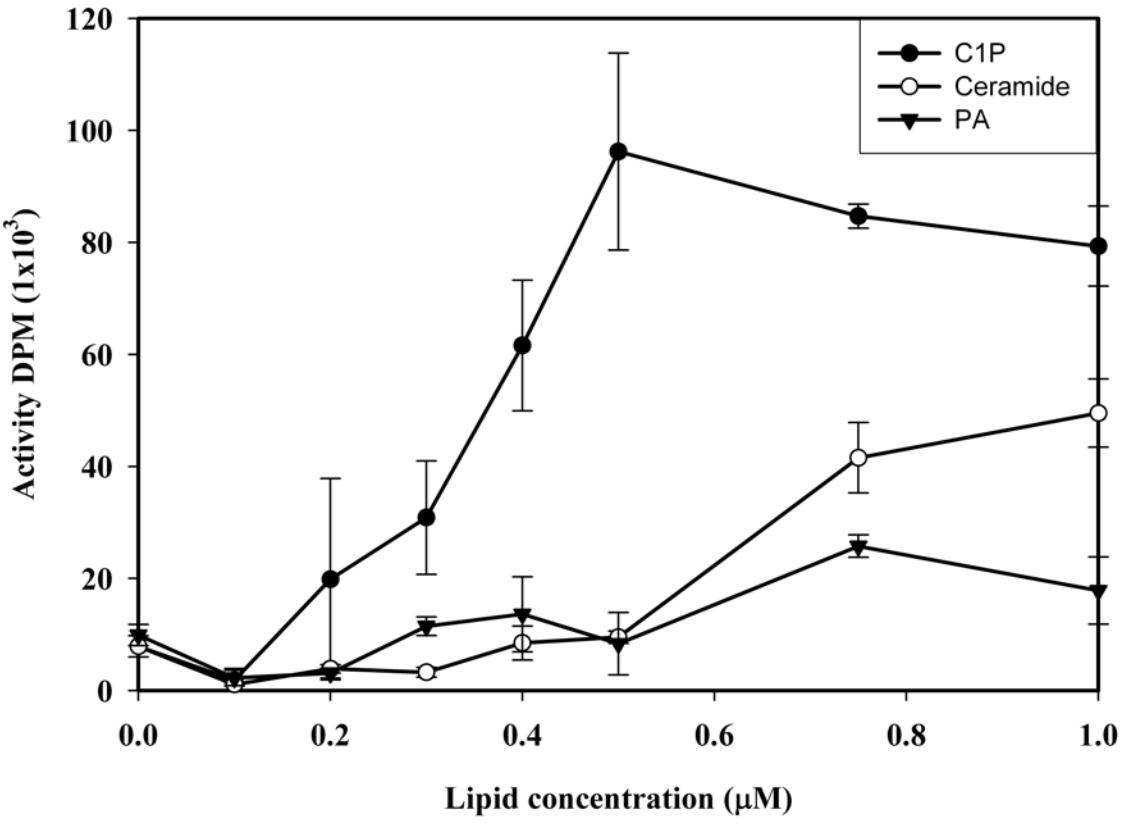

Figure 3.2: The effects of natural ceramide-1-phosphate on AA release and PGE_2 synthesis. Panel A. The effects of ceramide-1-phosphate on AA release is lipid specific at low doses. A549 cells (5 x 10^4) were labeled overnight with 5 μCi/mL [^{3}H]-arachidonic acid (5 nM). Cells were washed and placed in DMEM supplemented with 2% fetal bovine serum for two hours, followed by treatment with 0.1, 0.2, 0.3, 0.4, 0.5, 0.75 and 1 μM of D-e-$C_{18:1}$ C1P (●), 1-palmitoyl-2-oleoyl-*sn*-glycero-3-phosphate (PA) (▼) or D-e-$C_{18:1}$ ceramide (○) solubilized in 2% dodecane/98% EtOH (final concentration in treatments was 0.002% dodecane/0.098% EtOH) for 2 hours. For quantification of AA release, media was transferred to 1.5 mL polypropylene tubes, centrifuged 10,000 x g, and ^{3}H arachidonic acid determined by scintillation counting. The results are presented as DPM of ^{3}H-arachidonic

acid per mL of media controlled for equivalent number of cells by MTT assay. Data are representative of 15 separate determinations on 5 separate occasions.

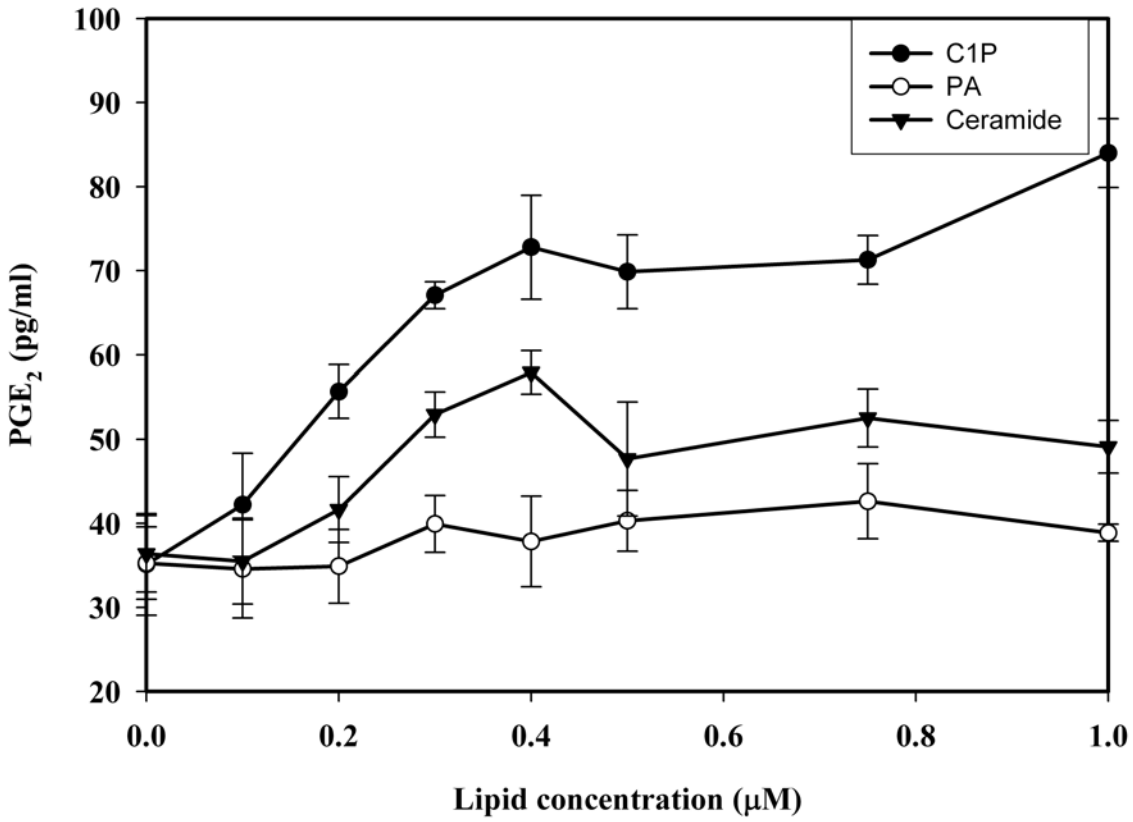

Figure 3.2. Panel B. Natural ceramide-1-phosphate, but not the structurally similar PA nor ceramide is capable of inducing PGE_2 synthesis. A549 cells (5 x 10^4) were washed and placed in DMEM supplemented with 2% fetal bovine serum for two hours. Cells were then treated with 0.1, 0.2, 0.4, 0.5, 0.75 and 1 μM D-e-$C_{18:1}$ C1P (●), 1-palmitoyl-2-oleoyl-*sn*-glycero-3-phosphate (PA) (○) or D-e-$C_{18:1}$ ceramide (▼), solubilized in 2% dodecane/98% EtOH (final concentration in treatments was 0.002% dodecane/0.098% EtOH) for 2 hours. For measurement of PGE_2 levels, media were assayed according to manufacturer's instructions using the Prostaglandin E_2 monoclonal EIA Kit from Cayman Chemical (Ann Arbor, MI, Catalog No. 514010). Briefly, media

containing PGE_2 competes with PGE_2 acetylcholinestaerase conjugate for a limited amount of PGE_2 monoclonal antibody. The antibody-PGE_2 conjugate binds to a goat-anti-mouse antibody previously attached to the wells. The plate is washed to remove any unbound reagents and then the substrate to acetylcholinesterase is provided. The concentration of PGE_2 in a sample is inversely proportional to the yellow color produced. The results are presented as pg of PGE_2 per mL of media controlled for equivalent number of cells by MTT assay. Data are representative of 6 separate determinations on 2 separate occasions.

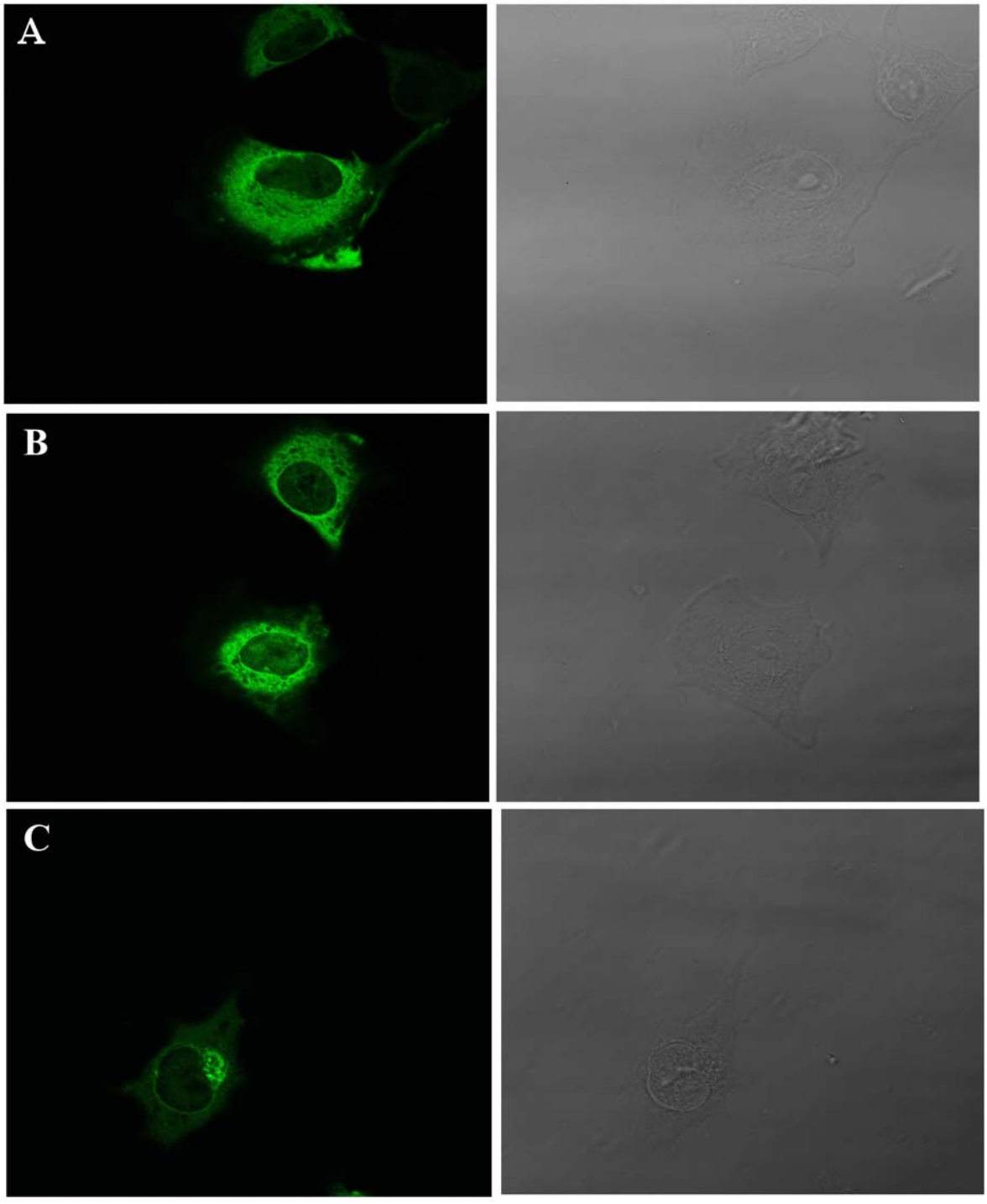

Figure 3.2 Panel C: cPLA$_2$α translocates specifically in response to ceramide-1-phosphate. A549 cells (1 x 10^5) were infected at 10 MOI with an adenoviral construct containing cPLA$_2$α-GFP. 48 hours post infection, cells were treated with 500 nM D-e-$C_{18:1}$ Ceramide (**A**), 500 nM 1-palmitoyl-2-oleoyl-*sn*-glycero-3-phosphate (PA) (**B**) and 500 nM D-e-$C_{18:1}$ceramide-1-phosphate (**C**), all solubilized in 2% dodecane/98% EtOH (final concentration in treatments was 0.002% dodecane/0.098% EtOH) for 2 hours. cPLA$_2$α localization was visualized using an Olympus BX50WI confocal microscope at 488 nM (Fluoview detector) using a 40x liquid immersable lens with a 1.5x-enhanced magnification. Data are representative of three separate determinations on 2 separate occasions.

To determine whether the activation of cPLA$_2\alpha$ by C1P was dependent on delivery of C1P by ethanol/dodecane, naturally occurring C1P was directly sonicated in water and delivered to NR8383 macrophages. A significant increase in AA release at 15 μM C1P was observed (Figure 3.3). In addition, the stimulation of AA release in the macrophages was specific for C1P as other related phospholipids S1P (data not shown) and PA had no effect (Figure 3.3). Although higher doses are required, C1P induces activation of the eicosanoid cascade irrespective of delivery vehicle and in a lipid-specific manner.

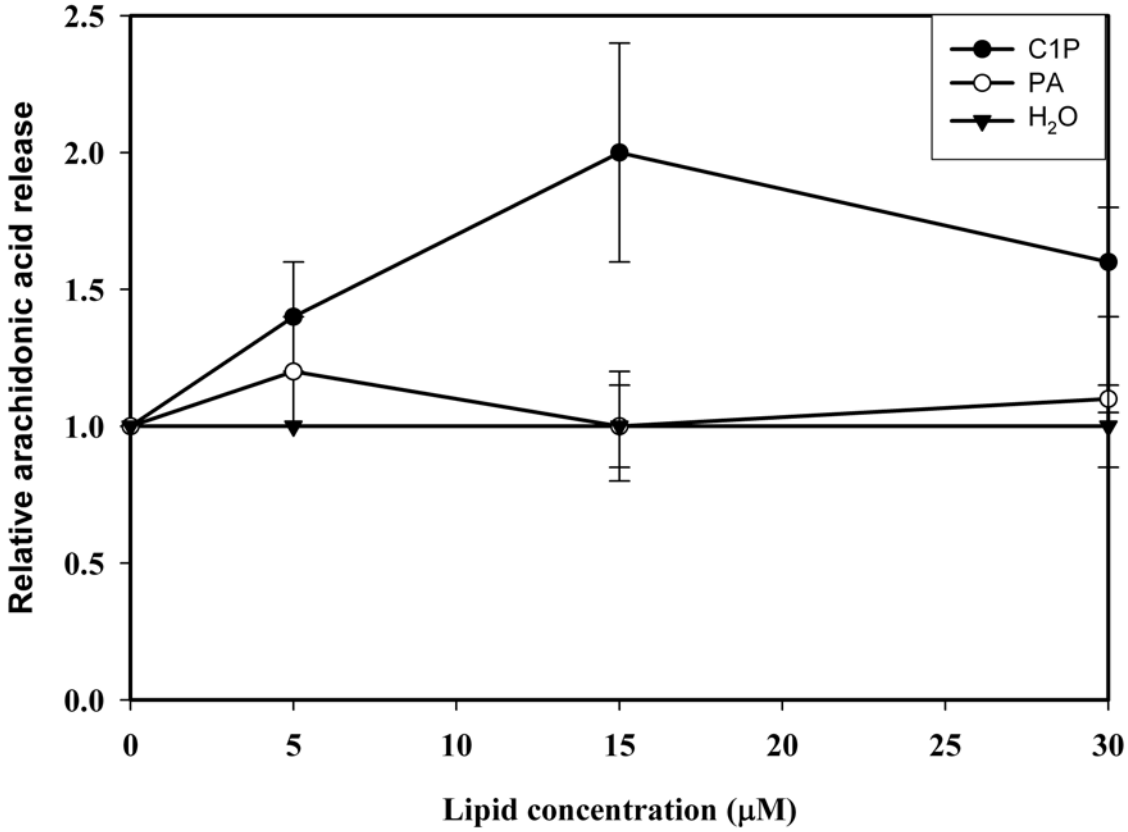

Figure 3.3. Activation of cPLA$_2\alpha$ by C1P is independent of its delivery medium. [^{3}H]-Arachidonic acid (0.20 μCi/ml) labeled NR8383 cells (1x10^6 cells/ml) were treated with C1P (●), PA (○) and H_2O (▼) sonicated in water at 5, 15 and 30 μM for six hours. For quantification the media was collected and centrifuged at 10000 x g for 5 minutes and the amount of [^{3}H] labeled arachidonic acid in the media was quantified by scintillation counting. The results are presented as DPM of radioactivity per mL of media.

Exogenous C1P is slowly metabolized to ceramide.

Bornancin and coworkers (96) reported that C1P delivered by EtOH/dodecane was rapidly metabolized, and its uptake was not enhanced by this delivery system. We hypothesized that this observation on uptake and metabolism by may be due to the toxicity induced by using 10 μM C1P delivered with EtOH/dodecane, or the use of the unnatural analogue, NBD-C1P. To determine, the kinetics of C1P metabolism and also examine cellular uptake, A549 cells were treated with natural (D-e-$C_{18:1}$) ceramide, and C1P, and the levels of these lipids were analyzed by mass spectrometry (Figure 3.4). C1P exogenously delivered by ethanol-dodecane demonstrated a rapid increase (within two hours) in the 18:1 acyl chain length of endogenous C1P in A549 cells (Figures 3.4). The data also demonstrate that C1P was slowly metabolized to ceramide in A549 cells (Figure 3.4 inset) with only a small increase in $C_{18:1}$ ceramide upon addition of D-e-$C_{18:1}$ C1P to cells. This translated into only a 2.8 % increase in total ceramide in accord with the recent collaboratory publication with Spiegel and co-workers (103). Thus, natural C1P delivered in low doses to A549 cells is not metabolized rapidly to ceramide at sub-micromolar concentrations.

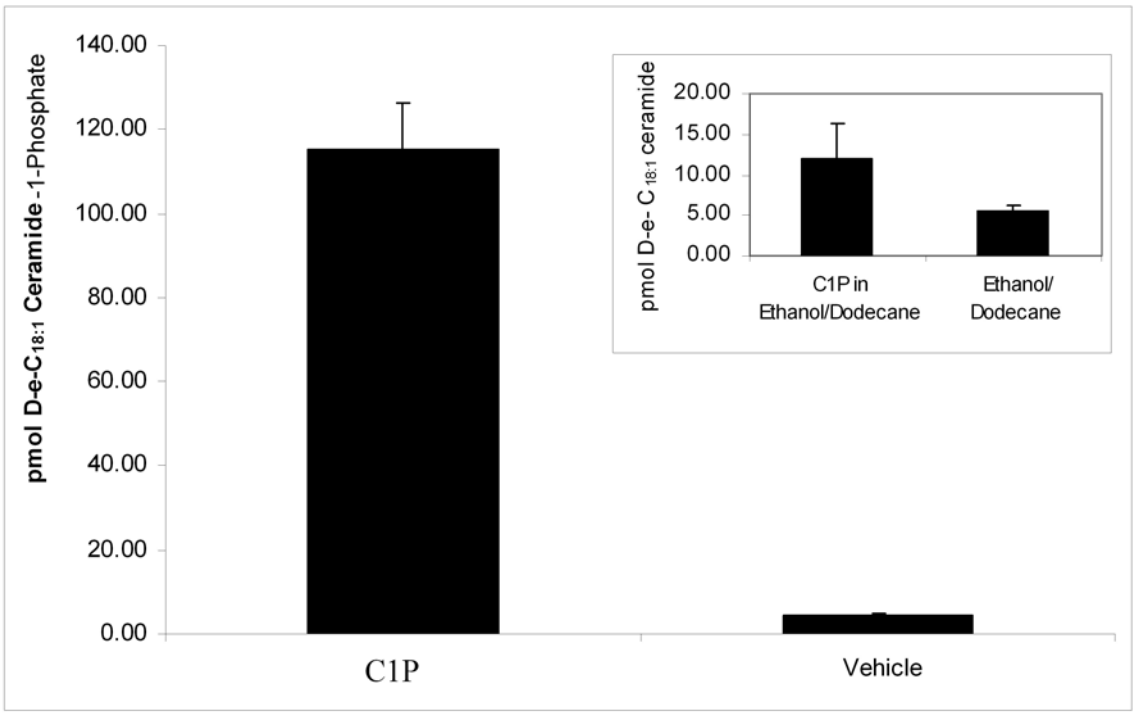

Figure 3.4: C1P is efficiently delivered to cells via EtOH/dodecane and is slowly metabolized to ceramide. A549 cells (1 x 10^6) were treated with 500μM D-e-$C_{18:1}$ C1P for 2 hours. The cells were then harvested and lipids extracted followed by analysis by mass spectroscopy. Data are presented as pmols of lipid. **Panel A inset.** Exogenously added C1P is slowly metabolized to ceramide. A549 cells (1 x 10^6) were treated with 500μM D-e-$C_{18:1}$ C1P for 2 hours. The cells were then harvested and lipids extracted followed by analysis by mass spectroscopy for C1P and ceramide (inset). Data is presented as pmols lipids.

C1P is delivered more efficiently to internal membranes with EtOH/dodecane.

Currently the delivery of C1P as vesicles is considered non-toxic to cells. However, the relative efficiency of this method for delivering C1P to internal membranes when compared to EtOH/dodecane system is not known. To investigate the uptake efficiency of C1P, we utilized ^{32}P-labeled C1P at low doses to examine the uptake of C1P delivered via ethanol/dodecane versus vesicle-based delivery (Figure 3.5). Following treatment (500 nM C1P for 2 hours), the concentration of radiolabeled C1P in the total internal membranes was found to be increased >2 fold when delivered via EtOH/dodecane versus vesicles (Figure 3.5A). Thus, C1P delivered via the EtOH/dodecane method is more efficient in delivering C1P to internal membranes.

In order to further compare the intracellular membranes for lipid delivery by ethanol/dodecane versus vesicles, radiolabeled C1P (^{32}P) was delivered using both ethanol/dodecane and sonicated vesicles followed by subcellular fractionation as previously described by our laboratory. The ethanol/dodecane delivery system was more efficient at delivering C1P to all internal membranes including the nucleus, mitochondria, *trans*-Golgi, the ER, and the *Cis*-Golgi when compared to vesicular delivery system (Figure 3.5B). Importantly, C1P was delivered > 3 fold by ethanol/dodecane to the site of cPLA$_2\alpha$ translocation (*trans*-Golgi enriched fraction) compared to sonicated vesicles.

Western analysis was used to confirm appropriate fractionation as previously described (Figure 3.5C) (104).

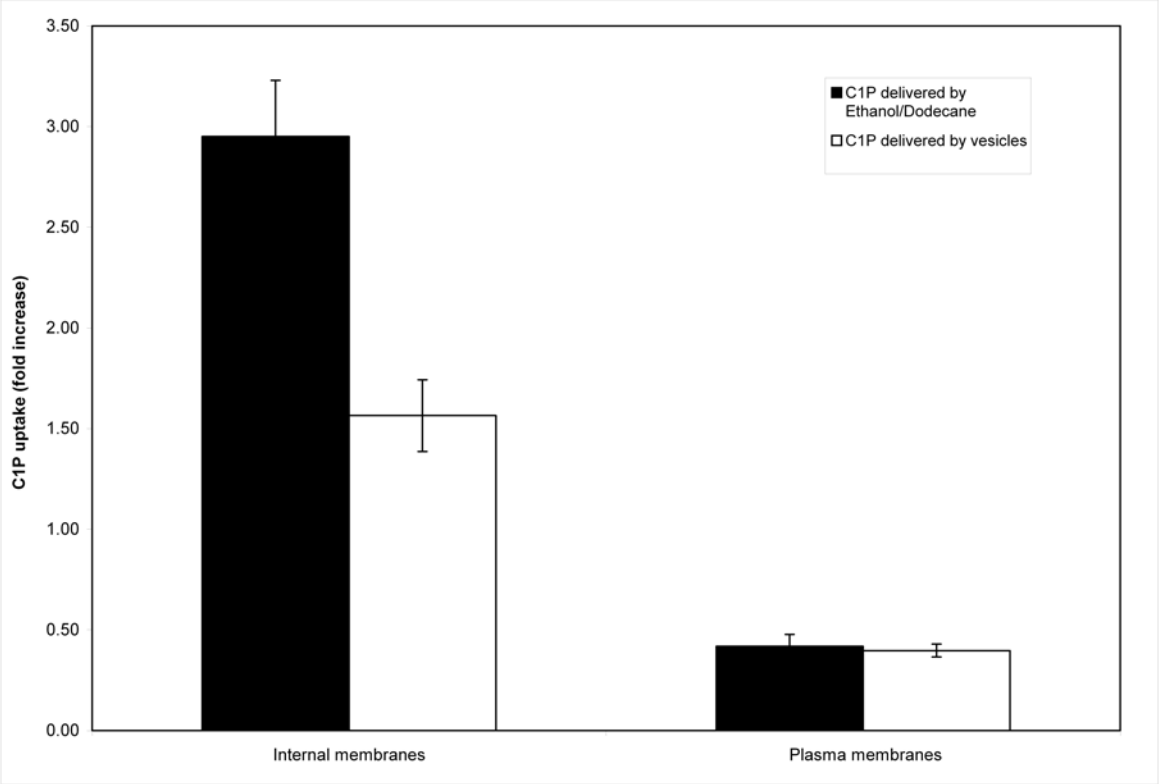

Figure 3.5: C1P is efficiently taken up by cells into internal membranes when delivered via ethanol/dodecane. Panel A. A549 cells (1 x 10^6) were treated for 2 hours with radiolabeled, 500μM D-e-$C_{18:1}$ C1P solubilized in either ethanol/dodecane or by sonication. The cells were then harvested and lysed by freeze thawing. The plasma membranes were separated from the internal membranes and the amounts of radiolabeled lipids in the different fractions measured by scintillation counting. The results are

presented as the fold increase of the levels of C1P over background in each fraction for the different methods of delivery.

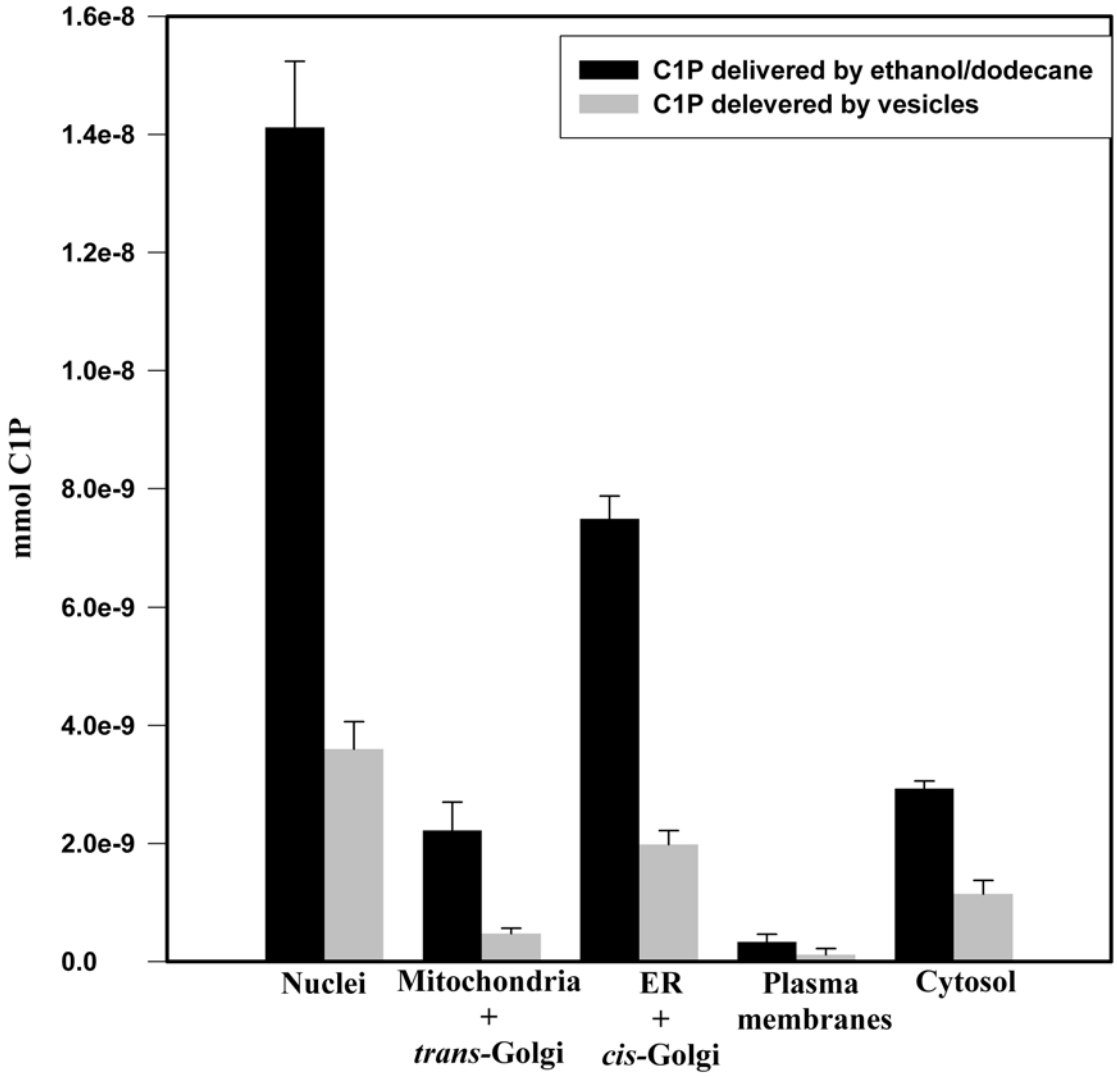

Figure 3.5 Panel B: C1P delivered via ethanol/dodecane system reaches specific internal membranes with higher efficiency. A549 cells (1 x 10^6) were treated for 2 hours with radiolabeled, 500μM D-e-$C_{18:1}$ C1P solubilized in either ethanol/dodecane or by sonication. The cells were then harvested and lysed by freeze thawing and homogenized. The resultant mixture was subjected subcellular fractionation via differential centrifugation

as previously described (104). All fractions were confirmed as previously described by our laboratory (104). The results are presented as a comparison of the levels of C1P in each fraction for the different methods of delivery of C1P.

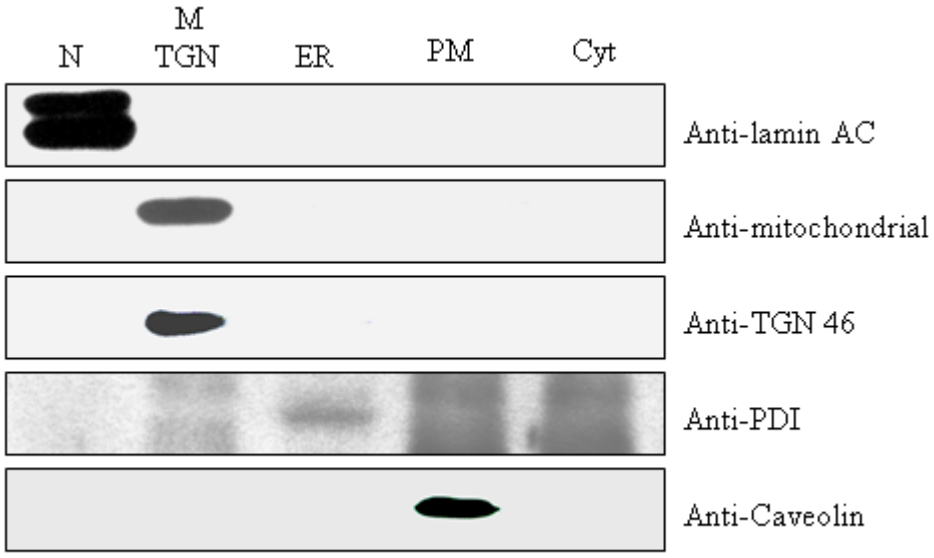

Figure 3.5 Panel C: Differential centrifugation allows the separation of the different organelles into different subcellular fractions. A_{549} cells treated and subjected to subcellular fractionation as in 5B to obtain nuclear (N), mitochondrial and trans-Golgi (M,TGN), Endoplasmic Reticulum (ER), plasma membrane (PM) and cytosolic (Cyt) fractions. All fractions were probed with organelle specific markers to assay for purity of the fractions. Anti-lamin AC (santa Cruz 1:1000) for nuclear, anti-mitochondrial (AbCam 1:1000), anti-TGN46 for trans-Golgi (AbCam 1:1000), anti- protein disulfide isomerase (PDI) for ER(AbCam 1:1000), anti-caveolin 1 for plasma membrane (Santa Cruz 1:1000). Note: Only the ER fraction demonstrated the proper PDI signal. The chemiluminescence signals observed in the other fractions are non-specific.

Long chain C1P specifically induces AA release by cPLA$_2$α

Once the ethanol/dodecane delivery system was established to deliver C1P to the proper organelles and produce a lipid specific activation of cPLA$_2$α, we investigated the effects of C_2, C_6, C_{16} and $C_{18:1}$ C1P treatment on cells. Although, the cellular concentration of C_2-C1P in internal membranes increased to the same extent as the $C_{18:1}$-C1P when delivered by the ethanol/dodecane delivery system (Figure 3.6A inset), induction of AA release was not observed (Figure 3.6A). Thus, intracellular activation of a PLA$_2$ species by C1P is also chain length specific.

To investigate, whether C_2-C1P could activate cPLA$_2$α in cells, we again delivered short chain (C_2) and long chain ($C_{18:1}$) C1P to A549 cells using the ethanol/dodecane system. The levels of membrane associated and cytosolic cPLA$_2$α following C1P treatment was measured. Western blot analysis revealed a significant increase of cPLA$_2$α in the membrane fraction of the $C_{18:1}$ treated cells. However, no increase in cPLA$_2$α in the membrane fraction was observed in C_2-C1P treated cells (Figure 3.6B).

Recently our laboratory has identified the C1P binding site on cPLA$_2$α which allowed us to generate a mutant cPLA$_2$α (R57A/K58A/R59A) that significantly reduced binding to C1P yet has no effects on structure, basal activity or the calcium response (105). Using GFP-tagged wild type and mutant cPLA$_2$α, we investigated their translocation in response to $C_{18:1}$-C1P delivered by ethanol/dodecane in A_{549} cells. Confocal analysis revealed > 3-fold

translocation of the wild type cPLA$_2$α compared to the mutant in response to $C_{18:1}$-C1P (Figure 3.6C). As all other functionalities of the mutant cPLA$_2$α are the same as the wild type, we conclude that activation of cPLA$_2$α by C1P is via a direct interaction and not through an indirect effect of other nonspecific biologies associated with the lipid.

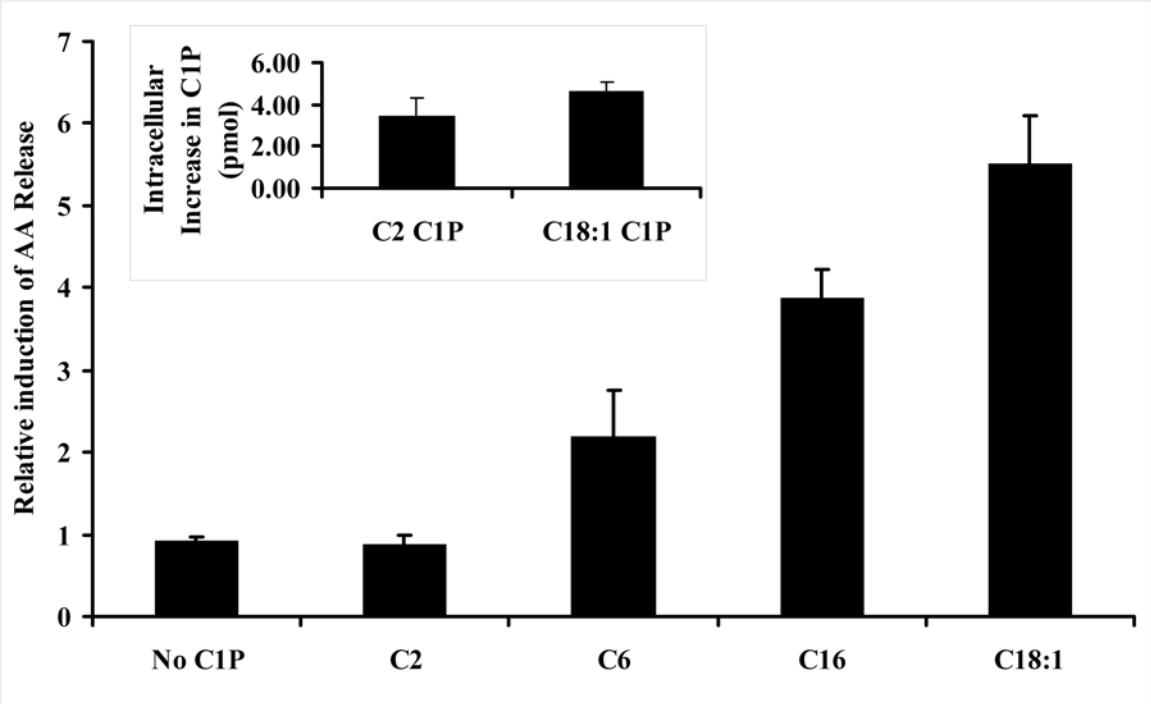

Figure 3.6. Naturally occurring C1P are the best activators of cPLA$_2\alpha$ *in-vivo*. Panel A. A549 cells (5 x 10^4) were labeled overnight with 5 μCi/mL [^{3}H]-arachidonic acid (5 nM). Cells were washed and placed in DMEM supplemented with 2% fetal bovine serum for two hours. Cells were then treated with either ethanol/dodecane alone, media (No C1P) or 0.5 μM D-*erythro* C_2, C_6, C_{16} and $C_{18:1}$ C1P solubilized in 2% dodecane/98% EtOH (final concentration in treatments was 0.002% dodecane/0.098% EtOH) as previously described for C1P(32) for 2 hours. For quantification of AA release, media was transferred to 1.5 mL polypropylene tubes, centrifuged 10,000xg, and ^{3}H cpm determined by scintillation counting. Results were controlled for equivalent number of cells quantified by WST assay. The results are presented as fold increase in AA release when compared to

ethanol/dodecane treatment. The results are an average of 3 experiments ± SD. **Panel A inset.** Ethanol/dodacane system successfully delivers both the long and short chain C1P's to cells. A549 cells (1 x 10^6) were treated for 2 hours with 1μM D-e-C_2 C1P or D-e-$C_{18:1}$C1P. The cells were then harvested and analyzed by mass spectrometry as previously described. Data are expressed as increase in pmol quantity of the lipid over that of the controls.

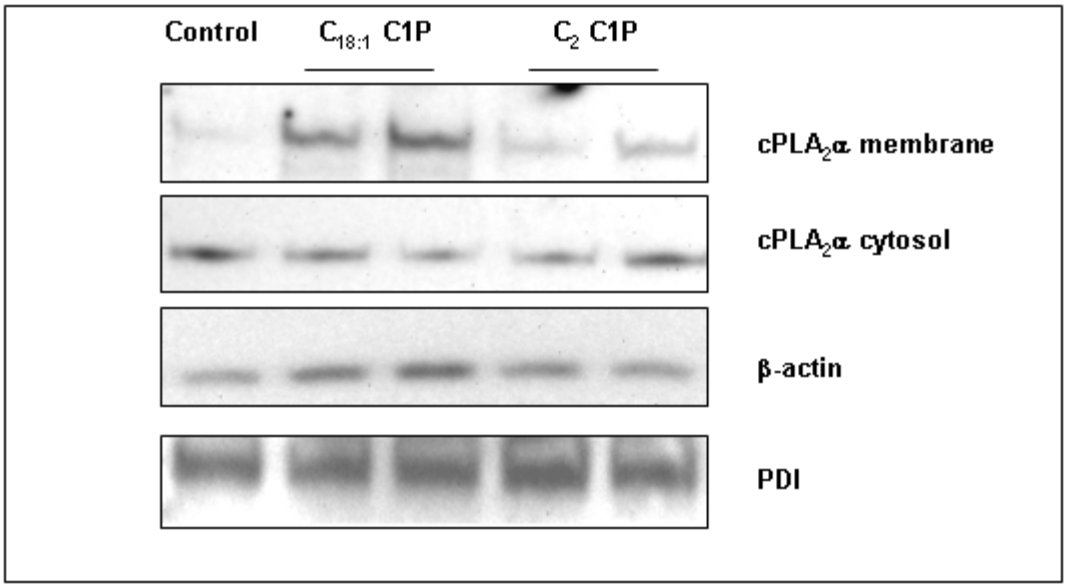

Figure 3.6. Panel B. cPLA$_2\alpha$ translocates to the membrane in response to natural long chain C1P but not the short C_2-C1P. A549 cells (1 x 10^5) were infected at 10 MOI with an adenoviral construct containing cPLA$_2\alpha$-GFP. 48 hours post infection, cells were treated with 500 nM D-e-$C_{18:1}$ C1P or C_2-C1P solubilized in 2% dodecane/98% EtOH (final concentration in treatments was 0.002% dodecane/0.098% EtOH) for 2 hours. The cells were subsequently lysed and centrifuged at 100,000 x g to separate membranes from the cytosol. Equal total protein from each fraction was subjected to western analysis and probed for the indicated proteins. Data are representative of three separate determinations on 2 separate occasions.

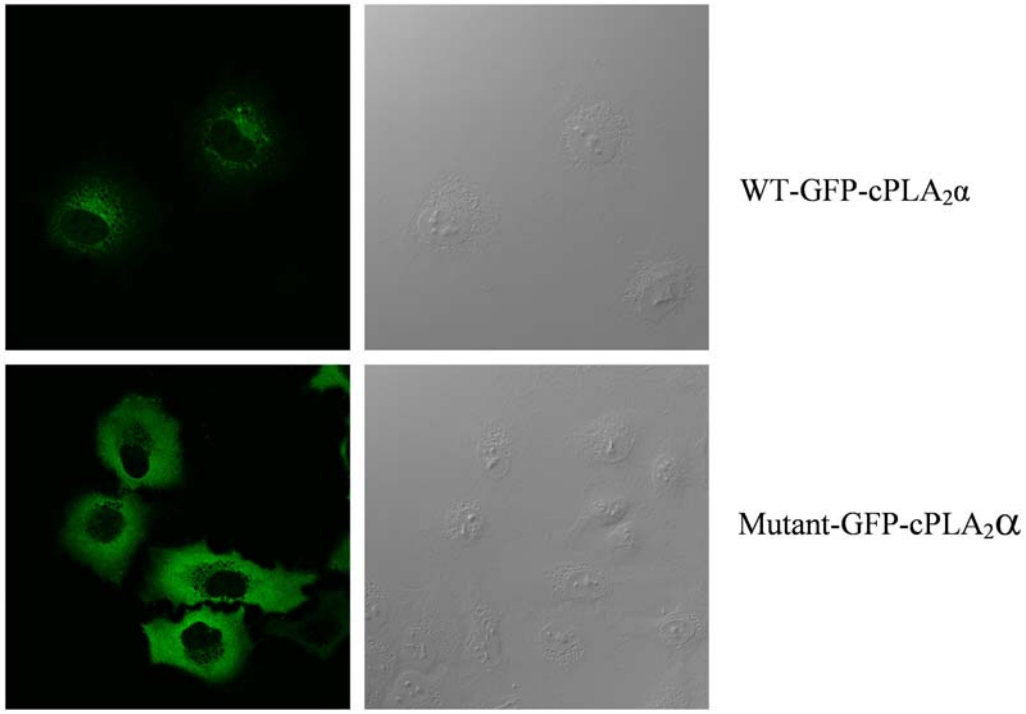

Figure 3.6. Panel C. Translocation of cPLA$_2$α in response to C1P is due to a direct interaction with C1P. A549 cells (1 x 10^5) were infected at 10 MOI with an adenoviral constructs containing wild type and mutant (R57A/K58A/R59A) cPLA2α-GFP. 48 hours post infection, cells were treated with 1μM D-e-$C_{18:1}$ C1P solubilized in 2% dodecane/98% EtOH (final concentration in treatments was 0.002% dodecane/0.098% EtOH) for 3 hours. cPLA$_2$α localization was visualized using an Olympus BX50WI confocal microscope at 488 nM (Fluoview detector) using a 40x liquid immersable lens with a 1.5x-enhanced magnification. Data are representative of three separate determinations on 2 separate occasions.

To further demonstrate that activation of cPLA$_2$α is limited to naturally occurring C1P, we compared the ability of the dimethyl ester of D-e-C$_{18:1}$ C1P and the naturally occurring D-e-C$_{18:1}$ C1P (Figure 3.7A) to activate cPLA$_2$α *in vitro* and in cells. Compared to the natural counterpart, dimethyl C1P was not able to activate of cPLA$_2$α in vitro (Figure 3.7B) and was a very poor inducer of AA release from cells (Figure 3.7C).

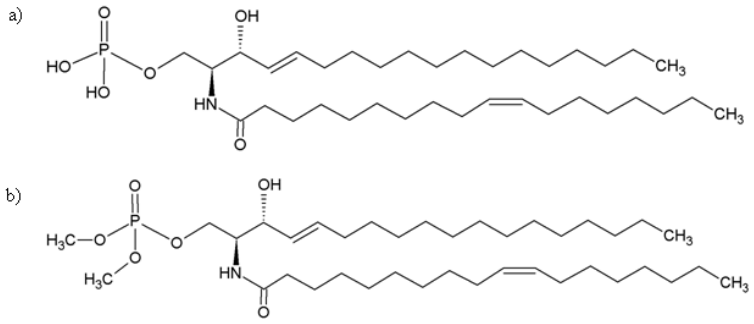

Figure 3.7 Panel A: D-e-C$_{18:1}$ dimethyl ester of C1P is structurally similar to D-e-C$_{18:1}$ C1P. a) D-e-C$_{18:1}$ C1P, b) D-e-C$_{18:1}$ dimethyl C1P.

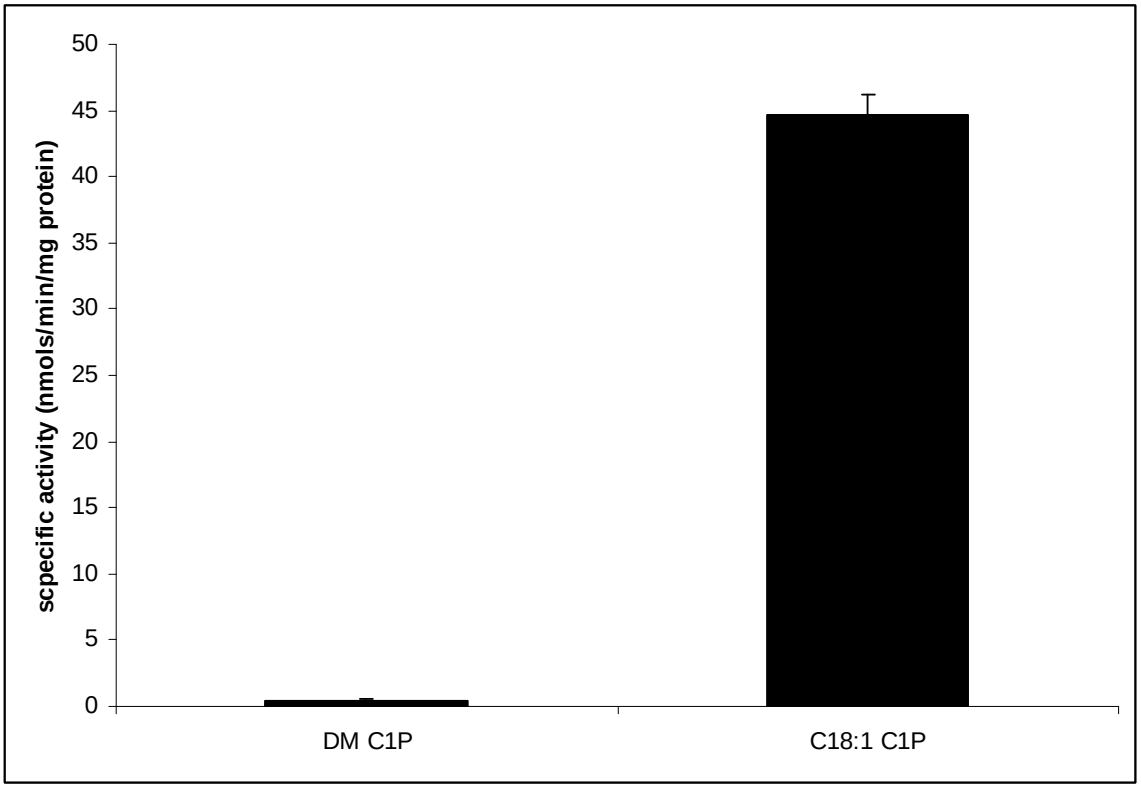

Figure 3.7 Panel B: The structurally similar dimethyl ester of D-e-$C_{18:}$ C1P does not activate cPLA$_2$α *in vitro*. cPLA$_2$α activity was measured as a function of PC molar concentration in the presence of 4 mol % D-e-$C_{18:1}$ C1P and dimethyl D-e-$C_{18:1}$ C1P for 45 min at 37 °C as described under "Experimental Procedures". The PC mole fraction was held constant at 0.137. Data are presented as cPLA$_2$α activity measured as nanomoles of arachidonic acid produced/minute/milligram of recombinant cPLA$_2$α± S.E.

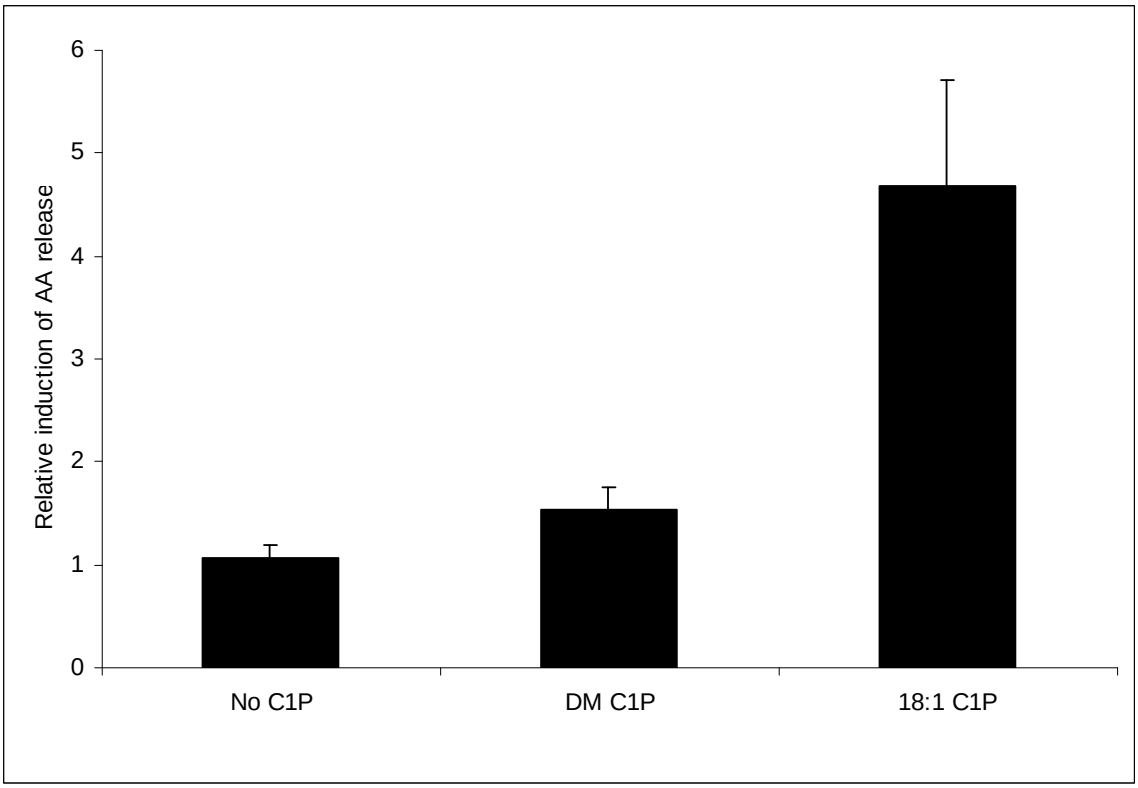

Figure 3.7 Panel C: Compared to naturally occurring C1P, the dimethyl ester of D-e-C_{18}: C1P is a very poor inducer of arachidonic acid release. A549 cells (5 x 10^4) were labeled overnight with 5 μCi/mL [^{3}H]-arachidonic acid (5 nM). Cells were washed and placed in DMEM supplemented with 2% fetal bovine serum for two hours. Cells were then treated with either ethanol/dodecane alone, media (No C1P) or 0.5 μM dimethyl ester of D-e-$C_{18:1}$ C1P or the naturally occurring D-e-$C_{18:1}$ C1P solubilized in 2% dodecane/98% EtOH for 2 hours (the final concentration in treatment groups was 0.002% dodecane/0.098% EtOH as previously described for C1P (32)). For quantification of AA release, media was transferred to 1.5 mL polypropylene tubes, centrifuged 10,000 x *g*, and ^{3}H cpm determined by scintillation counting. Results were controlled for equivalent

number of cells quantified by WST assay. The results are presented as fold increase in AA release when compared to ethanol/dodecane treatment. The results are an average of 3 experiments ± SD.

DISCUSSION

Previously, our laboratory reported in 2003 that C1P delivered in ethanol:dodecane stimulated cPLA$_2$α in A549 cells in a lipid-specific manner (32). However, the acyl chain length specificity of C1P for this interaction was not examined. In both *in-vitro* and cellular studies, C_2-C1P was not able to significantly increase AA release over control. Therefore, this study demonstrates that an acyl chain length of > 2 carbons was necessary for activation of cPLA$_2$α. Furthermore, data from cellular studies, where C1P was delivered in ethanol/dodecane, indicate that the naturally occurring C1P's are the most potent activators of cPLA$_2$α with C_{16} and $C_{18:1}$ C1P giving over a 4-fold increase in AA release over C_2-C1P.

These findings have relevance to the reported biological mechanisms attributed to exogenous C1P treatment. For example, several studies, using C_2 C1P have shown intracellular increases in Ca^{+2} (102, 106). As cPLA$_2$α is a calcium-stimulated enzyme, it may be argued that the activation of cPLA$_2$α by C1P is due to an increase in intracellular calcium. The current data clearly demonstrate that C_2 C1P does not cause activation of cPLA$_2$α *in vitro*, nor release arachidonic acid through the activation of cPLA$_2$α when delivered to cells. Thus the activation of cPLA$_2$α by C1P is not via an increases in the intracellular Ca^{+2} levels, corroborating our earlier findings that ceramide kinase is required for activation of cPLA$_2$α by calcium ionophores. Furthermore, induction of calcium release

observed in response to C_2-C1P is not via the reverse mechanism of activation of cPLA$_2\alpha$ and subsequent generation of PGE_2 a known inducer of Ca^{+2} release.

Thus, the current study also highlights the usefulness of C_2-C1P in studying the biological effects of C1P that are independent of the activation of cPLA$_2\alpha$. For example, the stimulation of DNA synthesis and cell division observed by exogenous treatment with C_2 C1P (37) is not due to any downstream effects of the activation of cPLA$_2\alpha$ and increases in eicosanoids. Therefore, C_2-C1P is now a "tool" to examine non eicosanoids biologies regulated by C1P. Furthermore, C_2-C1P may also be used to differentiate between direct targets of cPLA$_2\alpha$ and A-Smase.

This study also provides additional proof that translocation of cPLA$_2\alpha$ to membranes in response to C1P is via a direct interaction as C1P binding site mutants showed significantly reduced translocation (Figure 3.6C). This mutant can now be used as a tool to investigate C1P independent translocation of cPLA$_2\alpha$. As the mechanisms and triggers behind the generation of C1P is not currently understood, this is an important tool to differentiate between agonists causing C1P-independent translocation from those causing translocation via a direct increase in C1P.

The observation that cPLA$_2\alpha$ is activated by long chain naturally occurring C1P is in agreement with our previous work (41) with regards to ceramide kinase, the only known mammalian enzyme to date to produce C1P. Substrate preference of CERK is for

ceramides containing acyl chains of at least 12 carbons (41). Confocal studies demonstrate that in A_{549} cells CERK localizes to the Golgi apparatus, the site of AA release by $cPLA_2\alpha$. Thus, it is quite clear that ceramide phosphorylation by CERK is geared towards producing C1P causing maximal activation of $cPLA_2\alpha$.

This study also addresses the recent publication by Bornancin and co-workers, which raised doubts as to the lipid specificity of the activation of $cPLA_2\alpha$ by C1P when delivered via the well established ethanol/dodecane system (96). We specifically show that the stimulation of arachidonic acid release in the macrophages and A549 cells were specific for C1P as other related phospholipids such as ceramide and PA failed to do so. The lipid-specific effect required the use of low doses of C1P (≤ 1 μM) as previously reported by our laboratory. C1P at concentrations ≤ 500 nM demonstrated complete lipid specificity in the induction of AA release from A549 cells. In accord with the recent report by Bornancin and co-workers (96), lipid specificity was lost as concentrations of phospholipids increased above 1 μM. The loss of lipid specificity correlated with the loss of cell viability as recently reported by Spiegel and co-workers (103) and Bornancin and co-workers (96). Thus, our study demonstrates that the contrasting findings between the two laboratories was the difference in concentration of C1P utilized. C1P is indeed a specific activator of AA release and $cPLA_2\alpha$ activation when low concentrations are utilized and no loss of cell viability is observed.

In agreement with the lipid-specific effect of C1P on AA release, the presented data also shows that C1P dispersed in water interacts readily with NR8383 macrophages to induce arachidonic acid release. This was also found in A549 cells, but higher concentrations were required than with the use of the EtOH/dodecane system (data not shown). The observation that C1P can activate cPLA$_2\alpha$ in the absence of dodecane, or any other organic solvent, is also relevant because it discards any possible non-specific interaction of the phospholipid with the organic compounds used for its delivery to cells in culture. In this regard, it should be emphasized that the stimulatory effect of C1P on proliferation of rat-1 fibroblasts and the inhibition of apoptosis in bone marrow-derived macrophages were all observed using C1P dispersed in water, in the absence of any organic solvent (37, 39, 91). Therefore, ideally, lipids should be delivered in aqueous solutions so as to avoid any side effects that might be generated when organic solvents are added to biological tissues or cells in culture. Unfortunately, high concentrations of the phospholipids are required and in the case of some cell types (e.g. A549 cells), vesiculated phospholipids are not as efficiently transported to certain internal membranes (e.g. *trans*-Golgi). In these cases, the dodecane/alcohol delivery system is an alternative for the enhancement of lipid uptake.

In conclusion, the presented study answers the contrasting observations from several laboratories on the biological effects of lipids delivered by ethanol/dodecane. This study also demonstrates that the alcohol/dodecane delivery system can be utilized to examine biological effects by specific lipids as long as certain controls are observed. In particular, researchers need to utilize low doses of lipids, less than 1 μM. Doses higher than 1 μM

have effects on cell stress and viability, which can cause misinterpretation of results. The metabolism of the lipid is also of key importance as well as uptake, thus the utilization of closely-related lipids as well as direct metabolites of similar solubilities should be utilized as specificity controls. Importantly, all of these parameters need to be established for each specific cell type as viability may be affected at lower concentrations. Furthermore, monitoring of efficient uptake of the lipid should also be undertaken. With these measures observed, this study demonstrates that the dodecane delivery system for lipids can be utilized to study specific biological effects especially when coupled to genetic, cell biology, and enzymology approaches. Lastly, this study also demonstrates that the C1P-cPLA$_2$α interaction is structurally specific with proper acyl chain length being an essential criterion for activation of the enzyme. Furthermore, cellular biologies observed from treatment of cells with C_2-C1P cannot be attributed to cPLA$_2$α activation and subsequent eicosanoids synthesis.

CHAPTER 4: A VALIDATED METHOD FOR THE QUALITATIVE AND QUANTITATIVE ANALYSIS OF C1P

INTRODUCTION

It has been well over a decade since the first biological activity of Ceramide 1 phosphate was described by Gomez-Munoz. Since then the number of biological activities attributed to C1P has been steadily increasing further enhancing its recognition as an important lipid signaling molecule. Currently C1P has been demonstrated to play a role in DNA synthesis, activation of cPLA$_2\alpha$ leading to the production of inflammatory mediators, degranulation of mast cells, inhibition of apoptosis via inhibition of aSMase.

Our laboratory was the first to demonstrate that CERK and C1P have distinct roles in eicosanoid synthesis. We showed that treatment of several cell types with nanomolar concentrations of C1P induced arachidonic acid (AA) release and the synthesis of eicosanoids (9). Furthermore, studies using pulse labeling demonstrated that the increase in C1P is concurrent with the release of AA and eicosanoids in response to inflammatory agonists (16). Small interfering RNA (siRNA) technology to downregulate CERK blocked cytosolic phospholipase A$_2\alpha$ (cPLA$_2\alpha$) activation, AA release, and eicosanoid production in response to inflammatory cytokines, ATP, and the calcium ionophore A23187 (9). Lastly, our laboratory defined the first intracellular target of C1P, cPLA$_2\alpha$, demonstrating that C1P interacted directly with the enzyme and functioned to increase the association of

cPLA$_2\alpha$ with membranes (16). These data demonstrated a new role for CERK and its product, C1P, as major regulators of eicosanoid synthesis via the direct activation of cPLA$_2\alpha$ (16).

Until very recently an easy, accurate and reliable method for detecting cellular levels of C1P was unavailable. The method used by most involved either the steady state or pulse labeling of C1P be feeding cells with ^{32}P labeled ATP, followed by a bligh and dyer lipid extreaction with base hydrolysis. These samples were then separated by TLC with the appropriate standards. The TLC spots corresponding to C1P as indicated by the standards were analyzed either by densitometry of the relevant spot in an X-ray film or by scraping off the spot from the plate and counting the radioactivity by scintillation counting. These methods have several shortfalls. First, working with of ^{32}P is hazardous to the health. The use of extra protective equipment to minimize radiation exposure makes the experiments difficult to perform. Due to the large amount of radiation used in the labeling, in order to minimize effects on health the number of experiments that can be performed is limited.

The development of biological Mass Spectrometry gave rise to a new tool for investigating the lipidome. The new soft ionization methods allowed for the identification and quantitation of intact biological molecules based on their molecular mass. An added layer of molecule specific quantitation was achieved with the use of tandem mass spectrometry where a biomolecule of a particular m/z can be further fragmented to identify a molecule/ molecular class specific fragment. However isobaric molecular species that produce

identical or nearly identical product ions are common in biological samples. A classic example of this are the prostaglandins. PGE_2 and PGD_2 are indistinguishable using standard ms^2 mass spectrometry. The same is true for PGD_1 and PGE_1. However coupling mass spectrometry with a liquid chromatographic separation allows for such isobaric species to be separated providing an added layer of identification based on the retention time of the compound.

The key to analysis of any biological molecule by mass spectrometry is the ability to efficiently ionize the molecule of interest into the gas phase. This is not a problem in the case of volatile compounds. However for large molecules that are not volatile, special techniques need to be used to produce gas phase ions. One such method is the chemical derivatization of the compound of interest. This method in addition to being time consuming is also prone to errors that lead to inconsistent quantitations.

Several direct ionization methods are now available to study biological molecules by mass spectrometry. Of these the most applicable are the soft ionization methods which include matrix assisted laser desorption ionization (MALDI) and electrospray ionization (ESI). However, the most successful would be a method that allows for a chromatographic pre-separation prior to mass spectrometric analysis. This is best provided by the ESI technique and as such, this has become the most widely used ionization method used in the analysis of biomolecules by mass spectroscopy in conjunction with liquid chromatography.

ESI allows for continuous flow operation of HPLC-MS/MS system where compounds separated by the HPLC is directly fed into the ESI source for ionization and detection by the mass spectrometer. It is tolerant of a wide range of solvent types providing leeway in the development of chromatographic separation techniques. In addition ESI can accept a wide range of solvent flow rates and being a soft ionization method gives rise to intact ions. An added bonus is the ability to produce multiply charged ions which greatly extends the range of molecular weights that can be analyzed.

Merrill *et al* has published a protocol for the quantitiative analysis of long chain bases (i.e. sphingosines, sphinganines, sphingosine-1-phosphate and sphinganine-1-phosphates) and C1P in the same run using reverse phase HPLC with a C18 column and a set of internal standards consisting of compounds in the same class as the analytes but having negligible biological abundance (99). While the method is well suited for analyzing long chain bases (LCB's), it has two major drawbacks when used to analyze C1P which raise doubts as to the accuracy of data generated using mass spectroscopy. First, the reverse phase HPLC method show high carryovers between samples. Second, the levels of C1P reported were massively overestimated and not in agreement with quantification by steady state labeling. Thus we sought to modify this published method to allow us to accurately quantify C1P levels in cells that are in agreement with the amounts of C1P observed by traditional methods (i.e. steady state labeling studies).

In the course of this study it was found out that the protocol published by Merrill et all (99), resulted in carryovers in excess of 10% for $C_{16:0}$ C1P. In addition we discovered that the cause for overestimated amounts of C1P is the hydrolysis of SM due to the dry down of samples following base treatment without proper neutralization. This led us to re-evaluate the published protocol and to develop a more reproducible assay for quantification of C1P by LC MS/MS. We show here method for C1P that is both qualitative and quantitative. In addition the method has been validated using steady state labeling techniques.

EXPERIMENTAL PROCEDURES

Cell culture: All cultured cells were obtained from the American Type Culture Collection. A549 lung adenocarcinoma cells were grown in 50% DMEM (BioWhittaker) and 50% RPMI (BioWhittaker) supplemented with 10% fetal bovine serum (Invitrogen) and 2% penicillin/streptomycin (BioWhittaker). Cells were maintained under 5% CO2 at 37jC by routine passage every 3 days. For treatments, the medium was replaced 2 h before the addition of the agonist by DMEM containing 2% fetal bovine serum and 2% penicillin/streptomycin.

RNA interference: Sequence-specific silencing of CERK and CERT was performed using sequence-specific siRNA purchased from Dharmacon as described previously (18). The human CERK RNA interference sequence starts at 142 nucleotides from the start codon (UGCCUGCUCUGUGCCUGUAdTdT and UACAGGCACAGAGCAGGCAdTdT) (9).

The siRNA for human CERT was from Dharmacon (catalog No. M-012101-00). The sequence targets accession numbers NM_005713 and NM_031361. They were transfected into A549 cells using Dharmafect (Dharmacon) according to the manufacturer's instructions. After incubation for 24, 48, or 72 h, cells were analyzed by Western blotting using a specific antibody against CERK or CERT. After incubation for 48 h, cells were analyzed for C1P levels by TLC or mass spectrometry.

Treatment with CERT inhibitors: A549 cells were plated on 10 cm plates in the appropriate medium and grown at 37jC under 5% CO2 overnight such that the cells were 80% confluent on the next day. The following morning, the media was changed to 2% serum and the cells were incubated for 3hrs. Stock solutions of HPA-12 inhibitor and its inactive racemic mixturea were made at 2mM in DMSO and were added to cells at dilutions of 1:1000 and 1:5000 to obtain final concentrations of 2µM and 0.4µM. DMSO by itself at the same dilutions were uses as the controls.

Mass spectrometric analysis: A549 cells were plated on 10 cm plates in the appropriate medium and grown at 37^0C under 5% CO2 overnight. The next day, cells were subjected to the relevant treatment. After treatment, the plates were placed on ice and the cells were washed once with ice cold PBS and harvested by scraping in 200 µl of PBS. An aliquot of cells was taken for standardization (total protein). Lipids were extracted from the remaining cells as described by Merrill *et al* with slight modifications. In summary, to the remaining cells 1 ml of methanol was added and sonicated to obtain a homogeneous mix

followed by the addion of 500 µl of chloroform and 500 pmols of internal standards (Avanti). Internal standards used were $d_{18:1/12:0}$ ceramide-1-phosphate sphingomyelin, ceramide, glucosylceramide, lactosylceramide and $d_{17:1}$-sphingosine, sphinganine, sphingosine-1-phosphate, sphinganine-1-phosphate. The mixture was sonicated once again and incubated overnight at 48^0C. Following day the extracts was subjected to base hydrolysis for 2 hrs at 37 ^{0}C and neutralized. The neutralization was confirmed with pH paper. Half of the extract was transferred to another tube, dried down and resuspended in LCB running buffer C1P together with the long chain bases were quantified using the modified protocol from Merrill *et al* (99). To the remainder of the extract 1ml of chloroform and 2ml of water were added, and the lower phase was transferred to another tube, dried down and brought up in SL running buffer and used in the analysis of ceramides, monohexosyl ceramides and sphingomyelins and described by Merrill *et al* (99). The lipids were separated using a Discovery C18 column on a Shimadzu HPLC and subjected to mass spectrometric analysis using a 4000 Q-Trap (Applied Biosystems). Multiple reaction monitoring (MRM) transiton monitored were 562.4/264.4 ($d_{18:1/12:0}$), 590.4/264.4 ($d_{18:1/14:0}$), 618.4/264.4 ($d_{18:1/16:0}$), 620.4/264.4 ($d_{18:0/16:0}$), 644.4/264.4 ($d_{18:1/18:1}$), 646.4/264.4 ($d_{18:1/18:0}$), 674.4/264.4 ($d_{18:1/20:0}$), 702.4/264.4 ($d_{18:1/22:0}$), 728.4/264.4 ($d_{18:1/24:1}$), 730.4/264.4 ($d_{18:1/24:0}$), 756.4/264.4 ($d_{18:1/26:1}$), 758.4/264.4 ($d_{18:1/26:0}$) were used at collision energies +41, +43.5, +43.5, +46.0, +46.0, +48.5, +51.0, +53.5, +56.0, +56.0, +58.5, +58.5 V respectively. The chromatography column for C1P was a 5 cm3 2.1mmDiscovery C18 5mmHPLC column. The mobile phase solvent A for LCB and C1P was 58:41:1 CH3OH/water/HCOOH and solvent B was 99:1 CH3OH/HCOOH. Both

contained 5 mM ammonium formate (26). The mobile phase foe solvent A for sphingolipids are A: CH_3CN: H_2O:CH_3COOH 97:2:1, and solvent B: CH_3OH : H_2O : $CH_3(CH_2)_2CH_2OH$: CH_3COOH 64:15:20:1. Both caontained 5mM ammonium acetate.

RESULTS

Product ion spectra of C1P in positive ion mode gives rise to more structure specific fragments than that from the negative ion mode.

The product ion spectra of D-e-$C_{16:0}$ C1P was investigated in the positive and negative ion modes. The ionization of C1P is better in the positive ion mode in the tested pH range (pH 4-8) indicating that C1P act more like a base in the gas phase than an acid. Fragmentation of the precursor ion (m/z = 618.4) in the positive mode gave rise to the multiple structure indicative fragments of which the fragment for the sphingoid back bone was the most intense (m/z = 264.4) (Figure 4.1). Product ions obtained from fragmentation of the precursor ion in the negative ion mode was much less informative as to the structure of the species (Figure 4.2). The most prominent product ion in the negative ion mode is the PO_3^- fragment (m/z = 78.9). Neutral loss scan for the acyl chain (354.00) in the positive ion mode confirmed 618.4 (i.e. C_{16} C1P) as the only precursor ion only species in the mixture to contain a 16 carbon acyl chain (Figure 4.3).

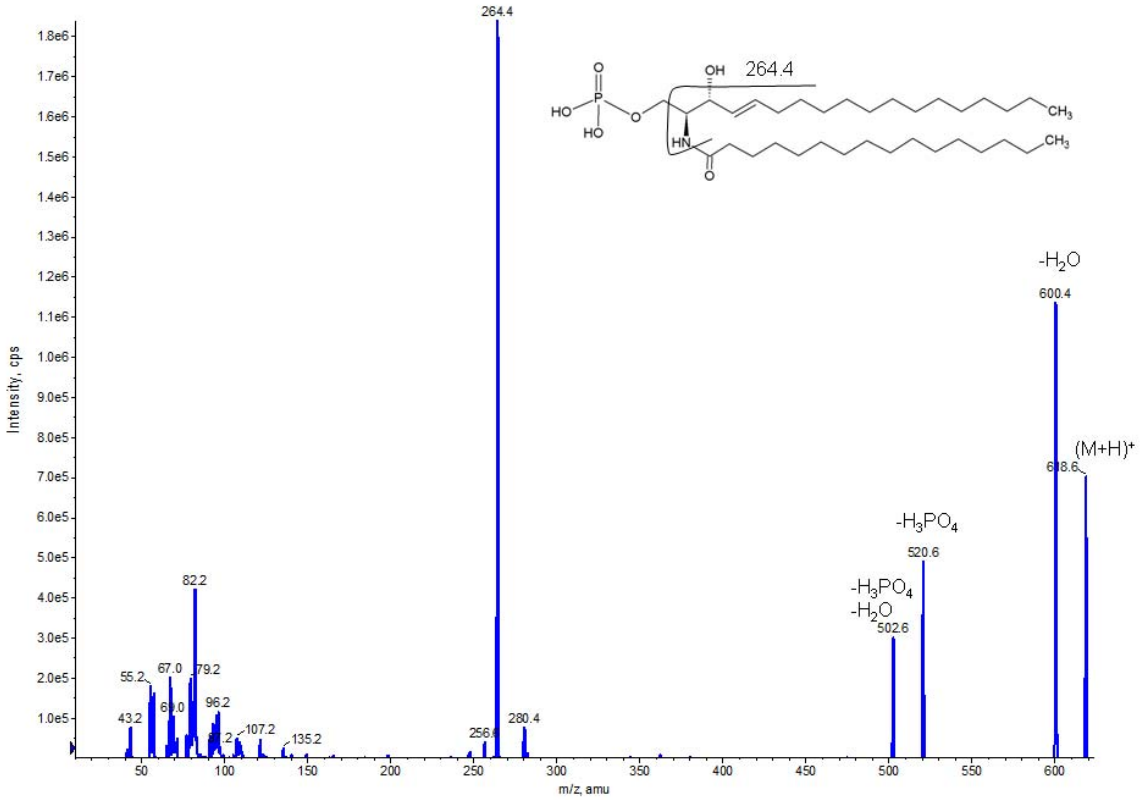

Figure 4.1. Product ion scan of D-e-C_{16} C1P in the positive ion mode. D-e-C_{16} C1P was infused at a rate of 10 µl/min and the product ion scans for 20 scans collected in the positive ion mode at a collision energy of 40 with a collision energy spread of 10.

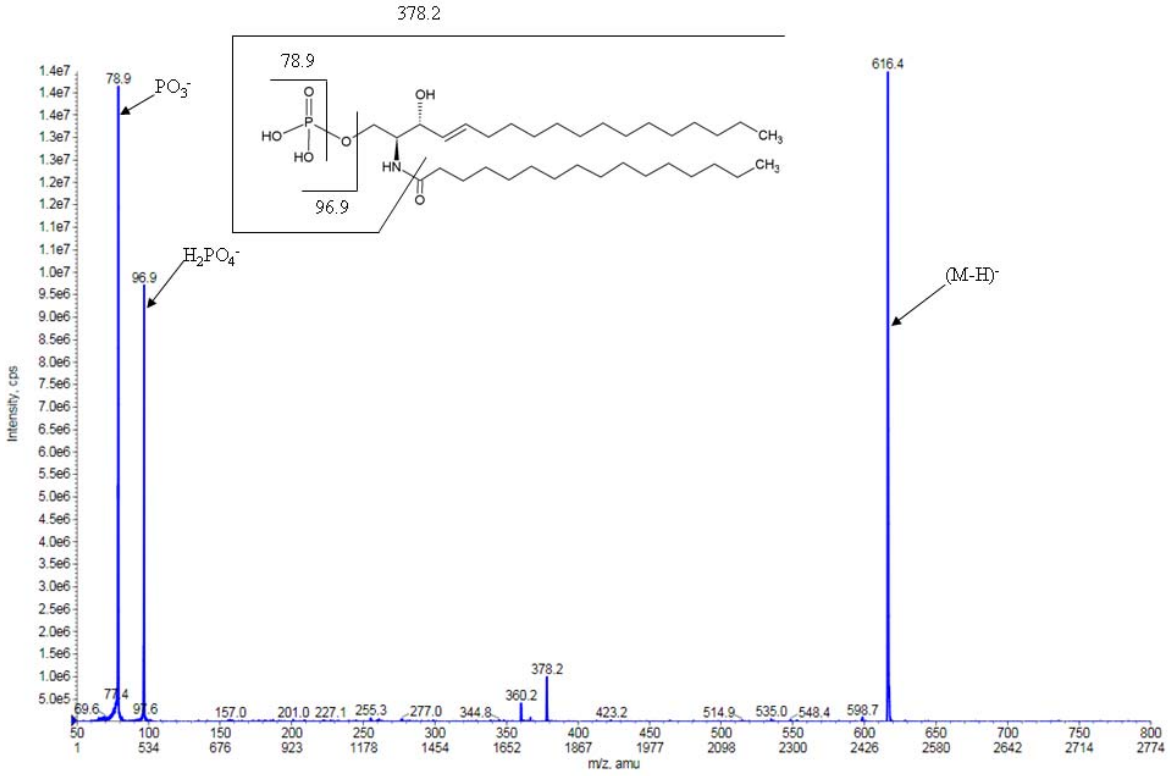

Figure 4.2. Product ion scan of D-e-C_{16} C1P in the negative ion mode. D-e-C_{16} C1P was infused at a rate of 10 µl/min and the product ion scans for 20 scans collected in the negative ion mode at a collision energy of 60 with a collision energy spread of 10.

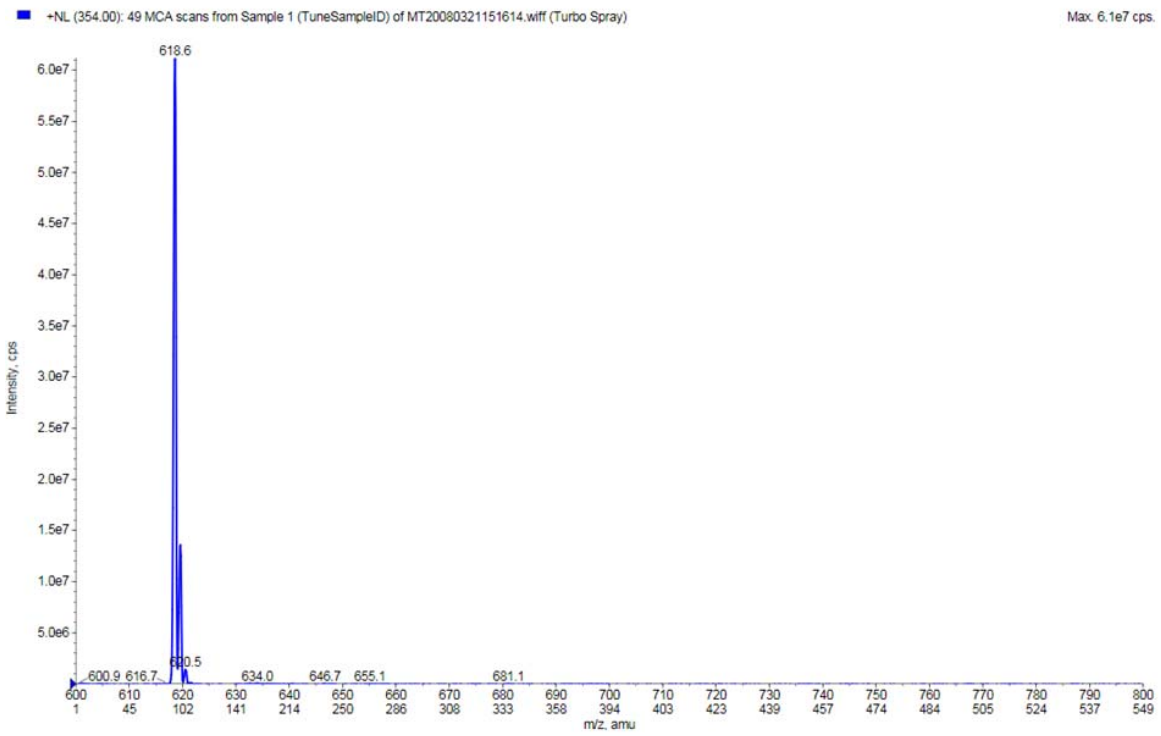

Figure 4.3. Neutral loss scan of D-e-C_{16} C1P in the positive ion mode for the loss of the acyl chain. D-e-C_{16} C1P was infused at a rate of 10 µl/min and the product ion scans for 20 scans collected in the negative ion mode at a collision energy of 40 with a collision energy spread of 10.

Column heating eliminates carryover of C1P between samples.

C18 columns are the most widely used reversed phase columns in the market. These are exceptionally well suited for the separation of lipids based on their chain lengths. However when used in the separation of C1P species using a methanol/water – methanol system a recurring problem has been carryovers between samples, sometimes in excess of 10%. This is especially the case for C_{16} C1P. A method used by Kester *et al* was shown to have less carryover using the same solvent system with the addition of tetrahydrofuran (THF) and heating of the column. Use of THF with heating causes a gummy substance to build up on the ESI source face plate leading to progressive deterioration of the signal when running multiple samples. Use of the methanol/water – methanol system by itself, together with the column heating and an extended run for 10 minutes was found to be sufficient to address the problem of carryover without the need for THF thereby avoiding the undesirable side effects. Using this method the column carryover after 10 injections of 10 pmols each of D-e-C_{12} C1P was less than 1%.

Heating of the column result in an increase of the signal strength and thereby the sensitivity due to increased the ionization efficiency of C1P.

In order to compare any detrimental effects on signal strength due to heating of the column, same quantity of D-e-C_{12} C1P was analyzed using the published protocol and the

modified protocol. Almost a two fold increase in the signal strength for C1P was achieved due to heating of the column to 60 ^{0}C (Figure 4.4)

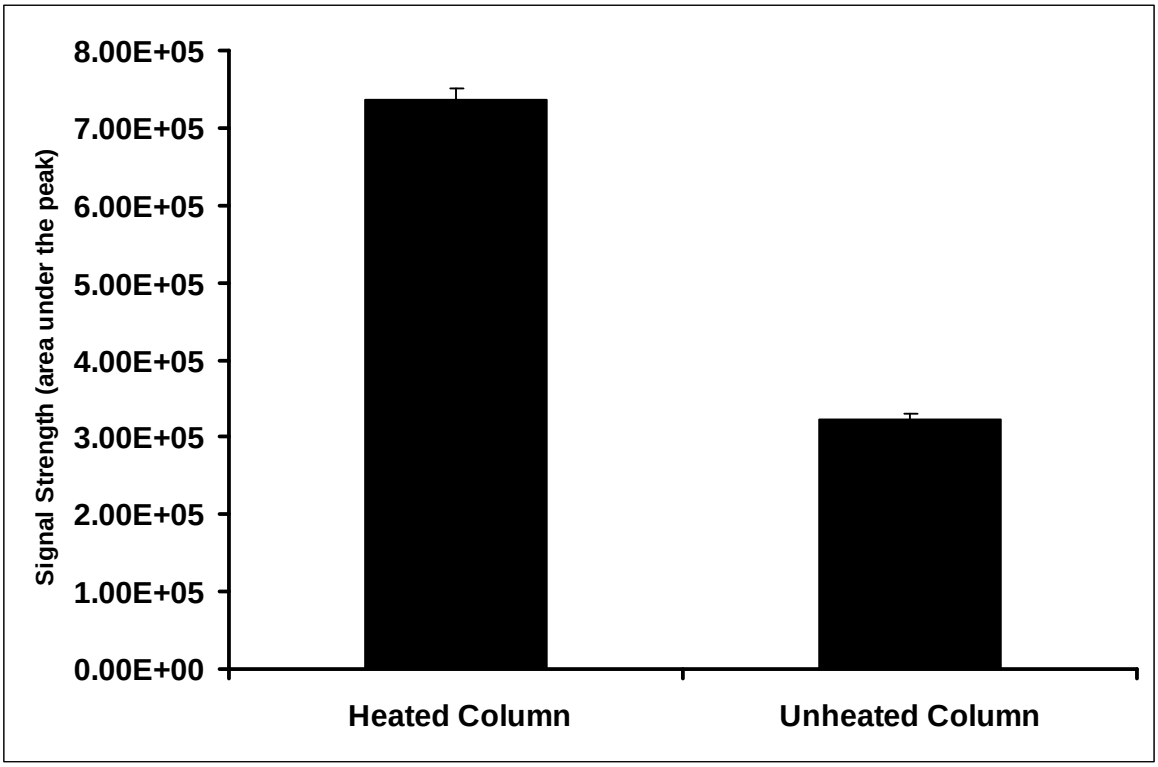

Figure 4.4: Heating of the C18 reverse phase column result in a two fold increase in signal strength. 8 pmols of D-e-C_{12} C1P was analyzed using a C18 reverse phase column as described in materials and methods with the column either heated at 60 ^{0}C or maintained at room temperature. The data are an average of 10 injections ± SD

The analytes are well separated in the modified method allowing for successful quantitation.

The standards by themselves and a mixture of long chain naturally occurring C1P's were analyzed using this modified method. The long chain bases and their phosphates elute first while the C1P's did not elute until the chromatographic conditions changed to 100% methanol. This separation allows for separately scanning for the two analyte groups there by allowing for additional increase in the sensitivity (Figures 4.5 and 4.6).

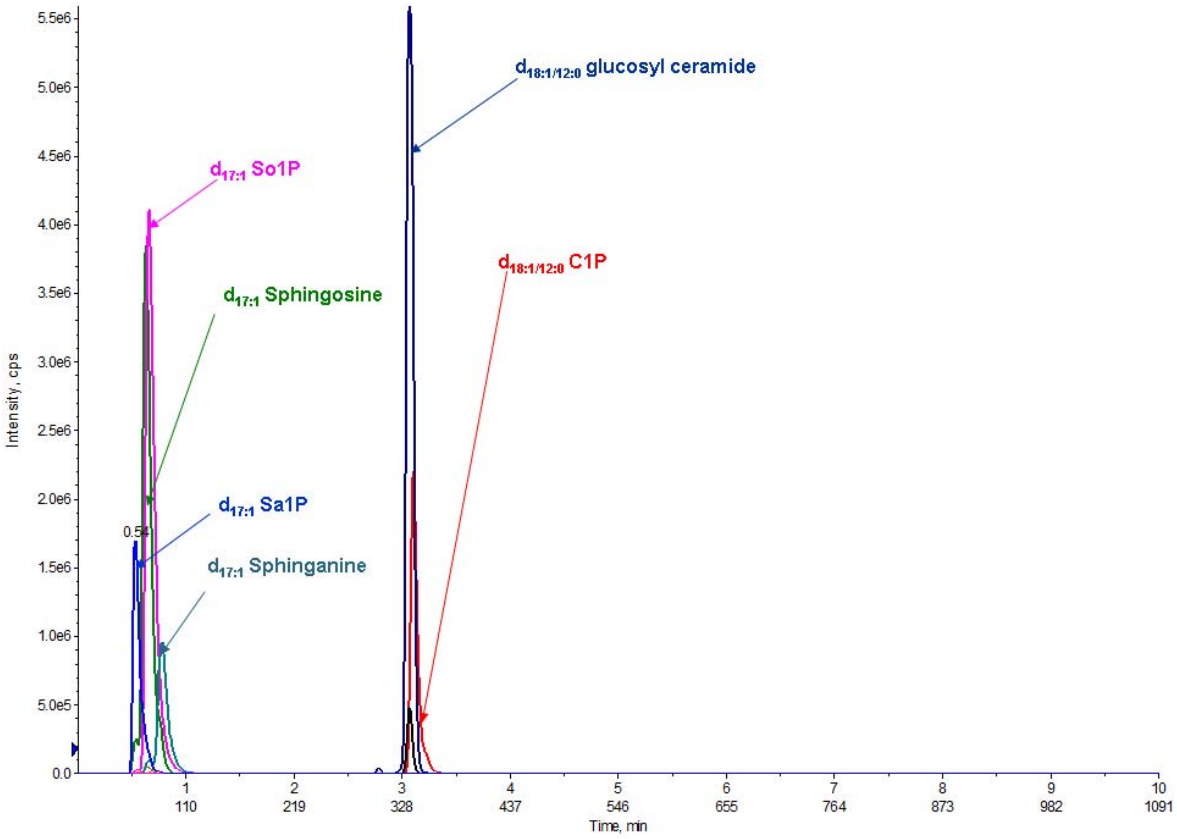

Figure 4.5: Excited Ion Chromatogram for LC-MS/MS from the reverse phase separation of standards used in the quantitation of long chain bases, long chain base 1 phosphates and C1P. Long chain bases and their phosphates elute first.

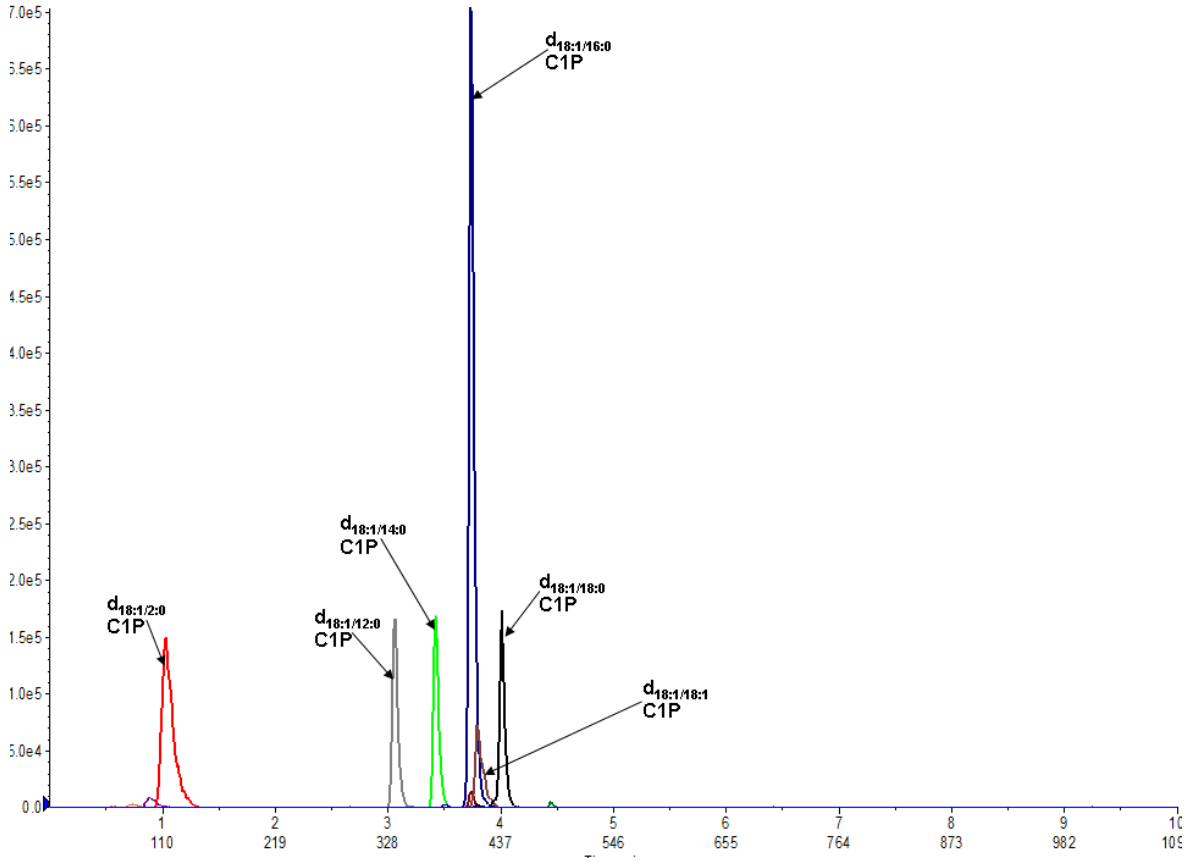

Figure 4.5: Excited Ion Chromatogram for LC-MS/MS from the reverse phase separation of selected synthetic C1P species. Separation was carried out using the modified HPLC protocol. All biologically relevent C1P species are eluting at 100 % methanol.

Sample dry down without proper neutralization causes SM to breakdown to C1P.

Previously C1P has been shown to be present in A549 cells in significant quantities. However the protocol used involved drying down the samples tested in a basic solution. We decided to test the possibility of lipid degradation due to drying under basic conditions. To our surprise the neutralized samples had three fold lower C1P than the un-neutralized. Examination of the SL fraction revealed SM to have decreased by a similar amount suggesting to us that during drying under basic conditions, SM is getting broken down to C1P (Figure 4.6A and 4.6B).

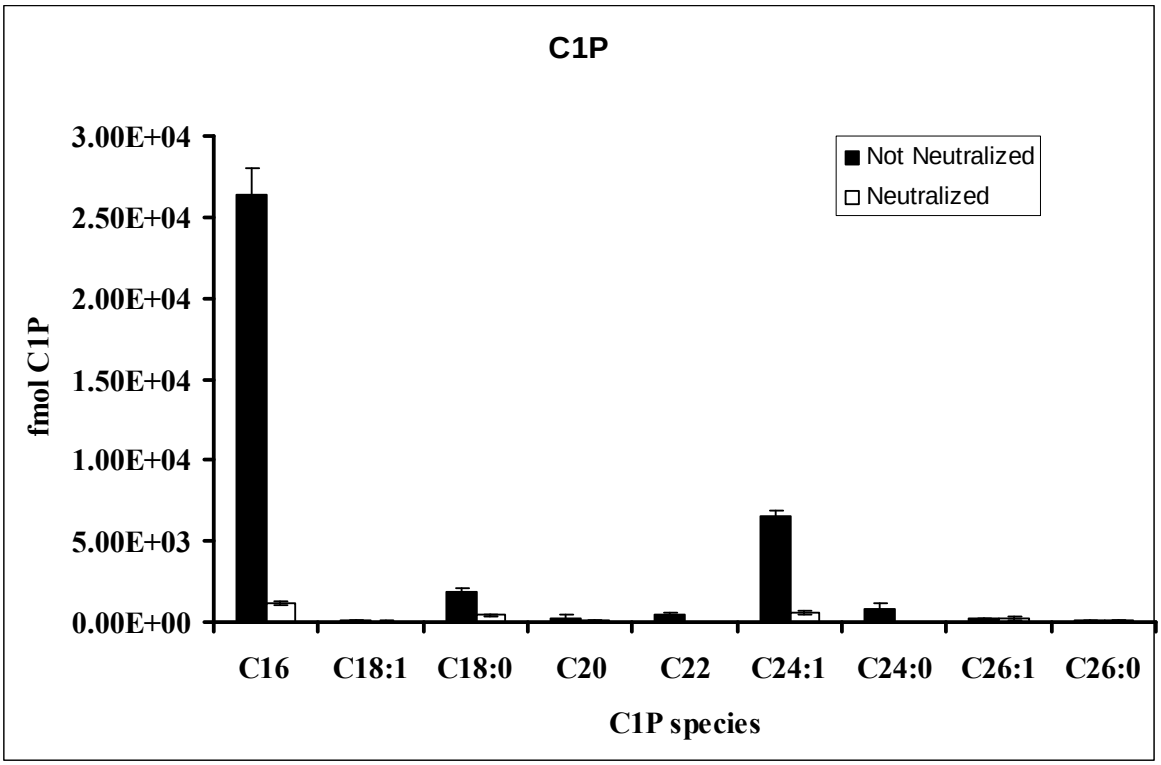

Figure 4.6A: Sample dry down following base hydrolysis without proper neutralization leads to increased amounts of C1P being present in the samples. A549 cells were plated on 10 cm plates in the appropriate medium and grown at 37^0C under 5% CO2 overnight. The next day, cells were harvested and lipids were extracted as mentioned in materials and methods. Following base hydrolysis one group of lipid extracts were dried down without neutralization (■) while the other dried down following neutralization (□). All samples were brought up in reversed phase loading buffer and subjected to analysis by HPLC-ESI MS/MS as described in materials and methods. The data are an average of 3 samples ±SD.

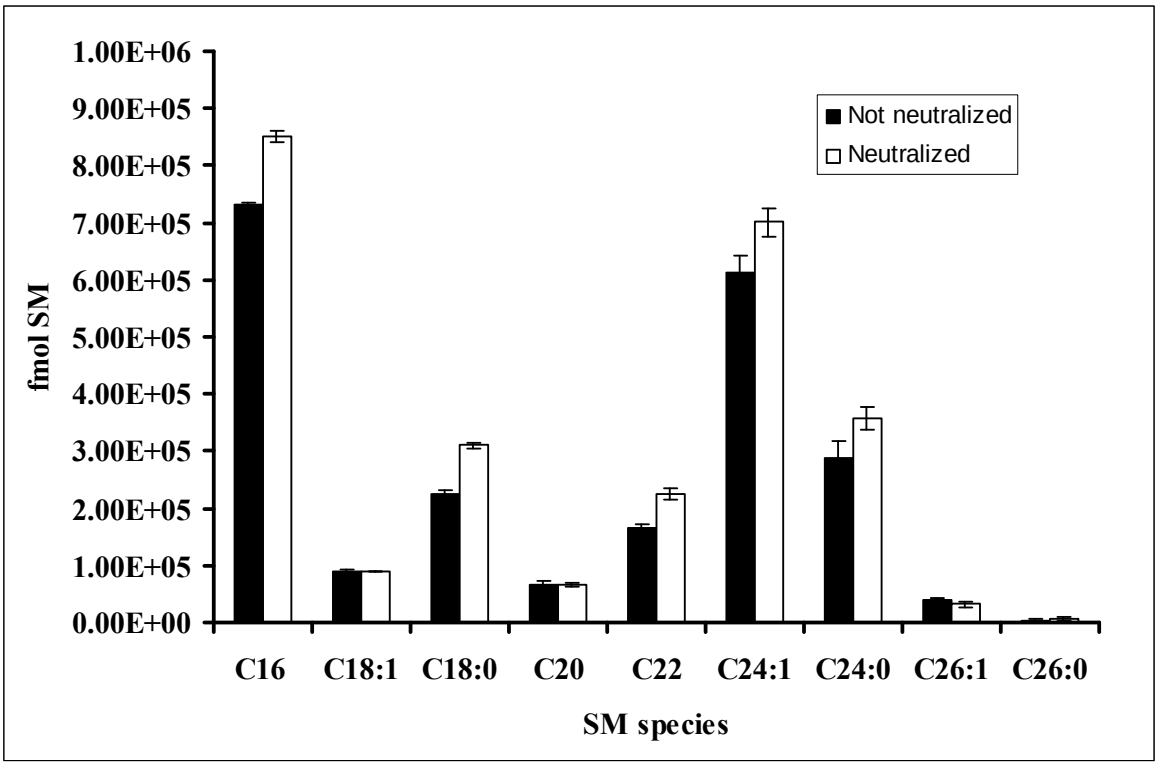

Figure 4.6B: Sample dry down following base hydrolysis without proper neutralization leads to decreased amounts of SM being present in the samples. A549 cells were plated on 10 cm plates in the appropriate medium and grown at 37^0C under 5% CO2 overnight. The next day, cells were harvested and lipids were extracted as mentioned in materials and methods. Following base hydrolysis one group of lipid extracts were dried down without neutralization (■) while the other dried down following neutralization (□). All samples were brought up in reversed phase loading buffer and subjected to analysis by HPLC-ESI MS/MS as described in materials and methods. The data are an average of 3 samples ±SD.

The modified method has a linear quantitation range from 5 fmoles to >125 pmol when used with 4000 QTRAP mass spectrometer.

Current generation of mass spectrometers very often show sub pico molar sensitivities. However this sensitivity is mainly dependent on the ionization capability of the analyte under investigation. The fact that the naturally occurring levels of C1P is almost two orders of magnitude lower than previously reported brought to question the validity of using the previously used levels of internal standards for quantitation of C1P. Also of interest is the linear range of quantitation of the modified method. To investigate these questions, different quantities of the internal standard mix used was analyzed for LCB's ($d_{17:1}$ sphingosine, $d_{17:1}$ sphinganine, $d_{17:1}$ sphingosine-1-phosphate and $d_{17:1}$ sphinganine-1-phosphate) and C1P ($d_{18:1/12:0}$ C1P) using the now developed method. The amounts injected ranged from 5 femto moles to 125 pmols. Within this range all analytes tested showed linear signal response with increasing concentrations. This confirmed that the use of the internal standard mix described by Merrill *et al (99)* can still be used to quantify naturally occurring low levels of C1P and also that femto molar levels of changes in the LCB's can also be accurately quantified (Figure 4.7).

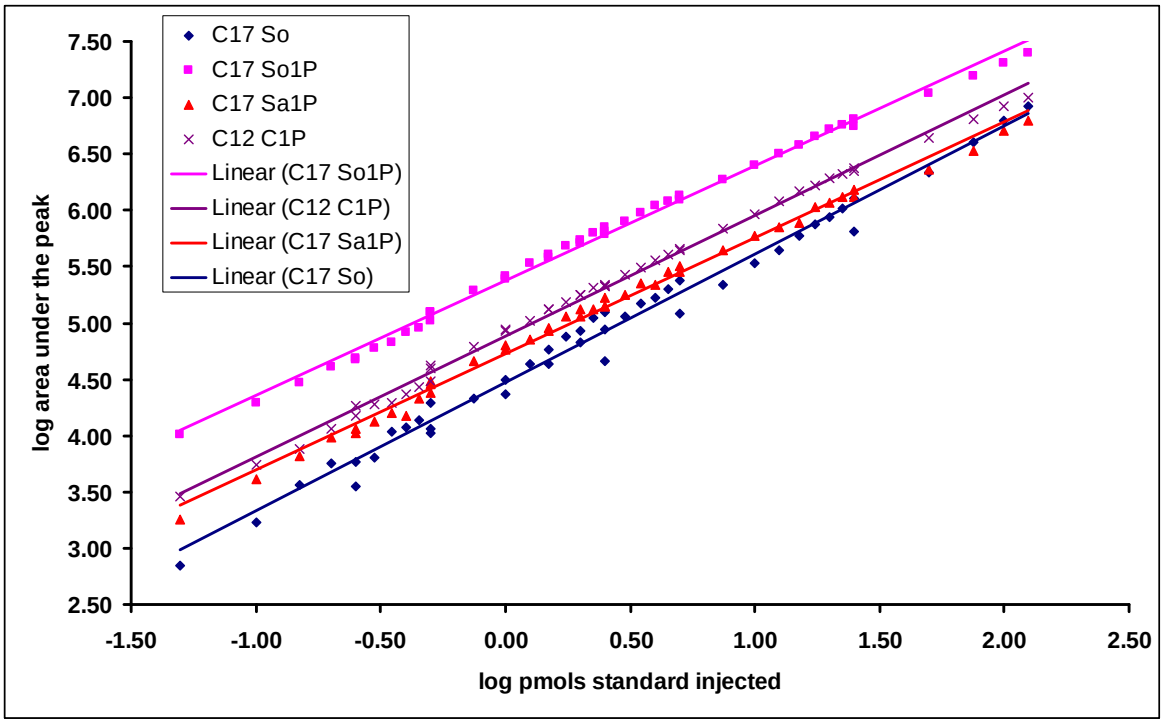

Figure 4.7: The modified method for detection of C1P shows a linear response in the range of 5 fmol to 125 pmols for C1P and LCB standards. 5 fmols to 125 pmols of standard solution in LCB buffer was analyzed using the method modified to overcome the carryover problem. The signal response as measured by the area under the peak vs the amount analyzed in pmols were plotted as a log-log plot.

D-e-C_{16} C1P is specifically decreased upon treatment of A549 cells with siRNA against Ceramide Kinase.

Previous studies using steady state labeling of C1P has shown that treatment of cells with si-CERK result in a decrease in the levels of D-e-C_{16} C1P. To date mass spectrometric analyses have failed to confirm this finding. Using the newly developed mass spectrometric assay for C1P, we quantified the levels of C1P in A549 cells where ceramide kinase has been down regulated by si-RNA. For the first time the results are in agreement with the steady state labeling data in that down regulation of CERK caused a corresponding decrease in the levels of D-e-$C_{16:0}$ C1P (Figure 4.8).

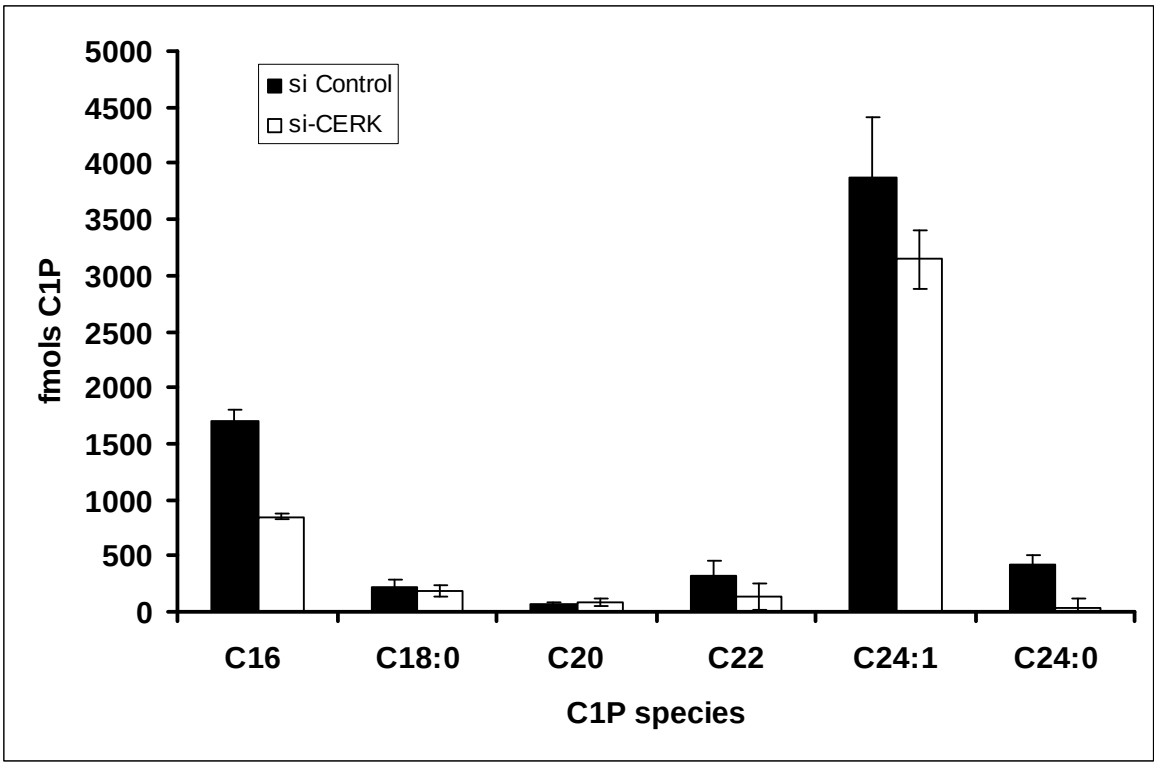

Figure 4.8: siRNA mediated downregulation of endogenous CERK in of A_{549} cells results in a concomitant decrease in the predominant C1P species. Sequence-specific silencing of CERT was performed using small interfering RNA (siRNA) as described in Experimental Procedures. 27 hours post treatment cells were harvested and the levels of C1P were measured using the newly developed HPLC ESI-MS/MS method. Results are the average of three experiments ± SD.

DISCUSSION:

Several times over, C1P has been shown to be an important bioactive molecules with activities implicated in biological processes that range from DNA synthesis to mast cell degranulation to apoptosis to name a few. Our laboratory has repeatedly shown the importance of C1P in inflammation by acting as an activator of $cPLA_2\alpha$. However, studies into metabolism of C1P has been hampered by the lack of a reliable and preferably nonradioactive method for detecting and quantifying cellular levels of C1P. The data generated using the currently available mass spectrometric methods were inconsistent with the levels of C1P measured using steady state labeling studies. In fact the levels of C1P were almost two orders of magnitude greater than expected. Here for the first time we describe a method that is validated using steady state labeling studies and thus can be used to reliably quantify cellular C1P levels.

C1P is not an easily ionizable species. Thus the signal strength is relatively low compared to S1P under the eluting conditions. This result in poor sensitivity and is especially a problem when trying to quantify low levels of C1P. As a result greater quantities of starting material is required. This is especially a problem when the starting material are from costly experiments like siRNA mediated gene knockdown. Thus any improvement is signal strength will help to bring down the amount of starting material needed. As indicated by Figure 4.2 and additional benefit of using a heated column is the twofold

increase in signal strength obtained. This now allows for lower quantities of starting material to be successfully analyzed for C1P.

A major hurdle to overcome in the development of the method was the absence of a commercially available panel of C1P's of different chain lengths to be used as standards. This problem is compounded by the appearance of in properly neutralized samples multiple peaks corresponding to a particular transition. This resulted in difficulties in the unambiguous assignment of peaks to the corresponding C1P species. To overcome this technical hurdle, C1P species of different chain lengths had to be custom synthesized at great cost. However, the discovery that one of the main problems of the existing method, namely the overestimation of C1P species due to the breakdown of SM (Figure 4.7A and 4.7B), turned out to be quite useful. This discovery was to our advantage since the same process allowed us to generate C1P that can be used to verify the retention times of the different chain lengths of C1P allowing for unambiguous peak assignment.

In summary, we have developed a HPLC ESI-MS/MS method that quantify cellular levels of C1P that are in agreement with the levels of C1P found to be present by steady state labeling studies. Using this method we have shown that, contrary to previous reports, the bioactive molecule C1P is present only in low abundance in cells. Ceramide Kinase, the only enzyme identified to date to produce C1P does not seem to be responsible for all the C1P species in cells. With the ever increasing use and the continuing decline in prize, mass spectrometers are becoming more commonplace in research institutes. The sub pico molar

sensitivity coupled with the availability of multiple levels molecular identification (molecular weight of the intact molecule, presence of signature fragments, retention time etc) are making mass spectrometers the most versatile bio-analytical tools available.

CHAPTER 5: SEARCH FOR THE ALTERNATE SOURCE(S) OF C1P

INTRODUCTION

The sphingolipid metabolite ceramide 1 phosphate was described by Gomez-Munoz. Since then the number of biological activities attributed to C1P has been steadily increasing further increasing its recognition as an important lipid signaling molecule. Currently C1P has been demonstrated to play a role in DNA synthesis, activation of $cPLA_2\alpha$ leading to the production of inflammatory mediators, degranulation of mast cells, inhibition of apoptosis via inhibition of aSMase.

Until recently the only known source of C1P has been ceramide kinase. However, siRNA mediated knockdown of ceramide kinase (80% knockdown) have consistently failed to decrease C1P levels by an amount proportional to the knockdown. Recent publicatons by Boath *et al* (107) and Graf *et al* (96) with regards to ceramide kinase knockout mouse has confirmed these findings by our laboratory. This raise the question as to what the other sources of C1P are. Here, using steady state labeling and the validated mass spectrometric methods we developed, we have attempted to identify the alternate source of C1P in mammalian cells.

EXPERIMENTAL PROCEDURES

Materials: CERK knockout mice was a donation as a result of collaboration with Frederick Bornancin (Novartis, Switzerland).

Cell culture: Mouse embryo fibroblasts were harvested from 5 day old embryos and cultured sunder standard incubator conditions in DMEM (4.5 g glucose l^{-1}) (BioWhittaker) supplemented with 10% fetal bovine serum (Invitrogen) and 2% penicillin/streptomycin (BioWhittaker). A549 cells were obtained from the American Type Culture Collection. A549 lung adenocarcinoma cells were grown in 50% DMEM (BioWhittaker) and 50% RPMI (BioWhittaker) supplemented with 10% fetal bovine serum (Invitrogen) and 2% penicillin/streptomycin (BioWhittaker). Cells were maintained under 5% CO2 at 37^0 C by routine passage every 3 days. For treatments, the medium was replaced 2 h before the addition of the agonist by DMEM containing 2% fetal bovine serum and 2% penicillin/streptomycin.

Treatment of cells with lipids: *E*thanol and dodecane is mixed at a ratio of 98:2, followed by vortexing and pre-warmed at 37 °C. Meanwhile, the lipid is dissolved in chloroform:methanol 1:1. The required volume is then dried down under N_2 gas. The pre-warmed alcohol:dodecane mixture is added to the dried C1P such that the final concentration is 2.5 mM (a stock solution up to 10 mM can be made). This mixture is thoroughly vortexed and incubated at 37°C for a further 20 minutes followed by further

vortexing. The stock solution, thus prepared, is diluted to the required concentration using ethanol/dodecane and used to treat the cells. This is incubated at 37 °C followed by vortexing. Lipid solution is diluted to the appropriate concentration in ethanol/dodecane solution, and added to cells at a dilution of 1:1000.

Pulse labeling and thin layer chromatographic detection of C1P: Pulse labeling. A549 cells were plated on 10 cm dishes at the concentration of 1.3 10^6 cells per plate. The next day, [^{32}P]orthophosphate (Perkin-Elmer) was added at 30 mCi/ml for 4 h. following incubation the cells were treated for two hour with the relevant lipid. The plates were then placed on ice, and the lipids were extracted using the Bligh and Dyer method followed by a base hydrolysis with 0.4 M methanolic NaOH for 2 h at 37 ^{0}C. The samples were dried under N2 and resuspended in chloroform-methanol (75:25) and spotted onto a 10 x 10 cm TLC plate (silica gel) (VWR International) together with standards. The lipids were separated using a chloroform-acetone-methanol-acetic acid-water (10:4:3:2:1) solvent mixture. The ^{32}P-labeled lipids were detected by exposing the plates to X-ray film.

Mass spectrometric analysis: A549 cells were plated on 10 cm plates in the appropriate medium and grown at 37^{0}C under 5% CO2 overnight. The next day, cells were subjected to the relevant treatment. After treatment, the plates were placed on ice and the cells were washed once with ice cold PBS and harvested by scraping in 200 µl of PBS. An aliquot of cells was taken for standardization (total protein). Lipids were extracted from the remaining cells as described by Merrill *et al* with slight modifications. In summary, to the

remaining cells 1 ml of methanol was added and sonicated to obtain a homogeneous mix followed by the addion of 500 µl of chloroform and 500 pmols of internal standards (Avanti). Internal standards used were $d_{18:1/12:0}$ ceramide-1-phosphate sphingomyelin, ceramide, glucosylceramide, lactosylceramide and $d_{17:1}$-sphingosine, sphinganine, sphingosine-1-phosphate, sphinganine-1-phosphate. The mixture was sonicated once again and incubated overnight at 48^0C. Following day the extracts was subjected to base hydrolysis for 2 hrs at 37 ^{0}C and neutralized. The neutralization was confirmed with pH paper. Half of the extract was transferred to another tube, dried down and resuspended in LCB running buffer C1P together with the long chain bases were quantified using the modified protocol from Merrill *et al* (99). To the remainder of the extract 1ml of chloroform and 2ml of water were added, and the lower phase was transferred to another tube, dried down and brought up in SL running buffer and used in the analysis of ceramides, monohexosyl ceramides and sphingomyelins and described by Merrill *et al* (99). The lipids were separated using a Discovery C18 column on a Shimadzu HPLC and subjected to mass spectrometric analysis using a 4000 Q-Trap (Applied Biosystems). Multiple reaction monitoring (MRM) transiton monitored were 562.4/264.4 ($d_{18:1/12:0}$), 590.4/264.4 ($d_{18:1/14:0}$), 618.4/264.4 ($d_{18:1/16:0}$), 620.4/264.4 ($d_{18:0/16:0}$), 644.4/264.4 ($d_{18:1/18:1}$), 646.4/264.4 ($d_{18:1/18:0}$), 674.4/264.4 ($d_{18:1/20:0}$), 702.4/264.4 ($d_{18:1/22:0}$), 728.4/264.4 ($d_{18:1/24:1}$), 730.4/264.4 ($d_{18:1/24:0}$), 756.4/264.4 ($d_{18:1/26:1}$), 758.4/264.4 ($d_{18:1/26:0}$) were used at collision energies +41, +43.5, +43.5, +46.0, +46.0, +48.5, +51.0, +53.5, +56.0, +56.0, +58.5, +58.5 V respectively.

pairs used were was carried out using m/z 644.6 (molecular ion) and m/z 78.9 (PO3 22 ion) for C12 C1P. The chromatography apparatus for C1P was a 5 cm3 2.1mmDiscovery C18 5mmHPLC column. The mobile phase solvent A for LCB and C1P was 58:41:1 CH3OH/water/HCOOH and solvent B was 99:1 CH3OH/HCOOH. Both contained 5 mM ammonium formate (26). The mobile phase foe solvent A for sphingolipids are A: CH_3CN: H_2O:CH_3COOH 97:2:1, and solvent B: CH_3OH : H_2O : $CH_3(CH_2)_2CH_2OH$: CH_3COOH 64:15:20:1. Both contained 5mM ammonium acetate.

RESULTS

C_{16} C1P is specifically decreased in the embryonic fibroblasts of ceramide kinase knockout mice.

Currently two groups have published phenotypic data on ceramide kinase knockout mice. Both groups report the mice being as aphenotypical with slightly altered C1P profiles (108-110). A collaboration with Novartis (Switzerland) allowed us to establish a ceramide kinase knockout mouse breeding colony together with their wild type counterparts. This enabled us to harvest and use mouse embryonic fibroblasts in assaying the effects of ceramide kinase knockdown on cellular physiology. We first compared changes in the C1P profiles of MEF's between ceramide kinase knockout mice and their wild type counterparts. The data revealed that the levels of C_{16} C1P is reduced by half in the

embryonic fibroblasts of the knockout mice compared to those of wild type mice. The other chain lengths of C1P were not affected (Figure 5.1).

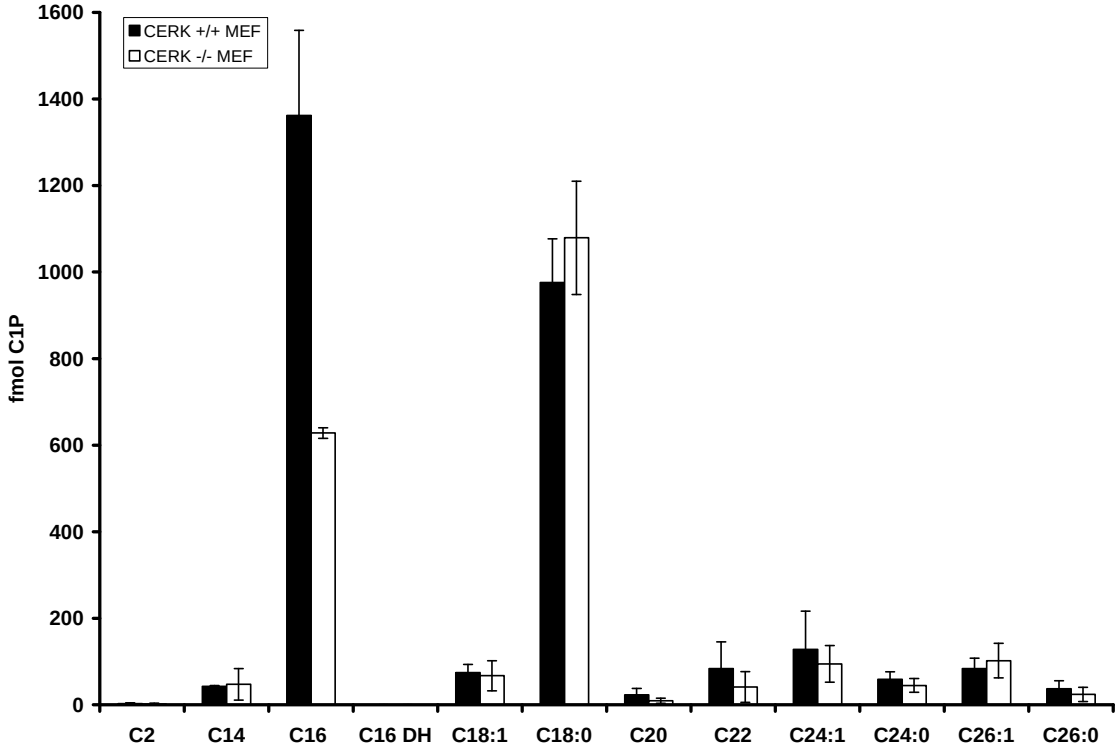

Figure 5.1: CERK -/- mice has decreased levels of C_{16} C1P. Mouse embryo fibroblasts obtained from CERK +/+ and -/- mice were cultured upto passage 3 as indicated in materials and methods. At passage 3 same number of cells were plated in 10 cm plates and allowed to adhere overnight. These cells were harvested and the lipids were extracted and quantified as described in materials and methods. The data show is the mean of three experiments ±SD.

Treatment of A549 cells with radiolabeled S1P results in an increase of radiolabeled C1P.

The presence of C1P in ceramide kinase knockout model is a clear indication as to the presence of additional sources of C1P. One possibility is via the acylation of S1P. To investigate this, ^{32}P labeled S1P was delivered to cells via ethanol/dodecane. The lipids were extracted from these cells and separated by TLC together with the standards as mentioned in materials and methods. The treatment resulted in an increase in radiolabeled C_{16} C1P.

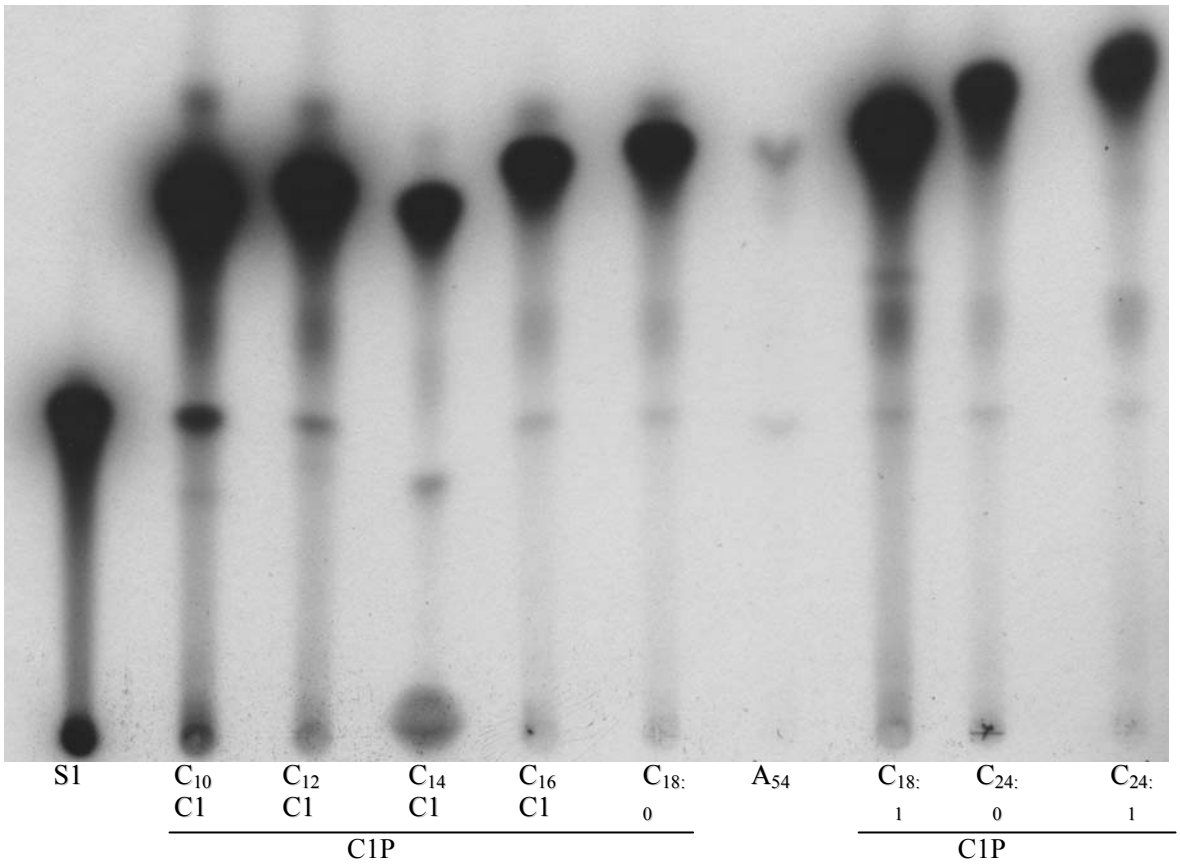

Figure 5.2A: Treatment of A_{549} cells with ^{32}P labeled S1P results in an increase in ^{32}P labeled C1P. A_{549} cells rested for two hours in % FBS containing A_{549} medium were treated with a mix of radiolabeled and unlabeled S1P 500 nM for two hours in 2% medium Following treatment cells were harvested and lipids extracted followed by thin layer chromatography as described in materials and methods. The results are representative of three separate reactions from three separate reactions.

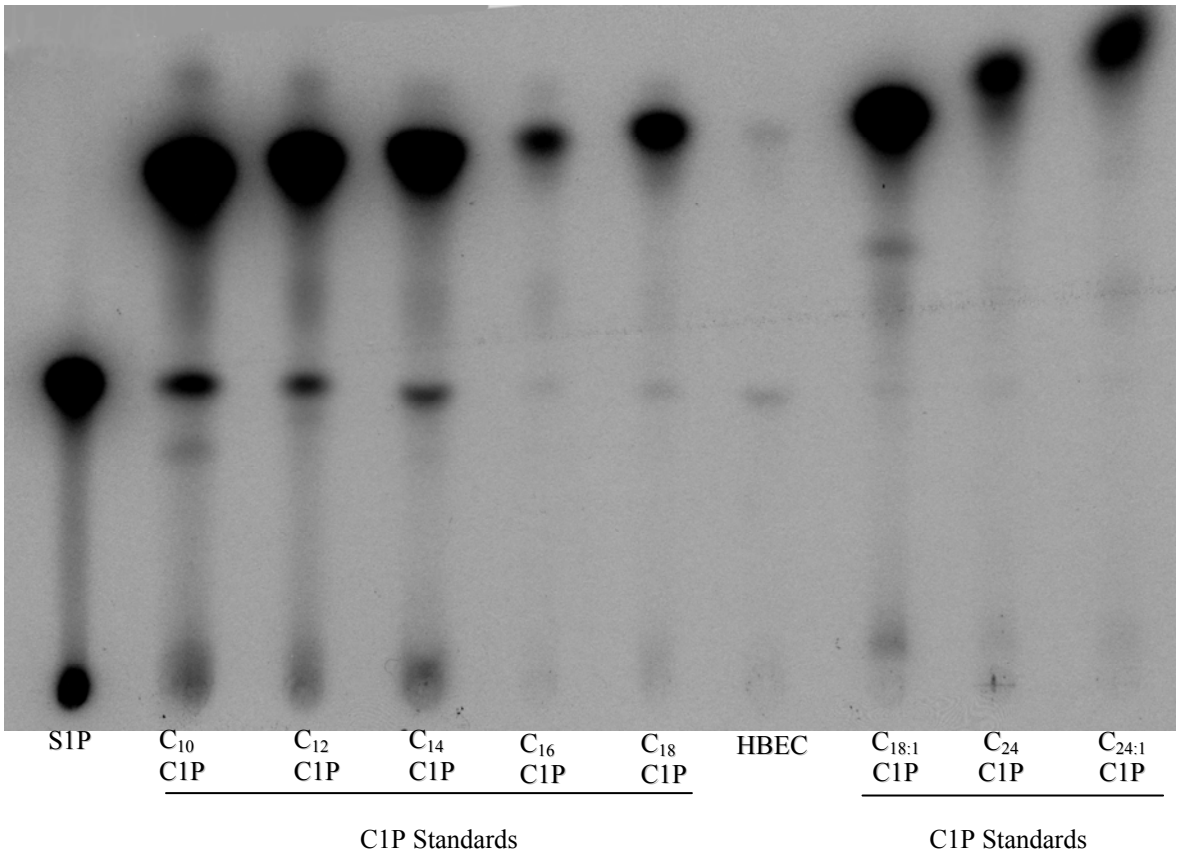

Figure 5.2B: Treatment of HBEC cells with ^{32}P labeled S1P results in an increase in ^{32}P labeled C1P. HBEC cells rested for two hours in % FBS containing HBEC medium were treated with a mix of radiolabeled and unlabeled S1P 500 nM for two hours in 2% medium Following treatment cells were harvested and lipids extracted followed by thin layer chromatography as described in materials and methods. The results are representative of three separate reactions from three separate reactions.

Treatment of ceramide kinase knockout mouse embryo fibroblasts with $d_{17:1}$ S1P results in an increase of $d_{17:1}$ C1P

Radiolabeling studies demonstrated that S1P can be acylated to produce C_{16} C1P. The levels of this lipid in A_{549} cells where ceramide kinase is downregulated by siRNA is half that of the cells with normal levels of CERK (Chapter 4 Figure 4.8). Similar effects are observed in the MEF's of CERK knockout mice. All these data indicates an alternate source of C1P. We hypothized that acylation of S1P is responsible at least in part for the CERK independent generation of C_{16} C1P. To investigate this possibility, we treated CERK knockout MEF with $d_{17:1}$ S1P and looked for the occurrence of $d_{17:1}$ C1P by mass spectrometry. The results show that the major portion of $d_{17:1}$ C1P is $d_{17:1/16:0}$ species (Figure 5.3).

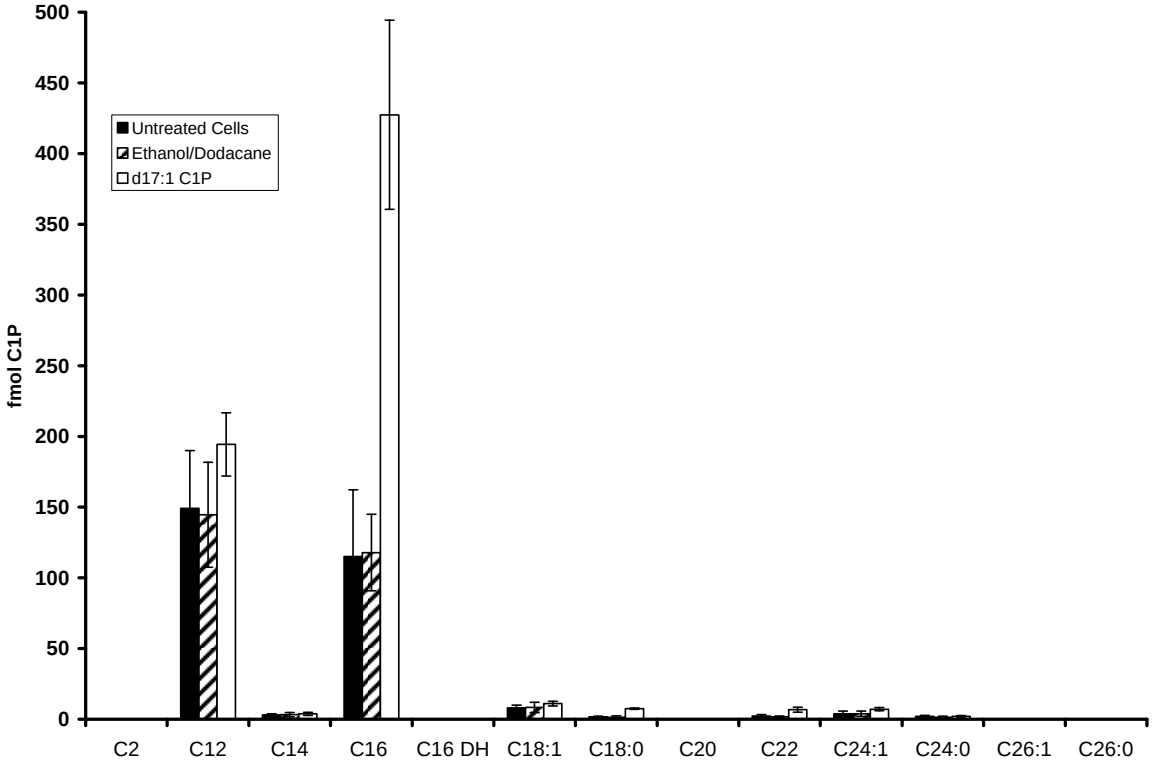

Figure 5.3: S1P is acylated into C_{16} C1P in ceramide kinase knockout MEF's. Ceramide kinase knockout MEF's were treated with $d_{17:1}$ S1P (500 nM) for two hours. Following incubation, the lipids were extracted from the cells and subjected to analysis by mass spectroscopy. The data are an average of three experiments ± SD.

DISCUSSION:

Currently C1P has been implicated in many biological processes. The only enzyme found to produce C1P directly is ceramide kinase. However, down regulation of CERK by siRNA has not resulted in proportional downregulation of C1P indicating the presence of alternate sources of C1P. Similar results were observed with CERK knockout mice. Downregulation of C1P was however found to be chain length specific in both instances with D-e-C_{16} C1P being downregulated by around 50%. This leads to the interesting possibility that CERK is mainly involved in the generation of the 16 C chain length of C1P. Since our previous published results prove that the substrate specificity of CERK with regards to all chain lengths longer than 14 C are more or less the same, the specific decrease in C16 C1P observed here would be due to an availability effect.

Many possibilities exist that may account for the CERK independent C1P in cells. These include an as yet undiscovered enzyme with a Smase D function; an unidentified novel enzyme with a ceramide kinase function or an enzyme capable of acylating S1P and thereby producing C1P. We decided to investigate this last possibility. Currently there are 6 identified ceramide synthases expressed in mammalian cells. The substrate specificity of all these are not well studied. Therefore the possibility exists that at least one may be able to use S1P as the substrate to produce C1P. To this extent, delivery of 32P labeled S1P to cells resulted in an increase of ^{32}P labeled C1P indicating the existence of an acylation pathway for the synthesis of C1P from S1P (Figures 5.2A and 5.2B). This hypothesis is

further strengthened by the observation that treatment of cells with $d_{17:1}$ S1P also resulted in an increase in $d_{17:1}$ C1P. Taken together these observations provide compelling evidence for generation of C1P via a pathway that involve a direct conversion of S1P.

The fact that the major form of C1P through the acylation pathway investigated above was C_{16} C1P raises the interesting possibility that the remaining C_{16} C1P in cells that do not contain CERK is via an acylation pathway. C_{16} C1P is the major form of C1P in cells. The availability of multiple pathways to produce the lipid indicate that it is an important lipid in the function of the cell. Also of importance is the fact that the acylation of S1P did not result in a significant increase in the other forms of C1P. This would indicate the presence of additional pathways for the synthesis of those different chain lengths of C1P.

In summary the study confirms previous studies that CERK is responsible for only a subset of C1P found in cells (namely C_{16} C1P). The data provides compelling evidence for the existence of an acylation pathway for production of C1P from S1P. The main form of C1P produced via this pathway appears to be C_{16} C1P. This seems to indicate the existence of other pathways that are responsible for other chain lengths of C1P. Taken together the data indicate that C1P is an important lipid in cells with multiple pathways responsible for its production. Further studies are needed to identify the particular acylase responsible for production of C1P from S1P

Literature Cited

1. Sims, P. J., and T. Wiedmer. 2001. Unraveling the mysteries of phospholipid scrambling. *Thromb Haemost* **86**: 266-275.
2. Naka, T., N. Fujiwara, I. Yano, S. Maeda, M. Doe, M. Minamino, N. Ikeda, Y. Kato, K. Watabe, Y. Kumazawa, I. Tomiyasu, and K. Kobayashi. 2003. Structural analysis of sphingophospholipids derived from Sphingobacterium spiritivorum, the type species of genus Sphingobacterium. *Biochimica et Biophysica Acta (BBA) - Molecular and Cell Biology of Lipids* **1635**: 83-92.
3. Pinto, W. J., B. Srinivasan, S. Shepherd, A. Schmidt, R. C. Dickson, and R. L. Lester. 1992. Sphingolipid long-chain-base auxotrophs of Saccharomyces cerevisiae: genetics, physiology, and a method for their selection. *J Bacteriol* **174**: 2565-2574.
4. Adachi-Yamada, T., T. Gotoh, I. Sugimura, M. Tateno, Y. Nishida, T. Onuki, and H. Date. 1999. De Novo Synthesis of Sphingolipids Is Required for Cell Survival by Down-Regulating c-Jun N-Terminal Kinase in Drosophila Imaginal Discs. *Mol. Cell. Biol.* **19**: 7276-7286.
5. Hojjati, M. R., Z. Li, and X.-C. Jiang. 2005. Serine palmitoyl-CoA transferase (SPT) deficiency and sphingolipid levels in mice. *Biochimica et Biophysica Acta (BBA) - Molecular and Cell Biology of Lipids* **1737**: 44-51.
6. Merrill, Jr., M. C. Sullards, J. C. Allegood, S. Kelly, and E. Wang. 2005. Sphingolipidomics: High-throughput, structure-specific, and quantitative analysis of sphingolipids by liquid chromatography tandem mass spectrometry. *Methods* **36**: 207-224.
7. Robson, K. J., M. E. Stewart, S. Michelsen, N. D. Lazo, and D. T. Downing. 1994. 6-Hydroxy-4-sphingenine in human epidermal ceramides. *Journal of Lipid Research* **35**: 2060-2068.
8. Ferguson-Yankey, S. R., M. S. Skrzypek, R. L. Lester, and R. C. Dickson. 2002. Mutant analysis reveals complex regulation of sphingolipid long chain base phosphates and long chain bases during heat stress in yeast. *Yeast (Chichester, England)* **19**: 573-586.

9. Hanada, K., K. Kumagai, S. Yasuda, Y. Miura, M. Kawano, M. Fukasawa, and M. Nishijima. 2003. Molecular machinery for non-vesicular trafficking of ceramide. *Nature* **426**: 803-809.
10. Funato, K., and H. Riezman. 2001. Vesicular and nonvesicular transport of ceramide from ER to the Golgi apparatus in yeast. *J. Cell Biol.* **155**: 949-960.
11. Vallee, B. a., and H. Riezman. 2005. Lip1p: a novel subunit of acyl-CoA ceramide synthase. *The EMBO Journal* **24**: 730?741-730?741.
12. Mizutani, Y., A. Kihara, and Y. Igarashi. 2005. Mammalian Lass6 and its related family members regulate synthesis of specific ceramides. *Biochemical Journal* **390**: 263?271-263?271.
13. Pewzner-Jung, Y., S. Ben-Dor, and A. H. Futerman. 2006. When Do Lasses (Longevity Assurance Genes) Become CerS (Ceramide Synthases)?: INSIGHTS INTO THE REGULATION OF CERAMIDE SYNTHESIS. *J. Biol. Chem.* **281**: 25001-25005.
14. Yamaoka, S., M. Miyaji, T. Kitano, H. Umehara, and T. Okazaki. 2004. Expression Cloning of a Human cDNA Restoring Sphingomyelin Synthesis and Cell Growth in Sphingomyelin Synthase-defective Lymphoid Cells. *J. Biol. Chem.* **279**: 18688-18693.
15. Huitema, K., J. v. d. Dikkenberg, J. F. H. M. Brouwers, and J. C. M. Holthuis. 2004. Identification of a family of animal sphingomyelin synthases. *The EMBO Journal* **23**: 33?44-33?44.
16. Ichikawa, S., H. Sakiyama, G. Suzuki, K. I. Hidari, and Y. Hirabayashi. 1996. Expression cloning of a cDNA for human ceramide glucosyltransferase that catalyzes the first glycosylation step of glycosphingolipid synthesis. *Proceedings of the National Academy of Sciences of the United States of America* **93**: 12654-12654.
17. Schulte, S., and W. Stoffel. 1993. Ceramide UDPgalactosyltransferase from myelinating rat brain: purification, cloning, and expression. *Proceedings of the National Academy of Sciences of the United States of America* **90**: 10265?10269-10265?10269.
18. Graf, C., S. Niwa, M. M?ller, B. Kinzel, and F. d. r. Bornancin. Wild-type levels of ceramide and ceramide-1-phosphate in the retina of ceramide kinase-like-deficient mice. *Biochemical and Biophysical Research Communications* **In Press, Uncorrected Proof**.
19. Sugiura, M., K. Kono, H. Liu, T. Shimizugawa, H. Minekura, S. Spiegel, and T. Kohama. 2002. Ceramide kinase, a novel lipid kinase. Molecular cloning and functional characterization. *J Biol Chem* **277**: 23294-23300.
20. Ishii, I., N. Fukushima, X. Ye, and J. Chun. 2004. Lysophospholipid receptors: signaling and biology. *Annu Rev Biochem* **73**: 321-354.
21. Radeff-Huang, J., T. M. Seasholtz, R. G. Matteo, and J. H. Brown. 2004. G protein mediated signaling pathways in lysophospholipid induced cell proliferation and survival. *J Cell Biochem* **92**: 949-966.

22. Ghosh, M., D. E. Tucker, S. A. Burchett, and C. C. Leslie. 2006. Properties of the Group IV phospholipase A2 family. *Prog Lipid Res* **45**: 487-510.
23. Yedgar, S., M. Krimsky, Y. Cohen, and R. J. Flower. 2007. Treatment of inflammatory diseases by selective eicosanoid inhibition: a double-edged sword? *Trends Pharmacol Sci* **28**: 459-464.
24. Rivera, J., and A. Olivera. 2007. Src family kinases and lipid mediators in control of allergic inflammation. *Immunol Rev* **217**: 255-268.
25. Bajjalieh, S. M., T. F. Martin, and E. Floor. 1989. Synaptic vesicle ceramide kinase. A calcium-stimulated lipid kinase that co-purifies with brain synaptic vesicles. *J Biol Chem* **264**: 14354-14360.
26. Dressler, K. A., and R. N. Kolesnick. 1990. Ceramide 1-phosphate, a novel phospholipid in human leukemia (HL-60) cells. Synthesis via ceramide from sphingomyelin. *J Biol Chem* **265**: 14917-14921.
27. Kolesnick, R. N., and M. R. Hemer. 1990. Characterization of a ceramide kinase activity from human leukemia (HL-60) cells. Separation from diacylglycerol kinase activity. *J Biol Chem* **265**: 18803-18808.
28. Kim, T. J., S. Mitsutake, and Y. Igarashi. 2006. The interaction between the pleckstrin homology domain of ceramide kinase and phosphatidylinositol 4,5-bisphosphate regulates the plasma membrane targeting and ceramide 1-phosphate levels. *Biochem Biophys Res Commun* **342**: 611-617.
29. Carre, A., C. Graf, S. Stora, D. Mechtcheriakova, R. Csonga, N. Urtz, A. Billich, T. Baumruker, and F. Bornancin. 2004. Ceramide kinase targeting and activity determined by its N-terminal pleckstrin homology domain. *Biochem Biophys Res Commun* **324**: 1215-1219.
30. Mitsutake, S., and Y. Igarashi. 2005. Calmodulin is involved in the Ca2+-dependent activation of ceramide kinase as a calcium sensor. *J Biol Chem* **280**: 40436-40441.
31. Kertesz, Z., B. B. Yu, A. Steinkasserer, H. Haupt, A. Benham, and R. B. Sim. 1995. Characterization of binding of human beta 2-glycoprotein I to cardiolipin. *Biochem J* **310 (Pt 1)**: 315-321.
32. Pettus, B. J., A. Bielawska, P. Subramanian, D. S. Wijesinghe, M. Maceyka, C. C. Leslie, J. H. Evans, J. Freiberg, P. Roddy, Y. A. Hannun, and C. E. Chalfant. 2004. Ceramide 1-phosphate is a direct activator of cytosolic phospholipase A2. *J Biol Chem* **279**: 11320-11326.
33. Pettus, B. J., A. Bielawska, S. Spiegel, P. Roddy, Y. A. Hannun, and C. E. Chalfant. Biol Chem 2003 Oct 3. Ceramide kinase mediates cytokine- and calcium ionophore-induced arachidonic acid release. *J* **278**: 38206-38213.
34. Subramanian, P., R. V. Stahelin, Z. Szulc, A. Bielawska, W. Cho, and C. E. Chalfant. 2005. Ceramide 1-phosphate acts as a positive allosteric activator of group IVA cytosolic phospholipase A2alpha and enhances the interaction of the enzyme with phosphatidylcholine. *J Biol Chem* **280**: 17601-17607.

35. Mitsutake, S., T. J. Kim, Y. Inagaki, M. Kato, T. Yamashita, and Y. Igarashi. 2004. Ceramide kinase is a mediator of calcium-dependent degranulation in mast cells. *J Biol Chem*.
36. Hinkovska-Galcheva, V. T., L. A. Boxer, P. J. Mansfield, D. Harsh, A. Blackwood, and J. A. Shayman. 1998. The formation of ceramide-1-phosphate during neutrophil phagocytosis and its role in liposome fusion. *J Biol Chem* **273**: 33203-33209.
37. Gomez-Munoz, A., P. A. Duffy, A. Martin, O. B. L, H. S. Byun, R. Bittman, and D. N. Brindley. 1995. Short-chain ceramide-1-phosphates are novel stimulators of DNA synthesis and cell division: antagonism by cell-permeable ceramides. *Mol Pharmacol* **47**: 833-839.
38. Gomez-Munoz, A., L. M. Frago, L. Alvarez, and I. Varela-Nieto. 1997. Stimulation of DNA synthesis by natural ceramide 1-phosphate. *Biochem J* **325**: 435-440.
39. Gomez-Munoz, A., J. Y. Kong, B. Salh, and U. P. Steinbrecher. 2004. Ceramide-1-phosphate blocks apoptosis through inhibition of acid sphingomyelinase in macrophages. *J Lipid Res* **45**: 99-105.
40. Bajjalieh, S., and R. Batchelor. 2000. Ceramide kinase. *Methods Enzymol* **311**: 207-215.
41. Wijesinghe, D. S., A. Massiello, P. Subramanian, Z. Szulc, A. Bielawska, and C. E. Chalfant. 2005. Substrate specificity of human ceramide kinase. *J Lipid Res*.
42. Garavito, R. M., and S. Ferguson-Miller. 2001. Detergents as tools in membrane biochemistry. *J Biol Chem* **276**: 32403-32406.
43. Lichtenberg, D., R. J. Robson, and E. A. Dennis. 1983. Solubilization of phospholipids by detergents. Structural and kinetic aspects. *Biochim Biophys Acta* **737**: 285-304.
44. Robson, R. J., and E. A. Dennis. 1979. Mixed micelles of sphingomyelin and phosphatidylcholine with nonionic surfactants. Effect of temperature and surfactant polydispersity. *Biochim Biophys Acta* **573**: 489-500.
45. Robson, R. J., Dennis, E. A. 1983. *Accts. Chem. Res.* **16**: 251-258.
46. Hannun, Y. A., C. R. Loomis, A. H. Merrill, Jr., and R. M. Bell. 1986. Sphingosine inhibition of protein kinase C activity and of phorbol dibutyrate binding in vitro and in human platelets. *J Biol Chem* **261**: 12604-12609.
47. Okazaki, T., R. M. Bell, and Y. A. Hannun. 1989. Sphingomyelin turnover induced by vitamin D3 in HL-60 cells. Role in cell differentiation. *J Biol Chem* **264**: 19076-19080.
48. Mathias, S., K. A. Dressler, and R. N. Kolesnick. 1991. Characterization of a ceramide-activated protein kinase: stimulation by tumor necrosis factor alpha. *Proc Natl Acad Sci U S A* **88**: 10009-10013.
49. Dressler, K. A., S. Mathias, and R. N. Kolesnick. 1992. Tumor necrosis factor-alpha activates the sphingomyelin signal transduction pathway in a cell-free system. *Science* **255**: 1715-1718.
50. Hannun, Y. A. 1994. The sphingomyelin cycle and the second messenger function of ceramide. *J Biol Chem* **269**: 3125-3128.

51. Hannun, Y. A., and L. M. Obeid. 1995. Ceramide: an intracellular signal for apoptosis. *Trends Biochem Sci* **20**: 73-77.
52. Kolesnick, R., and D. W. Golde. 1994. The sphingomyelin pathway in tumor necrosis factor and interleukin-1 signaling. *Cell* **77**: 325-328.
53. Ballou, L. R., S. J. Laulederkind, E. F. Rosloniec, and R. Raghow. 1996. Ceramide signalling and the immune response. *Biochim Biophys Acta* **1301**: 273-287.
54. Gomez-Munoz, A. 1998. Addendum to 'Modulation of cell signalling by ceramides'. *Biochim Biophys Acta* **1394**: 261.
55. Dobrowsky, R. T., and Y. A. Hannun. 1993. Ceramide-activated protein phosphatase: partial purification and relationship to protein phosphatase 2A. *Adv Lipid Res* **25**: 91-104.
56. Lozano, J., E. Berra, M. M. Municio, M. T. Diaz-Meco, I. Dominguez, L. Sanz, and J. Moscat. 1994. Protein kinase C zeta isoform is critical for kappa B-dependent promoter activation by sphingomyelinase. *J Biol Chem* **269**: 19200-19202.
57. Westwick, J. K., A. E. Bielawska, G. Dbaibo, Y. A. Hannun, and D. A. Brenner. 1995. Ceramide activates the stress-activated protein kinases. *J Biol Chem* **270**: 22689-22692.
58. Verheij, M., R. Bose, X. H. Lin, B. Yao, W. D. Jarvis, S. Grant, M. J. Birrer, E. Szabo, L. I. Zon, J. M. Kyriakis, A. Haimovitz-Friedman, Z. Fuks, and R. N. Kolesnick. 1996. Requirement for ceramide-initiated SAPK/JNK signalling in stress-induced apoptosis. *Nature* **380**: 75-79.
59. Hayakawa, M., S. Jayadev, M. Tsujimoto, Y. A. Hannun, and F. Ito. 1996. Role of ceramide in stimulation of the transcription of cytosolic phospholipase A2 and cyclooxygenase 2. *Biochem Biophys Res Commun* **220**: 681-686.
60. Bourbon, N. A., L. Sandirasegarane, and M. Kester. 2002. Ceramide-induced inhibition of Akt is mediated through protein kinase Czeta: implications for growth arrest. *J Biol Chem* **277**: 3286-3292.
61. Schubert, K. M., M. P. Scheid, and V. Duronio. 2000. Ceramide inhibits protein kinase B/Akt by promoting dephosphorylation of serine 473. *J Biol Chem* **275**: 13330-13335.
62. Bajjalieh, S. M., T. F. Martin, and E. Floor. 1989. Synaptic vesicle ceramide kinase. A calcium-stimulated lipid kinase that co-purifies with brain synaptic vesicles. *J Biol Chem* **264**: 14354-14360.
63. Dressler, K. A., and R. N. Kolesnick. 1990. Ceramide 1-phosphate, a novel phospholipid in human leukemia (HL-60) cells. Synthesis via ceramide from sphingomyelin. *J Biol Chem* **265**: 14917-14921.
64. Rile, G., Y. Yatomi, T. Takafuta, and Y. Ozaki. 2003. Ceramide 1-phosphate formation in neutrophils. *Acta Haematol* **109**: 76-83.
65. Riboni, L., R. Bassi, V. Anelli, and P. Viani. 2002. Metabolic formation of ceramide-1-phosphate in cerebellar granule cells: evidence for the phosphorylation of ceramide by different metabolic pathways. *Neurochem Res* **27**: 711-716.

66. Carpio, L. C., E. Stephan, A. Kamer, and R. Dziak. 1999. Sphingolipids stimulate cell growth via MAP kinase activation in osteoblastic cells. *Prostaglandins Leukot Essent Fatty Acids* **61**: 267-273.
67. Pettus, B. J., A. Bielawska, S. Spiegel, P. Roddy, Y. A. Hannun, and C. E. Chalfant. 2003. Ceramide kinase mediates cytokine and calcium ionophore-induced arachidonic acid release. *J Biol Chem* **2003**: 10.
68. Usta, J., S. El Bawab, P. Roddy, Z. M. Szulc, Yusuf, A. Hannun, and A. Bielawska. 2001 Aug 14. Structural requirements of ceramide and sphingosine based inhibitors of mitochondrial ceramidase. *Biochemistry* **40**: 9657-9668.
69. Chalfant, C. E., Z. Szulc, P. Roddy, A. Bielawska, and Y. A. Hannun. 2004. The structural requirements for ceramide activation of serine-threonine protein phosphatases. *J Lipid Res* **45**: 496-506.
70. Bielawska, A., H. M. Crane, D. Liotta, L. M. Obeid, and Y. A. Hannun. 1993. Selectivity of ceramide-mediated biology. Lack of activity of erythro-dihydroceramide. *J Biol Chem* **268**: 26226-26232.
71. Herold, P. E. 1988. Synthesis of D-erythro and D-threo Sphingosine Derivatives from L-Serine. *J. Org. Chem.* **71**: 354-362.
72. Usta, J., S. El Bawab, P. Roddy, Z. M. Szulc, Yusuf, A. Hannun, and A. Bielawska. 2001. Structural requirements of ceramide and sphingosine based inhibitors of mitochondrial ceramidase. *Biochemistry* **40**: 9657-9668.
73. Das, S., J. D. Rafter, K. P. Kim, S. P. Gygi, and W. Cho. 2003. Mechanism of group IVA cytosolic phospholipase A(2) activation by phosphorylation. *J Biol Chem* **278**: 41431-41442.
74. Bittova, L., M. Sumandea, and W. Cho. 1999. A structure-function study of the C2 domain of cytosolic phospholipase A2. Identification of essential calcium ligands and hydrophobic membrane binding residues. *J Biol Chem* **274**: 9665-9672.
75. Bektas, M., P. S. Jolly, S. Milstien, and S. Spiegel. 2003. A specific ceramide kinase assay to measure cellular levels of ceramide. *Anal Biochem* **320**: 259-265.
76. Perry, D. K., A. Bielawska, and Y. A. Hannun. Enzymol 2000. Quantitative determination of ceramide using diglyceride kinase. *Methods* **312**: 22-31.
77. Pettus, B. J., M. Baes, M. Busman, Y. A. Hannun, and P. P. Van Veldhoven. 2004. Mass spectrometric analysis of ceramide perturbations in brain and fibroblasts of mice and human patients with peroxisomal disorders. *Rapid Commun Mass Spectrom* **18**: 1569-1574.
78. Kroesen, B. J., B. Pettus, C. Luberto, M. Busman, H. Sietsma, L. de Leij, and Y. A. Hannun. 2001. Induction of apoptosis through B-cell receptor cross-linking occurs via de novo generated C16-ceramide and involves mitochondria. *J Biol Chem* **276**: 13606-13614.
79. Pettus, B. J., B. J. Kroesen, Z. M. Szulc, A. Bielawska, J. Bielawski, Y. A. Hannun, and M. Busman. 2004. Quantitative measurement of different ceramide species from crude cellular extracts by normal-phase high-performance liquid chromatography coupled to atmospheric pressure ionization mass spectrometry. *Rapid Commun Mass Spectrom* **18**: 577-583.

80. El Bawab, S., J. Usta, P. Roddy, Z. M. Szulc, A. Bielawska, and Y. A. Hannun. Lipid Res 2002 Jan. Substrate specificity of rat brain ceramidase. *J* **43**: 141-148.
81. Crossman, M. W., and C. B. Hirschberg. 1977. Biosynthesis of phytosphingosine by the rat. *J Biol Chem* **252**: 5815-5819.
82. Sato, E., T. Uezato, M. Fujita, and K. Nishimura. 1982. Developmental profiles of glycolipids in mouse small intestine. *J Biochem (Tokyo)* **91**: 2013-2019.
83. Madison, K. C., D. C. Swartzendruber, P. W. Wertz, and D. T. Downing. 1990. Sphingolipid metabolism in organotypic mouse keratinocyte cultures. *J Invest Dermatol* **95**: 657-664.
84. Roberts, M. F., R. A. Deems, and E. A. Dennis. 1977. Dual role of interfacial phospholipid in phospholipase A2 catalysis. *Proc Natl Acad Sci U S A* **74**: 1950-1954.
85. Hannun, Y. A., C. R. Loomis, and R. M. Bell. 1985. Activation of protein kinase C by Triton X-100 mixed micelles containing diacylglycerol and phosphatidylserine. *J Biol Chem* **260**: 10039-10043.
86. Sugiura, M., K. Kono, H. Liu, T. Shimizugawa, H. Minekura, S. Spiegel, and T. Kohama. Biol Chem 2002 Jun 28. Ceramide kinase, a novel lipid kinase. Molecular cloning and functional characterization. *J* **277**: 23294-23300.
87. Paul, P., Y. Kamisaka, D. L. Marks, and R. E. Pagano. 1996. Purification and characterization of UDP-glucose:ceramide glucosyltransferase from rat liver Golgi membranes. *J Biol Chem* **271**: 2287-2293.
88. Stoffel, W., and I. Melzner. 1980. Studies in vitro on the biosynthesis of ceramide and sphingomyelin. A reevaluation of proposed pathways. *Hoppe Seylers Z Physiol Chem* **361**: 755-771.
89. Baumruker, T., F. Bornancin, and A. Billich. 2005. The role of sphingosine and ceramide kinases in inflammatory responses. *Immunol Lett* **96**: 175-185.
90. Kumagai, K., S. Yasuda, K. Okemoto, M. Nishijima, S. Kobayashi, and K. Hanada. 2005. CERT mediates intermembrane transfer of various molecular species of ceramides. *J Biol Chem* **280**: 6488-6495.
91. Gomez-Munoz, A., J. Y. Kong, K. Parhar, S. W. Wang, P. Gangoiti, M. Gonzalez, S. Eivemark, B. Salh, V. Duronio, and U. P. Steinbrecher. 2005. Ceramide-1-phosphate promotes cell survival through activation of the phosphatidylinositol 3-kinase/protein kinase B pathway. *FEBS Lett* **579**: 3744-3750.
92. Liu, X., P. Zhu, and B. D. Freedman. 2006. Multiple eicosanoid-activated nonselective cation channels regulate B-lymphocyte adhesion to integrin ligands. *Am J Physiol Cell Physiol* **290**: C873-882.
93. Sirous, Z. N., J. B. Fleming, and R. A. Khalil. 2001. Endothelin-1 enhances eicosanoids-induced coronary smooth muscle contraction by activating specific protein kinase C isoforms. *Hypertension* **37**: 497-504.
94. Pidgeon, G. P., J. Lysaght, S. Krishnamoorthy, J. V. Reynolds, K. O'Byrne, D. Nie, and K. V. Honn. 2007. Lipoxygenase metabolism: roles in tumor progression and survival. *Cancer Metastasis Rev* **26**: 503-524.

95. Claria, J. 2006. Regulation of cell proliferation and apoptosis by bioactive lipid mediators. *Recent Patents Anticancer Drug Discov* **1**: 369-382.
96. Graf, C., P. Rovina, L. Tauzin, A. Schanzer, and F. Bornancin. 2007. Enhanced ceramide-induced apoptosis in ceramide kinase overexpressing cells. *Biochem Biophys Res Commun* **354**: 309-314.
97. Ulevitch, R. J. S., M.; Watanabe, Y.; Lister, M.D.; Deems, R.A; Dennis, E. A. 1988. Solubilization, purification, and characterization of a membrane-bound phospholipase A2 from the P388D1 macrophage-like cell line. *J.Biol.Chem* **263**: 3079-3085.
98. Maceyka M., N. V., Milstien S., Spiegel S. 2004. Aminoacylase 1 is a sphingosine kinase 1-interacting protein. *FEBS letters* **568**: 30-34.
99. Merrill, A. H., Jr., M. C. Sullards, J. C. Allegood, S. Kelly, and E. Wang. 2005. Sphingolipidomics: high-throughput, structure-specific, and quantitative analysis of sphingolipids by liquid chromatography tandem mass spectrometry. *Methods* **36**: 207-224.
100. Van Overloop, H., Y. Denizot, M. Baes, and P. P. Van Veldhoven. 2007. On the presence of C2-ceramide in mammalian tissues: possible relationship to etherphospholipids and phosphorylation by ceramide kinase. *Biol Chem* **388**: 315-324.
101. Hogback, S., P. Leppimaki, B. Rudnas, S. Bjorklund, J. P. Slotte, and K. Tornquist. J 2003 Feb 15. Ceramide 1-phosphate increases intracellular free calcium concentrations in thyroid FRTL-5 cells: evidence for an effect mediated by inositol 1,4,5-trisphosphate and intracellular sphingosine 1-phosphate. *Biochem* **370**: 111-119.
102. Tornquist, K., T. Blom, R. Shariatmadari, and M. Pasternack. 2004. Ceramide 1-phosphate enhances calcium entry through voltage-operated calcium channels by a protein kinase C-dependent mechanism in GH4C1 rat pituitary cells. *Biochem J* **380**: 661-668.
103. Mitra, P., M. Maceyka, S. G. Payne, N. Lamour, S. Milstien, C. E. Chalfant, and S. Spiegel. 2007. Ceramide kinase regulates growth and survival of A549 human lung adenocarcinoma cells. *FEBS Lett* **581**: 735-740.
104. Lamour, N. F., R. V. Stahelin, D. S. Wijesinghe, M. Maceyka, E. Wang, J. C. Allegood, A. H. Merrill, Jr., W. Cho, and C. E. Chalfant. 2007. Ceramide kinase uses ceramide provided by ceramide transport protein: localization to organelles of eicosanoid synthesis. *J Lipid Res* **48**: 1293-1304.
105. Stahelin, R. V., P. Subramanian, M. Vora, W. Cho, and C. E. Chalfant. 2007. Ceramide-1-phosphate binds group IVA cytosolic phospholipase a2 via a novel site in the C2 domain. *J Biol Chem* **282**: 20467-20474.
106. Hogback, S., P. Leppimaki, B. Rudnas, S. Bjorklund, J. P. Slotte, and K. Tornquist. 2003. Ceramide 1-phosphate increases intracellular free calcium concentrations in thyroid FRTL-5 cells: evidence for an effect mediated by inositol 1,4,5-trisphosphate and intracellular sphingosine 1-phosphate. *Biochem J* **370**: 111-119.

107. Boath, A., C. Graf, E. Lidome, T. Ullrich, P. Nussbaumer, and F. Bornancin. 2007. Regulation and traffic of ceramide-1-phosphate produced by ceramide kinase: Comparative analysis to glucosylceramide and sphingomyelin. *J Biol Chem*.
108. Mitsutake, S., U. Yokose, M. Kato, I. Matsuoka, J. M. Yoo, T. J. Kim, H. S. Yoo, K. Fujimoto, Y. Ando, M. Sugiura, T. Kohama, and Y. Igarashi. 2007. The generation and behavioral analysis of ceramide kinase-null mice, indicating a function in cerebellar Purkinje cells. *Biochem Biophys Res Commun* **363**: 519-524.
109. Graf, C., S. Niwa, M. Muller, B. Kinzel, and F. Bornancin. 2008. Wild-type levels of ceramide and ceramide-1-phosphate in the retina of ceramide kinase-like-deficient mice. *Biochem Biophys Res Commun* **373**: 159-163.
110. Graf, C., B. Zemann, P. Rovina, N. Urtz, A. Schanzer, R. Reuschel, D. Mechtcheriakova, M. Muller, E. Fischer, C. Reichel, S. Huber, J. Dawson, J. G. Meingassner, A. Billich, S. Niwa, R. Badegruber, P. P. Van Veldhoven, B. Kinzel, T. Baumruker, and F. Bornancin. 2008. Neutropenia with impaired immune response to Streptococcus pneumoniae in ceramide kinase-deficient mice. *J Immunol* **180**: 3457-3466.

APPENDIX A.1

Table A.1. AB 4000 Mass Spectrometer settings and retention times for reverse chromatographic separation under the described conditions for long chain bases, long chain base phosphates and C1P.

	Precursor ion *m/z*	Product ion *m/z*	DP	CE	CXP	Retention time
$d_{17:1}$ So	286.40	268.30	135.00	15.00	15.00	0.569
$d_{17:1}$ Sa	288.40	260.20	50.00	21.00	15.00	0.688
$d_{18:1}$ So	300.50	282.30	50.00	21.00	16.00	0.587
$d_{18:1}$ So	302.50	284.30	50.00	23.00	16.00	0.725
$d_{17:1}$ So1P	366.40	250.40	50.00	23.00	16.00	0.706
$d_{17:1}$ Sa1P	368.40	252.40	50.00	25.00	16.00	0.844
$d_{18:1}$ So1P	380.40	264.40	81.00	25.00	16.00	0.954
$d_{18:1}$ Sa1P	382.40	266.40	81.00	25.00	16.00	0.697
$d_{18:1/2:0}$ C1P	422.30	264.40	81.00	27.50	16.00	1.21
$d_{18:1/12:0}$ C1P	562.40	264.40	81.00	41.00	16.00	3.24
$d_{18:1/14:0}$ C1P	590.40	264.40	81.00	43.50	16.00	3.44
$d_{18:1/16:0}$ C1P	618.50	264.40	81.00	46.00	16.00	3.82
$d_{18:0/16:0}$ C1P	620.50	266.40	81.00	46.00	16.00	3.95

$d_{18:1/18:1}$ C1P	644.50	264.40	81.00	48.50	16.00	3.85
$d_{18:1/18:0}$ C1P	646.50	264.40	81.00	48.50	16.00	4.05
$d_{18:1/20:0}$ C1P	674.60	264.40	81.00	51.00	16.00	4.15
$d_{18:1/22:0}$ C1P	702.70	264.40	81.00	53.50	16.00	4.38
$d_{18:1/24:1}$ C1P	728.60	264.40	81.00	56.00	16.00	4.58
$d_{18:1/24:0}$ C1P	730.60	264.40	81.00	56.00	16.00	4.66
$d_{18:1/26:1}$ C1P	756.70	264.40	81.00	58.50	16.00	4.68
$d_{18:1/26:0}$ C1P	758.70	264.40	81.00	58.50	16.00	4.71

VITA

Dayanjan Shanaka Wijesinghe is from Sri Lanka. He received his Bachelor of Science degree from the University of Peradeniya majoring in Botany with Molecular biology and Biotechnology as the minor. He received a second degree at the same time from the Institute of Chemistry (College of Chemical Sciences) majoring in Chemistry. He enrolled in the PhD program in the fall of 2003.

While in the program, Shanaka was the recipient of the 2005 Clayton Award for the most outstanding second year graduate student, the Phi Kappa Phi scholarship Nomination award and the Evans Award for the most outstanding final year graduate student in 2008. In 2008 he was nominated into the phi kappa phi honor society. He also received a Student Fellowship Award for a poster presentation at the 3rd International Charleston Ceramide Conference.